Universidad de Huelva

Departamento de Química y Ciencia de los Materiales

Production, characterization and utilization of the biomass from various sources

Memoria para optar al grado de doctor
presentada por:

Živan Gojkovic

Fecha de lectura: 9 de junio de 2014

Bajo la dirección de los doctores:

Inés Garbayo Nores
Ivana Márová

Huelva, 2014

VYSOKÉ UČENÍ TECHNICKÉ V BRNĚ
BRNO UNIVERSITY OF TECHNOLOGY

FAKULTA CHEMICKÁ
ÚSTAV CHEMIE POTRAVIN A BIOTECHNOLOGIÍ

FACULTY OF CHEMISTRY
INSTITUTE OF FOOD SCIENCE AND BIOTECHNOLOGY

UNIVERSIDAD DE HUELVA
UNIVERSITY OF HUELVA

FACULTAD DE CIENCIAS EXPERIMENTALES
FACULTY OF EXPERIMENTAL SCIENCES

PRODUCTION, CHARACTERIZATION AND UTILIZATION OF THE BIOMASS FROM VARIOUS SOURCES

*****

PRODUKCE, CHARAKTERIZACE A VYUŽITÍ BIOMASY RŮZNÉHO PŮVODU

*****

PRODUCCIÓN, CARACTERIZACIÓN Y APLICACIÓN DE BIOMASA DE DIVERSO ORIGEN

DIZERTAČNÍ PRÁCE
DOCTORAL THESIS
TESIS DOCTORAL

AUTOR PRÁCE Ing. ŽIVAN GOJKOVIC
AUTHOR
AUTOR

VEDOUCÍ PRÁCE
CZECH SUPERVISOR
DIRECTOR TESIS
doc. RNDr. IVANA MÁROVÁ, CSc.

VEDOUCÍ PRÁCE VE ŠPANĚLSKU
SPANISH SUPERVISOR
CO-DIRECTOR TESIS
Dr. INES GARBAYO NORES

BRNO 2014

BRNO UNIVERSITY
OF TECHNOLOGY

FACULTY OF CHEMISTRY
INSTITUTE OF FOOD
SCIENCE AND
BIOTECHNOLOGY

Universidad de Huelva

Facultad de Ciencias Experimentales

PRODUCTION, CHARACTERIZATION AND UTILIZATION OF THE BIOMASS FROM VARIOUS SOURCES

*

PRODUKCE, CHARAKTERIZACE A VYUŽITÍ BIOMASY RŮZNÉHO PŮVODU

*

PRODUCCIÓN, CARACTERIZACIÓN Y APLICACIÓN DE BIOMASA DE DIVERSO ORIGEN

DOCTORAL THESIS

AUTHOR Ing. ŽIVAN GOJKOVIC
SUPERVISOR doc. RNDr. IVANA MÁROVÁ, CSc.
CO-SUPERVISOR Dr. INES GARBAYO NORES

BRNO 2014

Vysoké učení technické v Brně
Fakulta chemická
Purkyňova 464/118, 61200 Brno 12

Zadání dizertační práce

Číslo dizertační práce:	**FCH-DIZ0090/2013**	Akademický rok:	**2013/2014**
Ústav:	Ústav chemie potravin a biotechnologií		
Student(ka):	**Ing. et Ing. Živan Gojkovic**		
Studijní program:	Chemie a technologie potravin (P2901)		
Studijní obor:	Potravinářská chemie (2901V021)		
Vedoucí práce	**doc. RNDr. Ivana Márová, CSc.**		
Konzultanti:			

Název dizertační práce:

Produkce, charakterizace a využití biomasy různého původu

Zadání dizertační práce:

1) Rešerše - přehled současných poznatků o zpracování a využívání biomasy různého původu.
2) Charakterizace kolagenu izolovaného z různých typů živočišných tkání pomocí biochemických a fyzikálně-chemických metod.
3) Řízená produkce primární biomasy mikrořas Chlorella sorokiniana v režimu vsádkové i kontinuální kultivace.
4) Charakterizace a účinky vybraných selenoproteinů řasy Ch. sorokiniana - experimenty realizovány v rámci bilaterálního mezinárodního projektu CEIA3 ve Španělsku (Universita Huelva, Institut CEICEM)
4) Diskuse a potenciální využití výsledků.

Termín odevzdání dizertační práce: 31.3.2014

Dizertační práce se odevzdává v děkanem stanoveném počtu exemplářů na sekretariát ústavu a v elektronické formě vedoucímu dizertační práce. Toto zadání je přílohou dizertační práce.

Ing. et Ing. Živan Gojkovic Student(ka)	doc. RNDr. Ivana Márová, CSc. Vedoucí práce	doc. Ing. Jiřina Omelková, CSc. Ředitel ústavu

V Brně, dne 1.9.2009

prof. Ing. Martin Weiter, Ph.D.
Děkan fakulty

ABSTRACT

Biomass management is one of the most important issues in modern natural science as it is the basic category which spans through various disciplines of biotechnology. Whether animal, plant or microbial by its origin, biomass presents a vast source of food components, fine chemicals and bioactive molecules, which extraction, characterization and formulation can result in interesting new products destined for human consumption or as new materials in biomedicine.

In the scope of this work, two natural biomass types were investigated – chicken skin as a source of collagen type I, and green microalga *Chlorella sorokiniana* biomass enriched in selenomethionine (SeMet).

Chicken skin it appears as a good alternative to traditional sources of collagen such as pork, bovine and carp that have some limitations. In the first part of this thesis, collagen type I from chicken skin was isolated, identified and characterized and molecular properties were compared to collagen from other animal skins. New methods (viscosimetry and ultrasonic spectroscopy) for molecular characterization of collagen were used. By ultrasonic attenuation, it has been determined that disaggregation and liquefaction phase starts at 40 °C in bovine collagen, whereas in chicken collagen starts at 50 °C. Using viscosimetry technique, denaturation temperature was found to be 50 °C, which is 10 °C higher than that obtained with bovine tendon collagen, confirming higher thermal stability of chicken skin collagen, probably because lysine levels in chicken collagen are two times higher than in bovine. Based on obtained results it could be concluded that due to its higher thermal stability and amino acid composition, chicken skin could be used as an excellent alternative source of collagen.

The second phase of the thesis focused on the enrichment of green microalga *C. sorokiniana* biomass in SeMet by exposing cultures to selenate Se (+VI) during batch and continuous cultivation, and it was performed at the laboratory of Biotechnology of Algae from the Faculty of Experimental Sciences at the University of Huelva in Spain.

Effect of selenate on viability, cell morphology and SeMet accumulation of the microalga *C. sorokiniana* grown in batch conditions was studied. Growth rate of cultures exposed to a sub-lethal 40 $mg \cdot L^{-1}$ (212 μM) of Se decreased about 25 % compared to control. EC_{50} of 45 $mg \cdot L^{-1}$ (238.2 μM) was determined for selenate. Ultrastructural studies with electronic microscope revealed cellular alterations. Electrophoresis of Se-exposed cell proteins suggests that selenate affects expression of the Rubisco gene. Microalga was able to accumulate up to 140 $mg \cdot kg^{-1}$ of SeMet in 120 h of cultivation.

The second type of microalgae experiments focused on the enrichment of *C. sorokiniana* in SeMet, grown in continuous conditions in a 2.2 L photobioreactor, in a medium supplemented with selenate concentrations ranging from 5 to 50 $mg \cdot L^{-1}$. Continuous cultivation at several dilution rates was performed at 40 $mg \cdot L^{-1}$ selenate obtaining a maximum of 246 $\mu g \cdot L^{-1} \cdot day^{-1}$ of SeMet. Results suggest that an efficient batch and continuous cultivation of *C. sorokiniana* for the production of biomass enriched in the high value amino acid SeMet, at laboratory scale is feasible by carefully selecting sub-lethal selenate concentrations in culture medium as well as the culture dilution rates.

KEYWORDS

Collagen, chicken skin, viscosimetry, ultrasonic spectroscopy, selenium, photobioreactor, microalga, bioaccumulation, selenomethionine

ABSTRAKT

Úprava biomasy je jedním z nejdůležitějších problémů v moderních přírodních vědách, protože je základní kategorií týkající se zemědělství, potravinářství, ekologie, zpracování odpadu a biotechnologie. Ať už živočišného, rostlinného nebo mikrobiálního původu, biomasa představuje obrovský zdroj surovin jako potravin, čistých chemikálií, bioaktivních molekul atd., jejichž izolace, charakterizace a formulace může vést k zajímavým novým produktům určeným pro lidskou spotřebu, nebo jako nový materiál v biomedicíně. Předložená studie byla zaměřena na výzkum dvou druhů biomasy - kuřecí kůže jako zdroje kolagenu t a biomasy mikrořasy *Chlorella sorokiniana* obohacené selenomethioninem (SeMet).

V první části práce byl z kuřecí kůže izolován, identifikován a charakterizován kolagen typu I. Molekulární vlastnosti kuřecího kolagenu byly analyzovány a srovnány s jinými kolageny z živočišných kůží. Pro molekulární charakterizaci kolagenu byla použita viskosimetrie a ultrazvuková spektroskopie. Ultrazvukovou spektroskopií bylo zjištěno, že disagregace a zkapalňování hovězího kolagenu začíná při teplotě 40 °C, zatímco u kuřecího kolagenu začíná až při 50 °C. Viskosimetrie dále potvrdila vyšší tepelnou stabilitu kolagenu z kuřecí kůže, jeho denaturační teplota byla 50 °C, což je rovněž o deset stupňů více než u hovězího kolagenu. Kuřecí kolagen obsahuje dvakrát vyšší množství lysinu, což poskytuje tepelnou stabilitu kolagenu. Na základě získaných výsledků lze říci, že vzhledem ke své vysoké tepelné stabilitě a vhodnému aminokyselinovému složení, kuřecí kůže může být použita jako alternativní zdroj kolagenu typu I s aplikacemi v potravinářském průmyslu a biomedicíně.

Druhá část práce byla zaměřena na obohacení biomasy zelené mikrořasy *C. sorokiniana* selenomethioninem. Experimentální část byla provedena v Laboratoři biotechnologie řas na Univerzitě Huelva ve Španělsku.

Cílem první části experimentů bylo studovat vliv selenu na životaschopnost řas, morfologii buněk a akumulaci SeMet v biomase mikrořasy kultivované v dávkových kulturách. Subletální koncentrace Se v živném médiu, 40 $mg \cdot L^{-1}$ (212 μM), snížila rychlost růstu o 25 % ve srovnání s kontrolní kulturou. Hodnota EC_{50} 45 $mg \cdot L^{-1}$ (238,2 μM) byla stanovena pro selenan. Ultrastrukturální studie ukazovaly na strukturální změny chloroplastu (granulární stroma, redukce thylakoid). Elektroforéza proteinů z biomasy mikrořasy ukazuje, že Se ovlivňuje expresi genu enzymu Rubisco. *C. sorokiniana* byla schopna akumulovat až 140 $mg \cdot kg^{-1}$ SeMet během 120 h kultivace.

Další část experimentální práce byla zaměřena na obohacování biomasy mikrořasy *C. sorokiniana* selenomethioninem během kontinuální kultivace s použitím 2,2 L bioreaktoru v kultivačním médiu s přídavkem koncentrace selenu v rozmezí od 5 do 50 $mg \cdot L^{-1}$. *C. sorokiniana* rostla stejně ve všech testovaných koncentracích selenu kromě koncentrace 50 $mg \cdot L^{-1}$, která byla již po krátké době kultivace letální. Během kontinuální kultivace se 40 $mg \cdot L^{-1}$ selenu, bylo získáno maximálně 246 $\mu g \cdot L^{-1}$ selenomethioninu denně. Výsledky ukazují, že kultivace v dávkových kulturách a dlouhodobá kontinuální kultivace mikrořasy *C. sorokiniana* pro získaní biomasy obohacené SeMet je možná pečlivým výběrem podmínek kultivace a subletálních koncentrací selenu v živném médiu.

KLÍČOVÁ SLOVA

Kolagen, kuřecí kůže, viskosimetrie, ultrazvuková spektroskopie, selen, mikrořasa, bioreaktor, bioakumulace, selenomethionin

RESUMEN

La utilización de la biomasa es uno de los principales temas de interés en Biotecnologia. Ya sea de origen animal, vegetal o microbiano, la biomasa es una fuente de sustancias bioactivas cuya extracción puede resultar de interés en la obtención de nuevos productos destinados al consumo humano y/o animal. En esta tesis, se han utilizado dos tipos de biomasa de origen natural: piel de pollo como fuente de colágeno tipo I y biomasa enriquecida en selenometionina *Chlorella sorokiniana.*

En la primera parte de esta tesis, la piel de pollo se presenta como una alternativa frente al empleo de otras fuentes de colágeno tales como el cerdo, el ganado vacuno o las carpas. El colágeno tipo I procedente de pollo ha sido aislado y sus propiedades moleculares comparadas con las del colágeno procedente de otros animales. Con técnicas como la espectroscopía ultrasónica, se ha determinado que la fase de licuefacción en el colágeno de origen bovino empezaba a 40 ºC, mientras que para el colágeno de pollo era 50 ºC. Usando la técnica de viscosimetría, se confirmó 50 ºC como Tª de desnaturalización para el colágeno de pollo lo que representa 10 ºC más que la obtenida con el colágeno de tendón bovino, confirmando así su alta estabilidad térmica debido posiblemente a su alto contenido en lisina. Basándonos en los resultados obtenidos, el colágeno de la piel de pollo podría ser usado como una excelente fuente alternativa de colágeno tipo I.

En la segunda parte de esta tesis, se realizaron experimentos enfocados al enriquecimiento de la biomasa de la microalga *Chlorella sorokiniana* en selenometionina añadiendo selenato Se (+VI) al medio de cultivo en condiciones de crecimiento tanto en discontinuo (baño) como en modo continuo. Esta parte se realizó en el laboratorio de Biotecnología de Algas de la Facultad de Experimentales de la Universidad de Huelva en España y fue parcialmente financiada con una ayuda eidA3-ceiA3 para la realización de tesis doctorales en cotutela por doctorandos extranjeros del Campus de Excelencia Internacional en Agroalimentación (ceiA3).

Los resultados muestran que la tasa de crecimiento en cultivos sometidos a concentraciones subletales de selenio de 40 $mg \cdot L^{-1}$ (212 µM*)*, disminuyó un 25 % respecto a la del cultivo control. También se determinó el valor de EC_{50} siendo éste de 45 $mg \cdot L^{-1}$ (238.2 µM). Estudios con microscopía electrónica revelaron daños en la estructura celular, mientras que los resultados de las electroforesis sugieren que se afecta al gen de la enzima Rubisco. Las células acumularon hasta 140 $mg \cdot kg^{-1}$ of SeMet tras 120 horas de cultivo.

Se obtuvo biomasa de forma continua y con concentraciones crecientes de Se de 5 a 50 $mg \cdot L^{-1}$ usando un fotobioreactor y consiguiendo un máximo en la acumulación de SeMet de 246 $\mu g \cdot L^{-1} \cdot dia^{-1}$ con 40 $mg \cdot L^{-1}$ de selenato. Los resultados apuntan a que es posible obtener biomasa enriquecida en SeMet en modo continuo y a lo largo del tiempo y con una máxima productividad de SeMet, escogiendo bien la concentración subletal de selenio y las tasas de dilución.

PALABRAS CLAVE

Colágeno, piel de pollo, viscosimetría, espectroscopia ultrasónica, selenio, microalga, fotobiorreactor, bioacumulación, selenometionina

DECLARATION

I declare that the diploma thesis has been worked out by myself and that all the quotations from the used literary sources are accurate and complete. The content of the diploma thesis is the property of the Faculty of Chemistry of Brno University of Technology and all commercial uses are allowed only if approved by both the supervisor and the dean of the Faculty of Chemistry, BUT.

.....

student's signature

ACKNOWLEDGEMENT

I would like to express my deepest appreciation and gratitude to my supervisor, Dr. Ivana Márová, for her thoughtful guidance that provided me with an excellent opportunity and for doing research in Czech Republic and abroad. Without her help and support I would never have been able to finish my dissertation.

I would also like to thank my co-supervisor from The University of Huelva in Spain, Dr. Ines Garbayo, for her excellent guidance and patience that lead to completion of this thesis.

Special thanks goes to Dr. Carlos Vílchez, head of the Algal Biotechnology Group of The University of Huelva, for guiding my research of green microalgae for the past several years and helping me to develop my background in microalgal biotechnology.

TABLE OF CONTENTS

1. SYMBOLS AND ABBREVIATIONS

BSE - Bovine spongiform encephalopathy
Car_{tot} - total carotenoids per dry weight of biomass ($mg \cdot g^{-1}$)
Chl_{tot} - total chlorophyll per dry weight of biomass ($mg \cdot g^{-1}$)
Cyt b_6f - cytochrome b_6f complex
D - dilution rate (h^{-1} or day^{-1})
EC_{50} - Se concentration which results in 50 % of growth rate inhibition [μM]
h - Planck constant ($6.626 \cdot 10^{-34}\ J \cdot s^{-1}$)
H - power density of the solar radiation, assuming Sun is a black body ($MW \cdot m^{-2}$)
H^C - combustion enthalpy of algae biomass ($0.477MJ \cdot C\text{-}mol^{-1}$)
LF - luminous flux (lm)
mol_{ph} - mol of photons
N_A - Avogadro's number ($6.022 \cdot 10^{23}\ mol_{ph}^{-1}$)
OD_{680} - optical density measured at wavelength of 680 nm
PAR - photosynthetic active radiation ($400 < \lambda < 700$)
PF - PAR flux ($mol_{ph}s^{-1}$)
PFD - photon flux density ($\mu mol_{ph} \cdot m^{-2}s^{-1}$)
PS I - Photosystem I electron carrier complex of thylakoid membrane
PS II - Photosystem II electron carrier complex of thylakoid membrane
P_v - volumetric productivity ($g \cdot L^{-1}day^{-1}$)
Q_A - plastoquinone A - primary acceptor in photosynthetic electron transport
rpm - revolutions per minute
Rubisco - Ribulose 1,5-bisphosphate carboxylase/oxygenase enzyme
Se(+IV) - selenite (SeO_3^{2-})
Se(+VI) - selenate (SeO_4^{2-})
SeMeSeCys - Se-methylselenocysteine
SeMet - selenomethionine
$(SeCys)_2$ - selenocystine
SPD - spectral power distribution of the radiation ($W \cdot m^{-1}$)
T_d - denaturation temperature
Y_{op} - Maximum quantum yield of PSII
$Y_{ph\text{-}lm}$ - conversion factor [lm - $mol_{ph}s^{-1}$]
$Y_{x,E}$ - biomass yield on light energy ($g \cdot mol_{ph}^{-1}$)
λ - wavelength (nm)
μ - Specific growth rate [h^{-1}]
μ_m - Maximal specific growth rate [h^{-1}]
Φ_{PSII} - Effective photochemical yield of PSII

2. INTRODUCTION

Classical definition states that biotechnology is “the way of manipulating life forms (organisms) to provide desirable products for human use”. This formulation is brought by Kimball's Glossary of biotechnology terms [1], and elegantly underlines essential role of biomass in modern biosciences. Biomass or as above described as “life forms” presents a basic tool, (whether directly or after processing), of every biotechnology process in entire scope of use like pharmaceutical, agricultural, industrial and environmental applications. Not only biomass itself, but also both concepts of cell growth and cell metabolic capability are fundamental to biotechnology [2].

Both classical and novel food technologies produce significant amounts of biomass of different origin. If this biomass is not primary product and can not be directly used, then the problem which eventually remains, is how to further manage this secondary biomass. If this biomass is of non-microbial origin the answer is to extract valuable biomolecules and to purify them. On the other hand, if it is microbial biomass then the possible solution is to use it as enriched biomass, adapting the organism or cultivation process so that during the cultivation it accumulates different valuable microcomponents (e.g. carotenoids, oligopeptides, polysaccharides, bioplastics). Investigation of biomass utilization, in existing processes with main product other than biomass itself, opens interesting possibilities of creating cheap, energy efficient bio-processes with high productivity, palette of valuable products and low waste production, which are compatible with contemporary public demand.

Biomass can be of animal, plant or microbial origin. As it covers basically all living biosystems, biomass study presents a vast area of interest which expands to many disciplines as agriculture, farming, livestock breeding, food technology, industrial biotechnology, waste treatment and ecology and pharmaceutical engineering.

In the theoretical part of this study, a brief summary of different biomass technologies will be presented. Afterward, theoretical study for two types of biomass of particular interest, chicken skin collagen isolation and green microalga biomass enriched in seleno-amino acids of nutritional and therapeutic interest, will be discussed in detail, followed by experimental results of investigation of these two biomass sources.

First experimental part of the thesis, aimed at isolation and characterization of animal skin collagen, was performed at the laboratory of Faculty of Chemistry at Brno University of Technology from Czech Republic. This experimental phase was supported by the project MSM 0021630501 of Czech Ministry of Education.

Second experimental part of this thesis, dealing with green microalga biomass enrichment in seleno-amino acids, was performed at the laboratory of Biotechnology of Algae from the Faculty of Experimental Sciences at the University of Huelva in Spain. Experimental work was partially financed by a Spanish grant from Agrifood Campus of International Excellence (ceiA3) for foreign PhD-students.

3. THEORETICAL BASICS OF THE STUDIED PROBLEMATIC

3.1 BIOMASS OF ANIMAL ORIGIN

Although, the most important use for animal biomass is primarily as a food source, nevertheless, there are many possibilities of biotechnological applications. For decades, tissues obtained from animals have been extensively used for the extraction of therapeutic protein products including enzymes, antibodies and other protein isolates. In this way, much of waste and non-edible animal parts are used for enzyme extraction or as a valuable macromolecules source (e.g. collagen, antibodies, hormones).

Biologically active enzymes may be extracted from any living organism. A very wide range of sources are used for commercial enzyme production. Of the total amount of enzymes that have industrial application, more than 50 % are from fungi and yeast, one third is isolated from bacteria, and the rest from animal (8 %) and plant (4 %) sources [2,3]. Industrial enzymes isolated from animal biomass include chymotrypsin, lipase, trypsin from pancreas, rennet and chymosin of lamb and bovine for milk coagulation and catalase from animal liver [2]. Preparation of biological starting materials demands that all animal organs must be transported and stored at low temperature to retain its enzymatic activity. Frozen organs can be minced with machines generally used in the meat industry, and the enzymes extracted with a buffer solution [4].

3.1.2 Animal skin tissue as a source of type I collagen

Collagen is the most common fibrous protein found in human and animals. It forms up to 30 % of total body proteins and makes up to 80 % of total skin proteins [5]. *In vivo* it is present in a form of fibrils, providing necessary mechanical strength of tissues exposed to constant tensile forces (skin, tendon, blood vessels). Collagen fibrils form extra-cellular matrix holding cells in place allowing cell adhesion and growth. Although, collagen occurs in six varieties with different biological roles, only type I is of importance as material for biomedical usage. Basic structure, as discovered five decades ago, is triple helix, each having 67 nm periodicity and $(Gly\text{-}X\text{-}Y)_n$ amino acid pattern [5], where X is frequently proline (Pro), and Y is frequently 4-hydroxyproline (4-Hyp) [6]. Collagen molecule is formed by three polypeptides, called α chains twisted about each other. The helical twisting is right-handed in collagen and has three amino acid residues per turn. Twisted α chains may have different sequences and each has about 10^3 amino acid residues. High glycine (Gly) content is important feature of collagen, because only Gly residues can be positioned at the very tight junctions between the individual α chains [6]. Collagen ($M_r = 3 \cdot 10^5$) is a rod-shaped molecule, about 300 nm long and 1.5 nm thick. Collagen fibrils consist of triple-helical collagen molecules associated by cross linking in order to provide different degrees of tensile strength. In fibrils, collagen molecules are cross-linked by unusual types of covalent bonds involving lysine (Lys), 5-hydroxylysine, or histidine (His) residues (see **Fig. 1**) [6].

Native collagen suspension is available commercially. Collagen from livestock animals is widely used as cooking ingredient in food industry and in production of cosmetics. Reconstituted fibrils can also be recovered from native suspension and used in biomedicine [7]. Because collagen is a major component of the human extracellular matrix and connective tissues and also because of its excellent biocompatibility, low antigenicity, and high

availability, collagen is widely used as a bio-material.

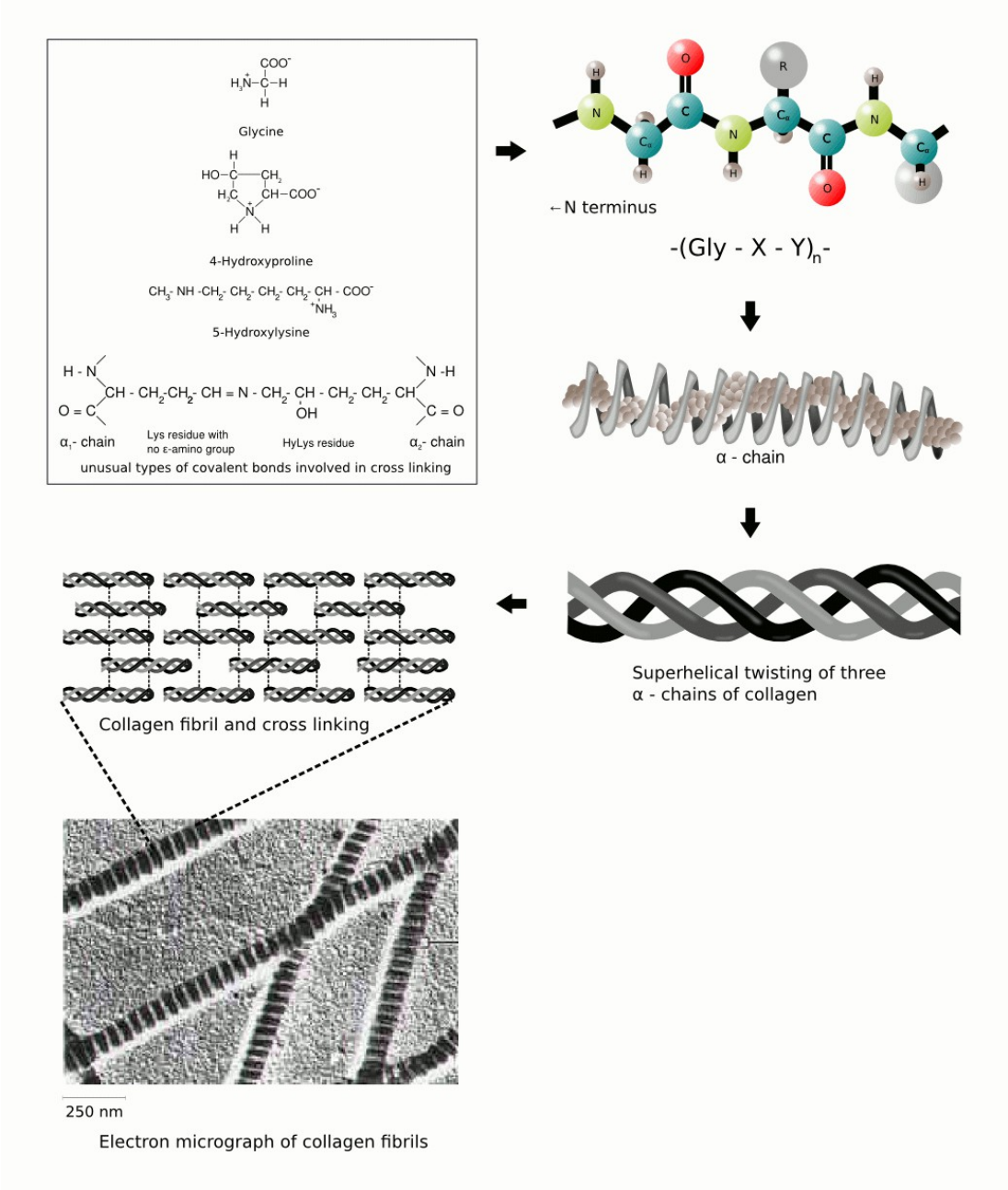

Figure 1. Structure of collagen fibrils which consists of the cross-linked collagen molecule triple helix formed by three supertwisted α chains consisting of repeating -(Gly-X-Y)-$_n$ pattern (adapted from [6]).

Various forms of collagen materials, such as films, sponges, gels, have been developed for medical applications. Collagen scaffolds have been widely used as a dermal equivalent to induce fibroblast infiltration and dermal regeneration [8]. However, they generally degrade quickly *in vivo*, so some treatments, such as glutaraldehyde cross-linking, thermal dehydration and UV radiation are used to increase its mechanical strength by introducing intra- and inter-molecular linkages as well as to decrease its degradation rate [8]. Scaffolds with

interconnected pores are prepared via freeze-drying of frozen hydro-gels made from collagen modified with chitosan nanofibres, hyaluronic acid, co-polymers based on polyethylene glycol (PEG), poly(lactic-co-glycolic acid) (PLGA), and itaconic acid (ITA), and hydroxyapatite nanoparticles. Hydroxyapatite containing scaffolds have the best resistance to hydrolytic degradation. Cartilage tissue generated using mesenchymal stem cells on porous collagen scaffolds with prescribed biomechanical properties is used as a novel material for hard tissue implants [9]. Also addition of hydroxyapatite or hyaluronic acid to the collagen matrix increases the rigidity [9].

In fish-eating and fish-processing countries such as China, carp skin is extensively studied as an alternative source of collagen [10,11]. Problem with application lays in fact that carp skin contains parvalbumins - small calcium-binding, heat resistant proteins which are extremely abundant allergen sources causing IgE-mediated food hypersensitivity [12]. These facts limit the possibility for application of fish skin collagen in biomedicine or in food industry.

The main industrial sources of collagen are pig and bovine skin, tendon and bones. But the outbreaks of BSE syndrome in recent years, and limited application of pork collagen due to religious issues draw attention to alternative collagen sources [11]. Consequently, collagens from other species may be used if they can meet appropriate standards, including lack of immunogenicity [13]. In the study of Penn et al. all responses in mice and rabbits were found only when immunizations were performed with adjuvant, and after multiple injections over a long period of time [13]. The fact that collagens are poor immunogens compared with ovalbumin indicates that chicken collagen may be useful in certain biomedical applications.

Poultry, especially chicken, is one of the most common meat sources in Europe, with annual production of $11.4 \cdot 10^6$ t [14]. During processing of chicken meat, skin is usually treated as waste although it contains high amount of valuable collagen. One of the objectives of this study was isolation and characterization of collagen type I proceeding from chicken skin tissue, as an interesting and cheap alternative collagen source.

3.2 BIOMASS OF PLANT ORIGIN

An enormous increase of global energy consumption produces, among other consequences, an extensive depletion of crude-oil reserves and is clearly unsustainable. On the other hand, only a small fraction of solar energy reaching Earth's surface is converted into biomass. The photosynthetic potential of plants for production of biomass as a renewable energy resource is recognized as a possible “green” energy solution [15]. There are some theoretical calculations that the word annual plant biomass production reaches the number of $17 \cdot 10^{10}$ t with total energy potential of $1.4 \cdot 10^{21}$ J [16]. That is almost five times more energy than world's annual fossil fuel consumption energy ($3 \cdot 10^{20}$ J) [16]. The fact that considerable part of the biomass can also serve as human food rises the ethical problem in this equation of biomass usage. Food versus energy controversy is best illustrated with the following example: ethanol production from maize, mainly in USA, is in direct conflict with global food prices, demand and consumption, as Earth population reaches 7th billion. Nevertheless, about 15 % of world corn production is annually converted into ethanol, while the third-world counties struggle daily with child malnutrition and poverty. The solution might be very obvious, in non-edible biomass conversion into energy [17].

Plant biomass composition has basic components as carbohydrates, lignin, proteins and

fats and other substances: vitamins, dyes, flavors and aromatic essences of different chemical structure. The estimated annual production of biomass by biosynthesis is approx. $17 \cdot 10^{10}$ t of which 75 % are carbohydrates as cellulose, starch, and sucrose, 20 % lignin and 5 % other components such as oils, proteins and other [18]. Plant biomass is a renewable resource that can be utilized for the supply of energy and chemicals, production of power alcohol from waste raw materials, production of biogas; extraction of various biomolecules from cellulosic and lignocellulosic materials [18]. Agronomic residues such as sugar cane waste, wheat or rice straw, forestry and paper mill waste can be converted to bio-ethanol, in the process of fermentation of released polymeric sugar from cellulose and hemicellulose [17]. The main technological concern is extraction of the carbohydrates and their conversion to chemical products or final products. Glucose, extracted by microbial or chemical methods is the basic chemical of interest because a broad palette of biotechnological or chemical products derived from it [18]. Of course, glucose is also the main carbon source for most of organotrophic microorganisms with industrial applications.

3.2.1 Macroalgae (seaweed) and biomass of microalgae as a food source

The term algae refers to a large variety of photosynthetic organisms both microscopic (microalgae) and macroscopic ones (macroalgae), within *Eukaryotes* and *Bacteria* which are not necessary closely related to each other [19]. Edible aquatic macroalgae comes from seven species of red macroalgae which contain pigment phycoerythrin, nine species of freshwater macroalgae and twenty one species of brown macroalgae which contain pigment fucoxanthin [20]. Some species of red macroalgae, such as laver (source of sushi), dulse, and Irish moss, are harvested for food.

Macroalgae biomass is used in the industrial production of phycocolloids like agar–agar, alginates or carrageenan. In total this macroalgae biotechnology represents a world market of approximately six billions of dollars per year; and more than $7.5 \cdot 10^6$ of tons per year of macroalgae are harvested from natural habitats or cultivated at seashore areas [20]. *Ulva lactuca* is harvested along the coast, during the low tide and is consumed by people living in Pacific coastal regions in salads and soups [20]. Macroalga farming is the 6th largest world aquatic-culture [21]. It is estimated that only in Japan, marine macroalgae cultures production worths total of more than 500 million dollars per year [20].

Since the middle 20th century intense efforts have been made to explore new and alternative food sources, primarily driven by increasing world population numbers. The estimated global production of microalgae is approximately $5 \cdot 10^3$ tons of dry biomass per year, of which about half correspond to green microalgae (*Chlorella* and *Dunaliella*) biomass [19,22-25]. Due to high production costs and technical problems as low digestibility of crude algae due to hemicellulotic cell walls, powder consistency, organoleptic issues and intense dark green colour microalgae still have not gained importance as a human food source [23]. Most of the global microalgae production is destined to animal feed (30 %) or as a health food products due to high content of various metabolites, polyunsaturated fatty acids, pigments, antioxidants [19,22,23,26]. Nevertheless, biomass of microalgae composition in terms of basics nutrient requirements such as proteins, carbohydrates and fats content is not inferior compared to meat, milk or soybean.

Table 1. Gross nutrient composition of different microalgae, in % of dry weight [27]

Microalga	Protein	Carbohydrates	Fats
Anabaena cylindrica	43 - 56	25 - 30	4 - 7
Chlamydomonas reinhardtii	48	17	21
Chlorella vulgaris	51 - 58	12 - 17	14 - 22
Dunaliella salina	57	32	6
Scenedesmus obliquus	50 - 56	10 - 17	12 - 14
Spirulina maxima	60 - 71	13 - 16	6 - 7

From data presented in **Tab. 1** it can be concluded that microalgae dried biomass generally contains more proteins and carbohydrates than meat and milk calculated as % of dry matter. Biomass is harvested from photobioreactors, separated from the growth media, washed and dried. The biomass of microalgae is usually formulated as sun-dried or spray-dried powder. In **Tab. 2** data of global production of some microalga species is presented.

Table 2. Estimated global production quantities for various microalgae [19].

Microalga	Annual production (t)
Spirulina	3000
Chlorella	2000
Dunaliella	1200
Nostoc	600

3.3 BIOMASS OF MICROBIAL ORIGIN

Microorganisms are a very diverse forms of life which account about 60 % of the Earth biomass [28]. The biosphere is dominated by microorganisms and contains about $4\text{-}6\cdot10^{30}$ of prokaryotic cells. This number represents at least two to three orders more than all of the plant and animal cells together. Microorganisms are ubiquitously present, have a diverse metabolism and unique survival and adaptation strategies under various conditions [29]. They have some advantages over plants or animals in biotechnology: faster growth and shorter generation time than plants and animals; they require less space (bioreactor volume vs. farm or land) and are not affected by diseases of plants and animals [30]. If one microorganism is used in an industrial process, it must comply to some basic characteristics: a) it must be able to grow in a simple and cheap medium, mineral if possible, preferably with only those growth factors (vitamins, nucleotides, micro-elements and acids), b) should be able to grow rapidly in the medium. A slow growing organism no matter how efficient it is, prolongs cultivation and risk of contamination [30], c) the products should not include toxic or undesirable materials, especially if they are destined for human consumption and should be suitable for product harvest at the end of the fermentation, and d) with physiological requirements that protect them against contaminants.

A microorganism with optimum growth and productivity at high temperatures, low pH values has great advantage over others. The microorganism should not be too demanding in oxygen, because of greater power consumption for aeration which makes about 20 % of the cost of the final product [30].

3.4 PRODUCTION, CHARACTERIZATION AND UTILIZATION OF MICROALGAL BIOMASS

Having in mind that estimated global biomass of microalgae production is about $5 \cdot 10^3$ $t \cdot y^{-1}$ and production of poultry about $11.4 \cdot 10^6$ $t \cdot y^{-1}$ only in Europe, it is obvious that microalgae can not compete with traditional food sources as optimistically projected in the first half of the 20th century [14,24,25]. Nevertheless, 2.5 billions of years of algae evolution and diversification resulted in over $3 \cdot 10^4$ aquatic photosynthetic species (**Fig. 2**) containing many metabolites (including lipids, PUFA, pigments, gellification agents and various bioactive molecules) with potential use in human nutrition [26]. Microalgae potential lies in the production of biofuels and nutraceutics industry of health food and natural pigments source [19,31]. Two major group of microalgae are widely investigated and commercialised: procaryotic cyanobacteria, (*Spirulina* and *Nostoc*), and eukaryotic green microalgae (*Chlorella* and *Dunaliella*) [19,32].

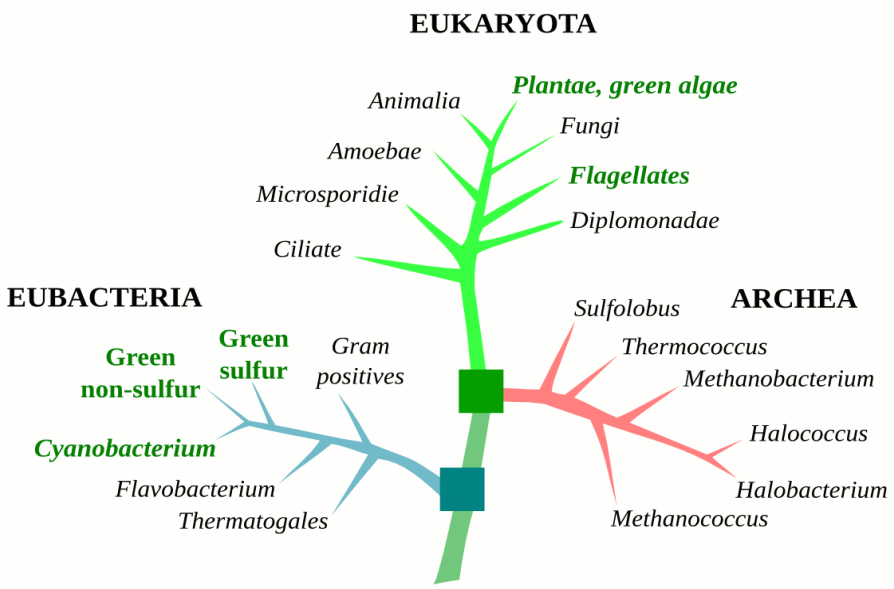

Figure 2. Phylogenetic tree of life - different groups spanning throughout three basic domains of life containing organisms able to perform photosyntheses are presented in green, squares represent common evolutionary ancestors (adapted from [33,34]).

Microalgae can be classified based on morphological, ultrastructural or molecular characteristics of the species. Traditional taxonomic approach uses the morphology of the vegetative state of the organisms for classification while ultrastructural concept uses the basal body orientation of the flagellar apparatus and cytokinesis [35]. Molecular classification is based on the phylogenetic analyses of molecular markers such as nuclear ribosomal operon DNA as well as several chloroplast and mitochondrial genes [35,36]. The largest group of

green microalgae, Chlorophyceae, originally contained all green microalgae but was subsequently reduced thanks to molecular data which showed the polyphyly within the genera, that reclassified many species into different taxonomic groups [37]. Relationship between many of the phylogenetic lineages of Chlorophyta remains subject to debate [35-38]. According to combined classification methods (morphology, ultrastructure, and molecular phylogeny) separation of genera and species within the Chlorophyta reveals three major taxa: Ulvophyceae, Chlorophyceae and Trebouxiophyceae [35,36]. The most important eukaryotic microalgal species from both commercial and scientific point of view, belong to the Chlorophyceae and Trebouxiophyceae classes [19,23,36].

Chlorophyta is a large group of aquatic photosynthetic organisms including microscopic eukaryotic algae as well as macroscopic forms divided into 6000 genera with 10000 species which share the following characteristics: 1) they contain chlorophyll a and b, 2) the chloroplasts have two envelope membranes and stacked thylakoids, 3) starch deposited inside the plastids as the main reserve polysaccharide [32,35].

C. reinhardtii is considered the type species of the genus *Chlamydomonas* which is one of the largest microalgae genera including more than 600 species of biflagellate microalgae which contain a single chloroplast with one or more pyrenoids and cell wall and have both flagellas of the same length and in close proximity to each other (**Fig. 3**) [39].

S. quadricauda belongs to a genus *Scenedesmus* comprising of approx. 70 colonial, chloroccocalean green microalgae species with 2 to 16 cells arranged in a row usually equipped with terminal spines [40]. *S. quadricauda* cell is 5 - 8 μm wide and twice as long and forms four-celled colonies with poles of terminal cells with single spine (**Fig. 3**) [40].

C. sorokiniana belongs to the genus *Chlorella* which is one of the best studied microalgae groups worldwide, with more than 100 unicellular members that are traditionally characterized by spherical cell shape, solitary life-form and the absence of mucilaginous envelopes. *C. sorokiniana* cell is spherical to oval with 5-10 μm in diameter, protected by hemicellulotic cell wall which also provides cells rigidity (**Fig. 3**) [23,38].

3.4.1 Photosynthesis as a life driving force of microalgae

Green microalgae contain chlorophyll a and b as photosynthetic pigments and several carotenoids as secondary pigments, which can be accumulated inside the cell in stress situations **(Fig. 4)**.

Chlorophyll a is found in all known eukaryotic photosynthetic organisms. Among prokaryotes, it is found in large quantities only in cyanobacteria. Chlorophyll b is the major accessory light-absorbing pigment in the majority of eukaryotic photosynthetic organisms, with the exception of the red and brown algae (**Tab. 3**). Chlorophyll b at the C-7 position has a formyl group where the chlorophyll a has methyl group. This change shifts the maximum absorption to shorter wavelengths [33]. Green microalgae have carotenoid composition of higher plants. Primary carotenoids include β-carotene, neoxanthin, lutein, and zeaxanthin, integrated in chloroplast lamella while secondary carotenoids such as equinenone, canthaxanthin and astaxanthin come later as final metabolites in biosynthesis pathway [51,52]. Reserve polysaccharide stored directly in chloroplasts is starch. Cell often contains pyrenoid with high concentration of Rubisco and other enzymes from the dark-phase of photosynthesis. Cellulose contained in the cell wall protects cells from external damage [32].

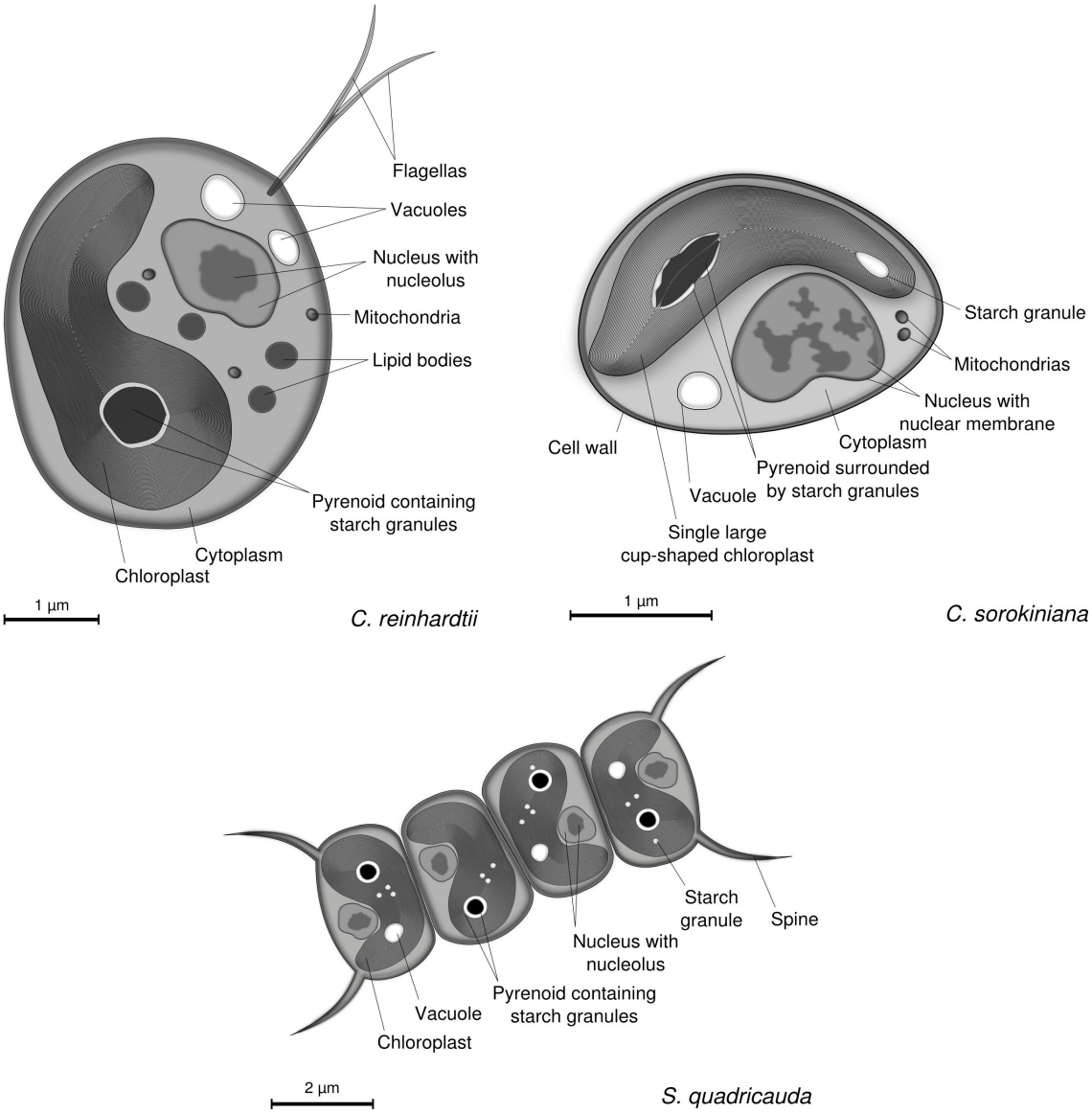

Figure 3. Structural drawings of three microalgae species which are frequently used as a target microorganisms in the study of Se effect on aquatic organisms [41-49].

All photosynthetic organisms that contain chlorophyll use antenna systems for light harvesting and energy transfer to the photosynthetic reaction centers. Two major light-harvesting complexes LHC I and LHC II are hydrophobic complexes of proteins and pigments containing chlorophyll a and b and carotenoids [55]. Photosystems are closely associated with the thylakoid membrane with several hundreds of antenna chlorophylls and accessory pigments packed around the reaction center. Antenna pigments are arranged in organized three-dimensional structures (**Fig. 5**).

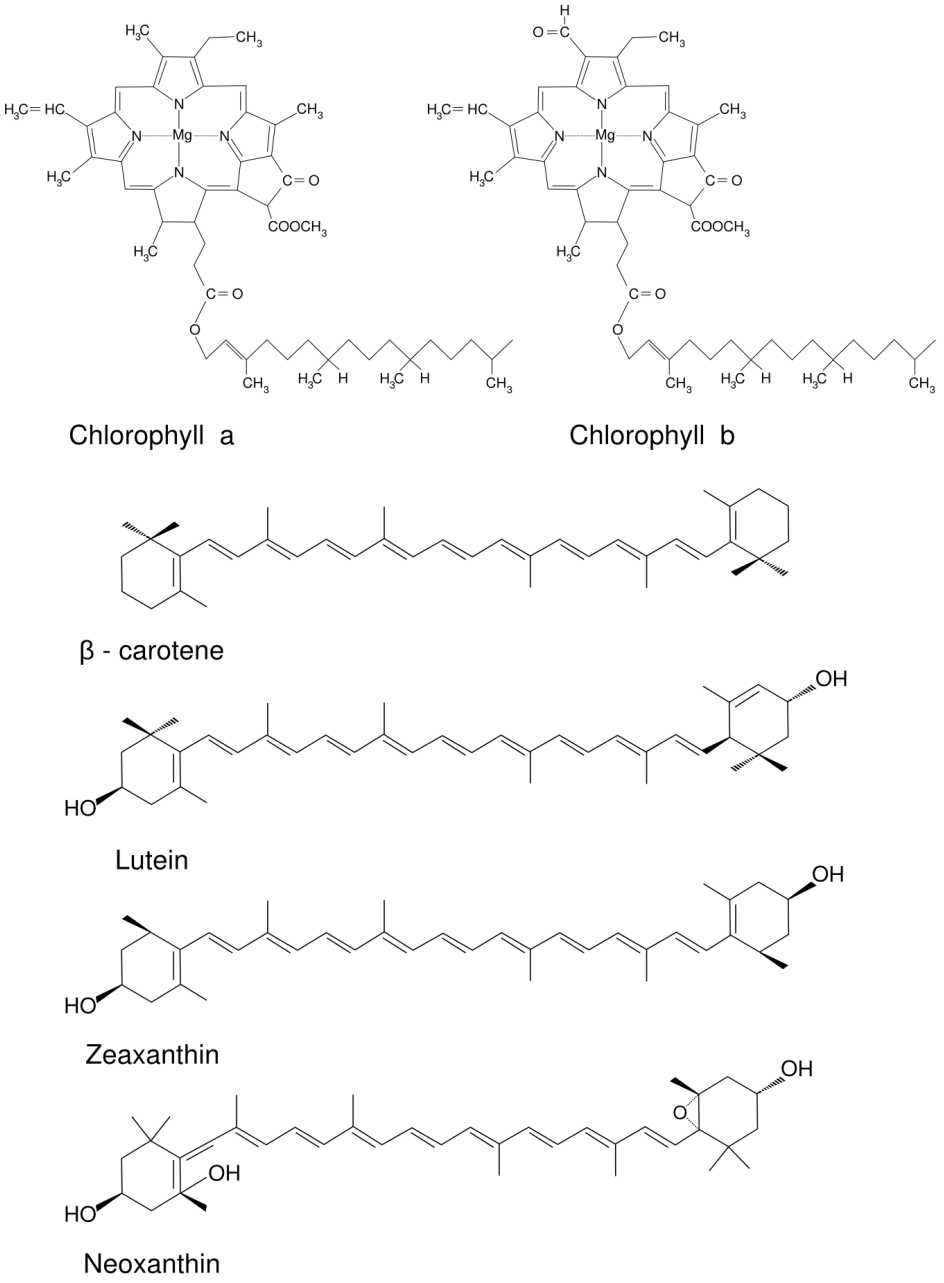

Figure 4. Structures of the primary photosynthetic pigments in microalgae – chlorophyll a and b and accessory group of pigments – carotenoids including β-carotene, lutein, zeaxanthin and neoxanthin. *C. sorokiniana* has a high content of accessory pigments whereas lutein, neoxanthin and β-carotene are the most abundant forms (adapted from [50]).

Not every chlorophyll molecule performs complete photosynthesis but transfers excitation to a reaction center. Number of photons that single chlorophyll molecule absorbs during the exposure to light can be roughly calculated making a few approximations.

Table 3. Distribution of primary and accessory pigments among the major microalgae groups (adapted from [53,54]).

Pigment type ⬇	Algal group ➡	Green Alga (*Chlorophyceae*)	Blue-green Alga (*Cyanophyceae*)	Red Alga (Rhodo*phyceae*)	Brown Alga (Phaeo*phyceae*)	Dinoflagellates (Dino*phyceae*)	Diatoms (Bacillario*phyceae*)	Naked Flagellates
Chlorophylls	Chlorophyll a	+	+	+	+	+	+	+
	Chlorophyll b	+						
	Chlorophyll c				+	+	+	+
Phycobillins	Phycocyanin		+	+				
	Phycoerythrin		+	+				
Carotenoids	β carotene	+	+	+	+	+	+	+
Xanthophylls	Lutein	+		+				
	Zeaxanthin	+	+	+	+			
	Fucoxanthin				+	+	+	+
	Diadinoxanthin				+	+	+	+
	Alloxanthin							+
	Peridinin					+		

The maximal intensity of sunlight expressed as molar photon flux density at a photosynthetically active radiation region PAR (400-700 nm) has the value of PFD = 1800 $\mu mol \cdot m^{-2}s^{-1}$. Flux density of photons can be calculated using Avogadro's number:

$PFD \cdot N_A = 1.8 \cdot 10^{-3} mol \cdot m^{-2}s^{-1} \cdot 6.022 \cdot 10^{23} mol^{-1} = 1.08 \cdot 10^{21} photons \cdot m^{-2}s^{-1} = 1.08 \cdot 10^{3} photons \cdot nm^{-2}s^{-1}$

If single chlorophyll molecule is approximated as a square with surface of 1 nm^2 then it will approximately get hit by 1080 photons every second, according to this calculation [33]. As demonstrated by Blankenship [33] no all of these 1080 photons will be absorbed. The actual number of incoming photons that will be absorbed is proportional to the molar absorption (or extinction) coefficient (ε) representing the strength of the absorption, which can be quantified by the Lambert–Beer law: $A = \varepsilon \cdot c \cdot l$; where ε is absorption coefficient of chlorophyll a (90 $mM^{-1} \cdot cm^{-1}$ at 680 nm), *c* is molar concentration of chlorophyll; *l* is a length of the light path (cm) and $A = \log(I \cdot I_0^{-1})$ is absorption. Having in mind that extinction coefficient depends on chlorophyll concentration and photon flux density gives maximal photon flux incoming to a chlorophyll (antenna) surface, the actual number of photons that are absorbed after hitting chlorophyll molecule can be approximated by multiplying this two parameters:

$$N_{hits} = PFD \cdot \varepsilon = 1800 \cdot 10^{-6} mol_{ph} \cdot m^{-2}s^{-1} \cdot 90\ mM^{-1} \cdot cm^{-1} =$$
$$= 1800 \cdot 10^{-6} mol_{ph} \cdot m^{-2}s^{-1} \cdot 90 \cdot 10^{3} (mol_{ch} \cdot dm^{-3}cm)^{-1} =$$
$$= 16\ mol_{ph} \cdot mol_{ch}^{-1}s^{-1}$$

which taking in account moles are proportional to particles number via Avogadro's number gives approx. 16 photons absorbed per chlorophyll molecule per second. It is important to note that this calculation is only a rough estimation, under ideal conditions, because molar absorption (or extinction) coefficient (ε) is not constant for all wavelengths of PAR spectrum, nor PFD always corresponds to maximal intensity of sunlight [33].

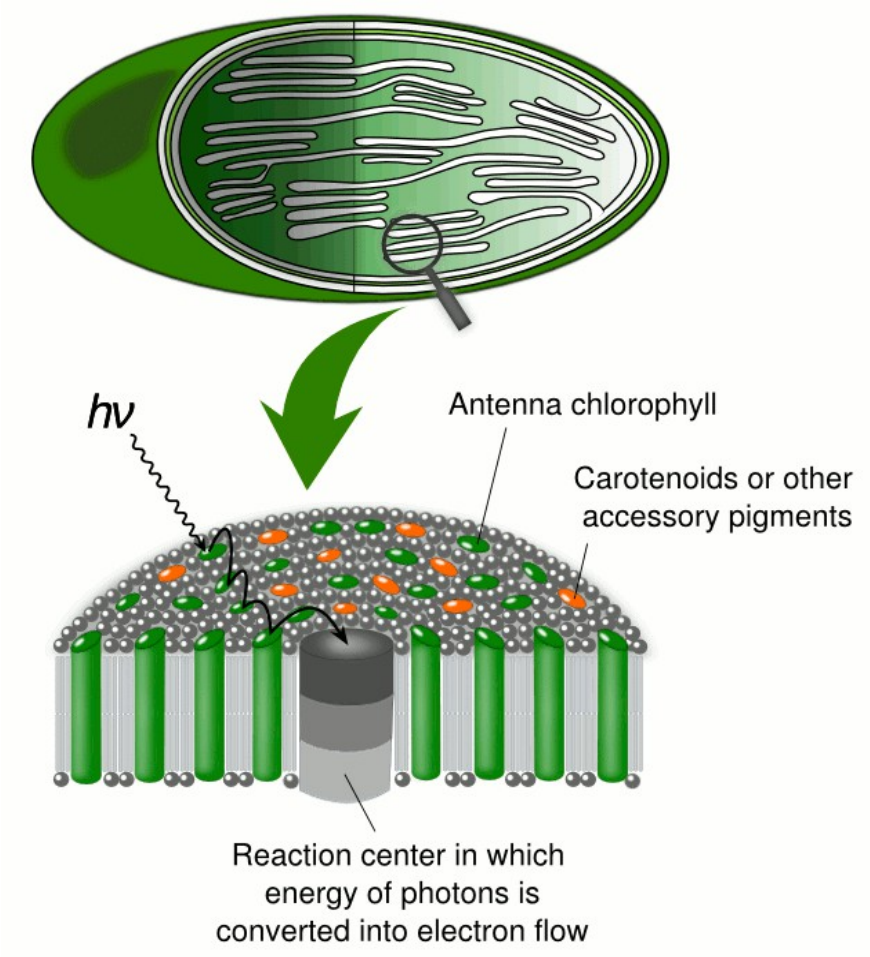

Figure 5. General structure of photosystem associated with thylakoid membrane (adapted from [6]). Photosystem function is to absorb light and transfer the energy in the light to a the reaction center which initiates photochemistry or deactivates the excited state (via fluorescence).

All photosynthetic light reactions are located on the thylakoid membrane of the chloroplast. This membrane is a lipid bilayer membrane arranged to form enclosed system which separates intrathylakoidal space called lumen from stroma surrounding thylakoid outer membrane [55] (**Fig. 6**). Thylakoid membrane consists of highly appressed region called grana or grana lamellae where several membranes are in contact (in algae thylakoids are organised as stacks of two or three) and non-appressed region called stromal lamellae with single thylakoid connecting grana [33,55].

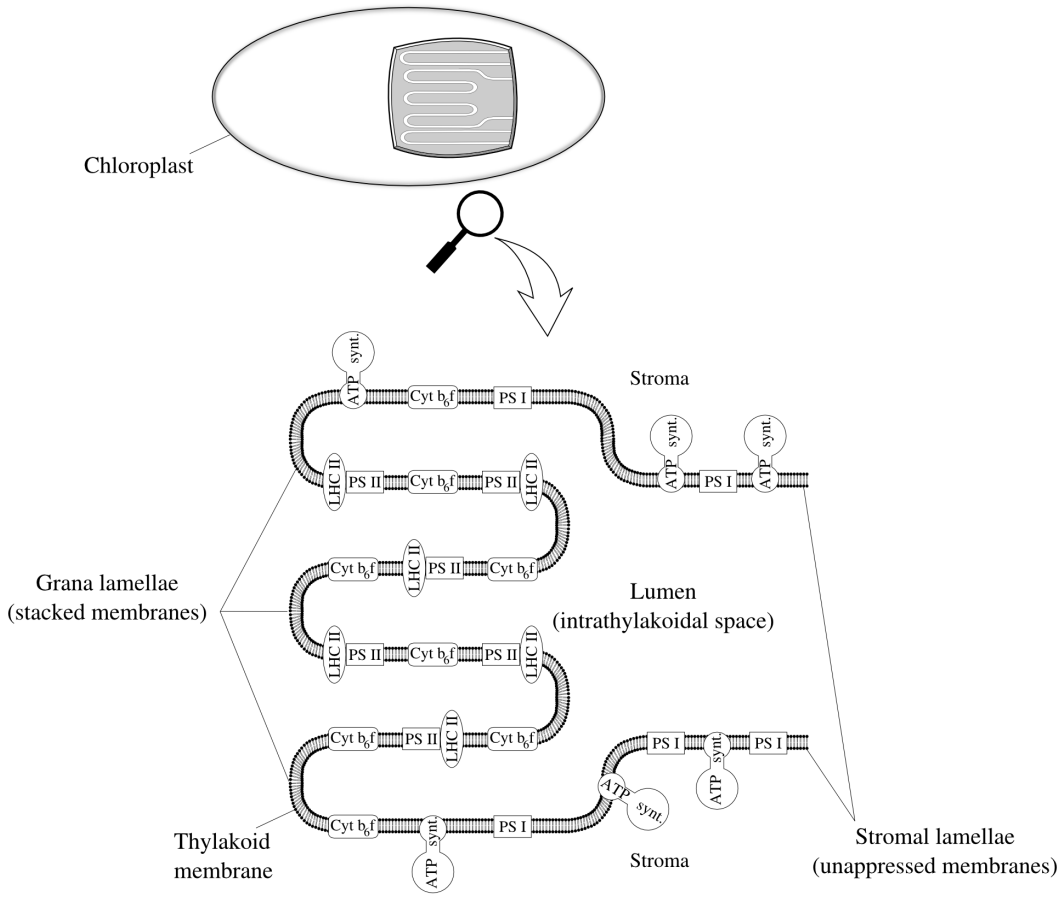

Figure 6. Distribution of photosystems I and II and other electron transfer complexes in thylakoid membrane inside chloroplast of algae and plants (adapted from [6,33]). PS II is located exclusively in the appressed regions (grana) associated to LHCII as well as Cyt b_6f complex. PS I and the ATP synthase are located in the nonappressed regions of single thylakoids (stromal lamellae) and on the edges of the grana. LHC II - light harvesting complex; PS I – Photosystem I; PS II - Photosystem II; Cyt b_6f - cytochrome b_6f complex; ATP synt. - ATP synthase.

Major components involved in photosynthetic electron transfer associated with thylakoid membrane are [56]:

- Photosystem II (PS II) - membrane-intrinsic, light-dependant H_2O/plastoquinone oxidoreductase which is associated with light harvesting complex II (LHC II);
- Cytochrome b_6f complex (Cyt b_6f)-membrane-intrinsic, light-independent plastoquinol/plastocyanin oxidoreductase;
- Photosystem I (PS I) - membrane-intrinsic, light-dependant plastocyanin/ferredoxin oxidoreductase;
- ATP synthase – a proton translocating ATP hydrolase [56].

These complexes are non-uniformly distributed on thylakoid membrane [6,33,55]. Photosystem PS II is located exclusively in the stacked regions of the membranes (grana) associated to LHC II which keeps thylakoids in appressed state, whereas PS I is located mainly in the nonappressed regions (stroma lamellae) and on the ends of the grana stacks [6,33]. The Cyt b_6f complex is mainly present in the grana. ATP synthase complex is like PSI

located mainly in the nonappressed thylakoid membranes (stromal lamellae), where it has access to ADP and $NADP^+$ concentrated in stroma [6].

3.4.1.1 Photosynthetically active radiation, Z scheme and calculation of photosynthetic efficiency

Driving force of photosynthesis, light is an electromagnetic radiation divided into several components based on its wavelength. Although sun emits radiation in the broad range of the wavelengths; chlorophylls, photosynthetic pigments of microalgae and plants, are absorbing in a narrow wavelength range of 400 to 750 nm usually named PAR range and almost equivalent to visible light wavelengths (**Fig. 7**).

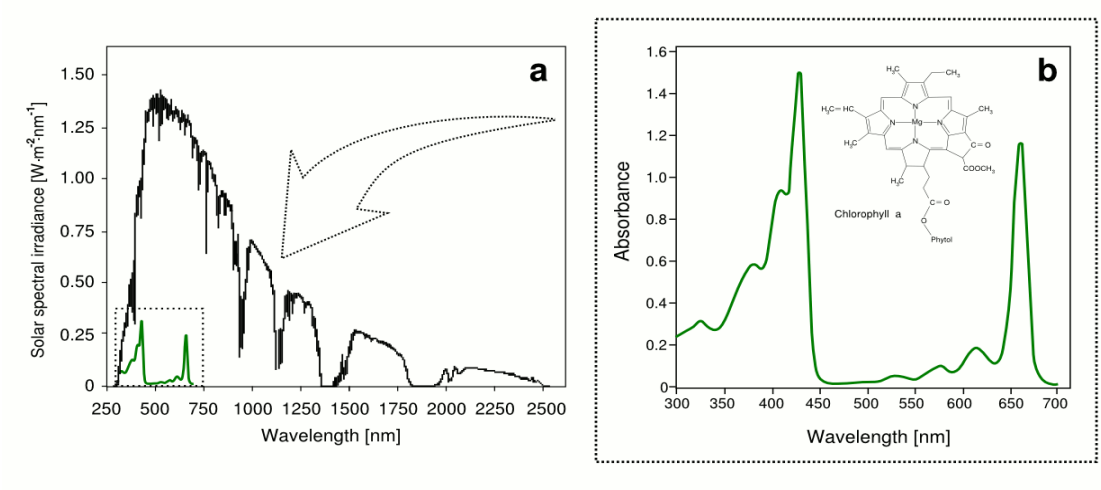

Figure 7. The distributions of terrestrial spectral irradiance of a solar spectrum **(a);** compared to absorption range of photosynthetic pigment chlorophyll **(b)** [33,57].

Light incoming from sun is usually described by power density of the solar radiation, assuming sun is a black body radiating H = 63 $MW \cdot m^{-2}$. Photon flux density (PFD) and spectral power density (SPD) are two important photosynthesis parameters used to describe sun radiation for every wavelength of sun spectrum. Photon flux density (PFD, $[mol_{ph} \cdot m^{-2} s^{-1}]$) is related to H via equation: $PFD = H \cdot \lambda \cdot (N_A hc)^{-1}$; where $h \cdot c \cdot \lambda^{-1}$ [J] represents photon energy at certain wavelength and N_A is Avogadro's number $6.022 \cdot 10^{23}$ mol^{-1}, at a fixed wavelength λ. Spectral power density SPD, $[W \cdot m^{-2} \cdot \mu m]$ or $[W \cdot m^{-1}]$ refers to the power density at a given wavelength and is related to H via $H = SPD \cdot \Delta\lambda$ equation. Using these equations both photon flux density (PFD) and spectral irradiance (SPD) can be calculated from Sun power density (H) for every given wavelength.

Visible light ranges from violet at 380 nm to red at 750 nm (**Fig. 8**). Ultraviolet, X rays and Gamma radiation have shorter wavelengths while infra-red, microwaves and radio waves have longer wavelengths than visible part of the light spectrum.

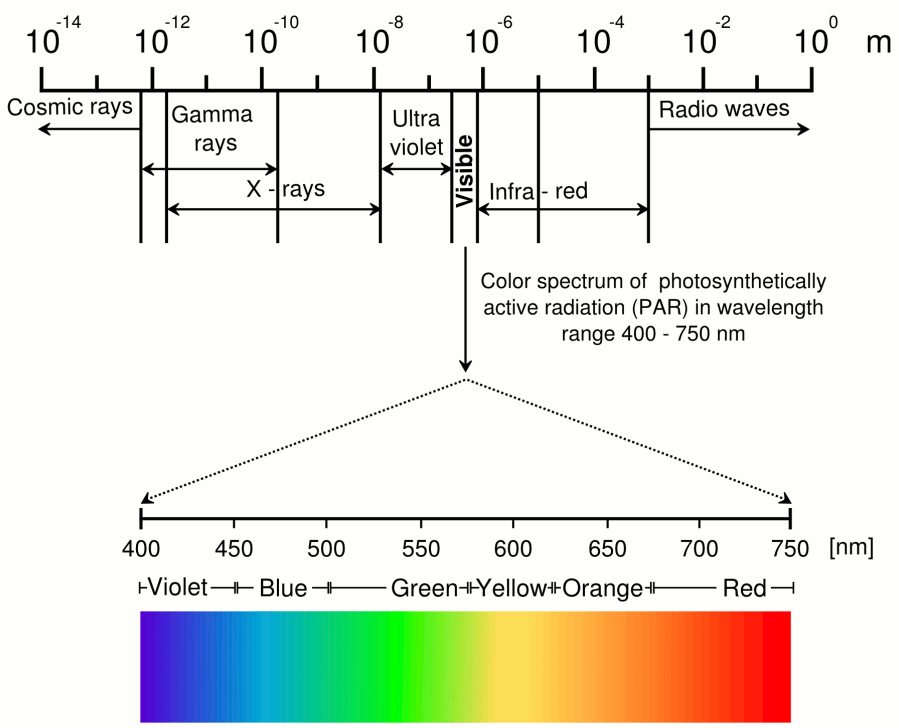

Figure 8. Spectra of electromagnetic radiation and visible light (adapted from [55]). Photosynthetically active radiation, denoted usually as PAR, ranges from 400 to 700 nm.

The shorter wavelength corresponds to mass energy of the radiation meaning violet has more energy than red light. The smallest units of irradiated light are quanta called photons which are absorbed by photosynthetic pigments. If the photon absorbed has sufficient energy to initiate charge separation and excite electron from pigment molecule such electron is transferred to the reaction centre initiating photochemistry reactions known as the Z scheme (**Fig. 9**). The Z scheme of presents chain of components involved in photosynthetic electron flow from water to $NADPH_2$. Components of the electron transport are ordered by their redox potential so that reactions go from a lower – negative redox potential to a higher – positive redox potential. As a result of illumination two electrons are separated from water molecule resulting in oxygen evolution, and transferred through Z chain to finally form one molecule of $NADPH_2$. During the process protons are pumped from stroma to intrathylakoidal lumen forming a pH gradient which drives synthesis of ATP in a reaction of photophosphorylation [55]. In total the process of electron transport with oxygen forming coupled with ATP production and NADP reduction is called photophospohorylation and has the following stoichiometry:

$$2NADP^+ + 2H_2O + 3ADP + 3P_i + 8\ photons \rightarrow 2NADPH + 3\ ATP + O_2$$

From the equation can be concluded that photosystems I and II must absorb eight photons in order to four electrons to be to extracted from H_2O and consequently passed to NADPH, one photon per electron at each photosystem reaction centre. Photosynthetic organisms use energy of eight photons of visible light for the synthesis of three molecules of ATP [6].

Photosynthetic efficiency can be calculated as a part of the solar energy absorbed by a microalgae and converted to glucose and oxygen under ideal conditions. Such efficiency of photosynthetic energy conversion can be calculated based on data of energy of process-driving photons originating from the solar irradiance and standard Gibbs free energy of

formation for oxygen and glucose as the end products of the photosynthetic process (calculation principle is adapted from [33]).

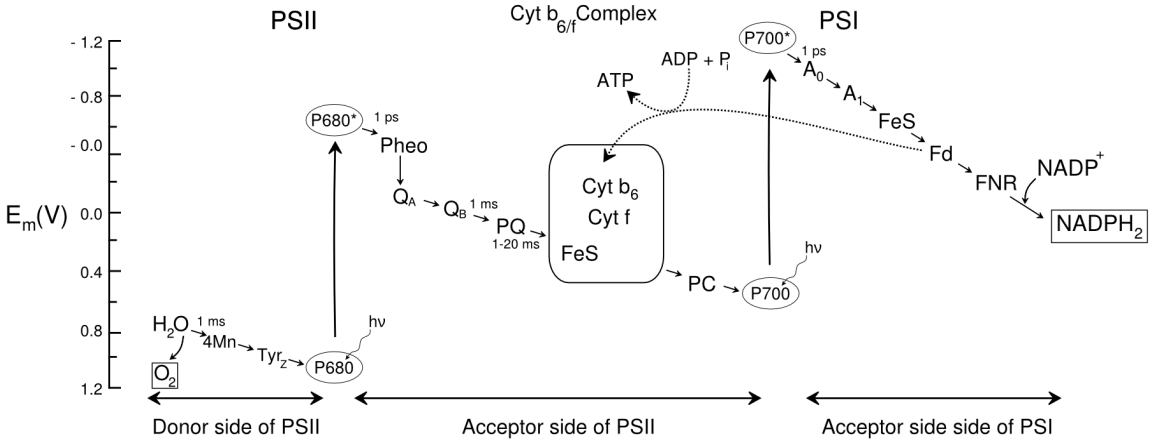

Figure 9. The Z scheme of photosynthetic electron flow from water to $NADPH_2$ [55]. Components of the electron transport are ordered by their redox potential so that reactions go from a lower – negative redox potential to a higher – positive redox potential. As a result of illumination two electrons are separated from water molecule resulting in oxygen evolution, and transferred through Z chain to finally form one molecule of $NADPH_2$.

Overall chemical equation of photosynthesis can be applied in order to calculate standard Gibbs free energy of formation for oxygen and glucose:

$$H_2O + CO_2 \rightarrow 1/6\ (C_6H_{12}O_6) + O_2$$

Standard free energy change (Gib's energy) of the overall chemical equation of photosynthesis reaction is:

$$\Delta G^{\theta} = 1/6\ \Delta_f G^{\theta}(C_6H_{12}O_6) + \Delta_f G^{\theta}(O_2) - \Delta_f G^{\theta}(H_2O) - \Delta_f G^{\theta}(CO_2)$$

$$\Delta G^{\theta} = 1/6(-914.54) + (0) - (-273.19) + (-394.38) = 479.14\ kJ\cdot mol^{-1}$$

In order to calculate photosynthetic efficiency obtained free energy change value has to be compared to energy imported by a mol of photons. As stated in previous chapter $h\cdot c\cdot\lambda^{-1}$,[J] represents photon energy at certain wavelength. If this value is multiplied with Avogadro's number, ($N_A = 6.022\cdot10^{23}\ mol^{-1}$) and quantum requirement (QR) number assuming wavelength to be at 680 nm which corresponds to PSII excitation, following equation is obtained:

$$E_{\lambda} = (QR)\cdot hc\lambda^{-1}\cdot N_A$$

representing the energy in [$kJ\cdot mol^{-1}$] of one mol of photons at 680 nm wavelength. If we assumed QR of oxygenic photosynthesis value to be 10, [33] energy of one mol of photons at 680 nm wavelength is:

$$E_{\lambda} = 1761.4\ kJ\cdot mol^{-1}$$

Finally, photosynthetic efficiency can be calculated as $(\Delta G^{\theta}\, E_{\lambda}^{-1})\cdot100$ which results in 27 % of efficiency in converting solar radiation energy to stored energy in form of glucose under ideal conditions [33].

3.4.1.2 Energy costs and efficiency of microalgae cultivation on artificial light

Energetic efficiency of artificial light sources is normally expressed in lumens per watt [lmW^{-1}], thus describing the amount of visible light produced for each watt of electricity consumed by the light source and this parameter is usually denominated luminous efficacy [25]. Light energy quanta consumed by microalgae communities for purposes of driving photosynthesis are expressed in number of photons, which when divided by Avogadro's number gives amount of photons [mol_{ph}] that comes convenient having in mind stoichiometry of photosynthetic chemical reactions. The most common artificial light sources used in microalgae biotechnology are fluorescent and white-LED with average luminous efficacy of 50-100 and 25-64 $lm \cdot W^{-1}$, respectively [25].

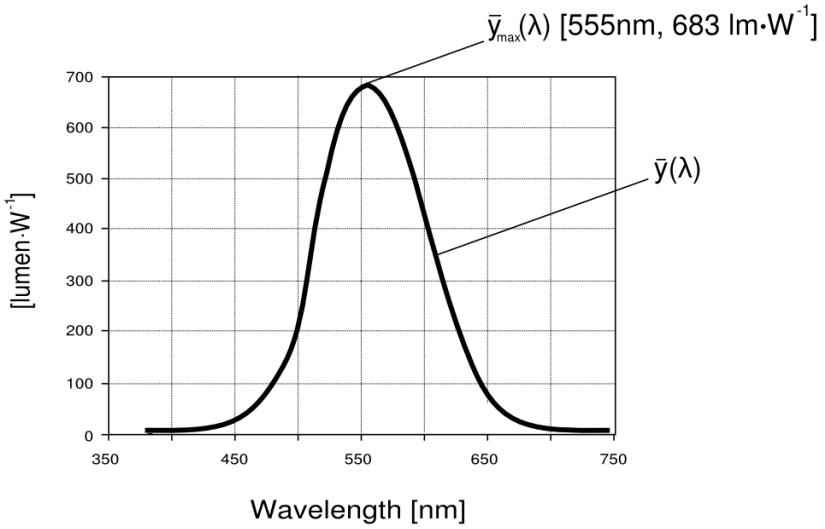

Figure 10. Standard CIE photopic luminosity function in visible spectrum [58]. It is used to convert radiant energy in Watts into visible energy expressed as luminous flux in lumens. Because it is dimensionless, in this graph the y-axis represents conversion factors values which correspond to luminosity function values (from 0 to 1.0), with a peak value of 683 $lm \cdot W^{-1}$ at 555 nm (green).

In order to convert luminous flux in lumens, as a measure of light intensity considering varying sensitivity of the human eye, to PAR efficiency, which describes the amount of photons (mol_{ph}) available for microalgae per light energy unit (W) and time (s), it is necessary to calculate the amount of photons per lumen, and both parameters depend on light wavelength [25]. Commission Internationale de l'Éclairage (CIE), is an international institution which defines CIE 1931 color space and standard photopic curve (**Fig. 10**) [25,58]. Photopic curve represents visible spectrum course of CIE luminosity function y(λ), which is dimensionless standard function used to convert radiant energy in Watts into visible energy - luminous flux in lumens, and vice versa. Luminous flux (LF in lm) is mathematically represented as an integral function calculated as a sum of luminous flux values (luminosity function y(λ) multiplied by SPD) for discrete wavelengths which are also available in tables provided by CIE for wavelengths from 380 nm to 780 nm [58]. PAR flux is mathematically represented as another integral function calculated as a sum of PAR efficiency values for discrete wavelengths from 380 nm to 780 nm or directly measured on the light source using dedicated spectrophotometer [25]. Luminous flux efficiency and PAR efficiency are consequently calculated by dividing corresponding flux with light flux (W). The key parameter which is used as conversion factor $Y_{ph/lm}$ is subsequently calculated by dividing the

two efficiencies. Consequently, PAR efficiency (PFE in $mol_{ph}W^{-1}s^{-1}$) of any artificial light source can be calculated by multiplying obtained conversion factor by luminous efficiency values of the source as declared by the producer [25].

$$LF(lm) = 683\ lmW^{-1}\int_{400}^{700} y(\lambda)SPD(\lambda)d(\lambda) = 683\ lmW^{-1}\sum_{400}^{700} y(\lambda)SPD(\lambda)\Delta\lambda$$

$$PF(mol_{ph}\cdot s^{-1}) = \int_{400}^{700} SPD(\lambda)\frac{\lambda}{N_A hc}\,d(\lambda) = \sum_{400}^{700} SPD(\lambda)\frac{\lambda}{N_A hc}\Delta\lambda$$

$$LFE(lmW^{-1}) = \frac{683\ lmW^{-1}\sum_{400}^{700} y(\lambda)SPD(\lambda)\Delta\lambda}{\sum_{400}^{700} SPD(\lambda)\Delta\lambda}$$

$$PFE(mol_{ph}\cdot s^{-1}\cdot W^{-1}) = \frac{\sum_{400}^{700} SPD(\lambda)\frac{\lambda}{N_A hc}\Delta\lambda}{\sum_{400}^{700} SPD(\lambda)\Delta\lambda}$$

$$Y_{ph\rightarrow lm}(mol_{ph}\cdot s^{-1}\,lm^{-1}) = \frac{\sum_{400}^{700} SPD(\lambda)\frac{\lambda}{N_A hc}\Delta\lambda}{683\ lmW^{-1}\sum_{400}^{700} y(\lambda)SPD(\lambda)\Delta\lambda}$$

Where used symbols represent: mol_{ph} – mol of photons; LF – luminous flux [lm]; PF – PAR flux [$mol_{ph}s^{-1}$]; LFE – luminous flux efficiency [$lm\cdot W^{-1}$]; PFE – PAR flux [$mol_{ph}s^{-1}W^{-1}$]; $Y_{ph\text{-}lm}$ – conversion factor; SPD - spectral power distribution of the radiation available as tabular value provided by CIE [$W\cdot m^{-1}$]; N_A – Avogadro's number ($6.022\ 10^{23}\ mol_{ph}^{-1}$); h – Planck constant ($6.626\ 10^{-34}$ J·s); λ – wavelength [nm]; c – speed of light in vacuum (approx. $3\cdot10^8$ $m\cdot s^{-1}$).

Supposing Cool-White LED provides luminous efficiency of 100 $lm\cdot W^{-1}$ at electric current of 1000 mA, PAR efficiency of the light source can be calculated. Assuming conversion factor $Y_{ph\text{-}lm} = 1.6\cdot10^{-2}\ \mu mol_{ph}lm^{-1}s^{-1}$, as a result of above calculations, PAR flux efficiency of the light source can be calculated:

PFE [$\mu mol_{ph}s^{-1}W^{-1}$] = $Y_{ph\text{-}lm}\cdot100\ lm\cdot W^{-1} = 1.6\ \mu mol_{ph}s^{-1}\ W^{-1}$

Based on the literature data, maximum biomass yield of microalgae per mol of light photons ($Y_{x,E}$) in the PAR range approximates 0.063 C-mol of biomass per mol of PAR photons [25]. Considering that the molecular weight of the microalgae (M_x) is approx. 24 $g\cdot C\text{-}mol^{-1}$ [59], the theoretical maximum biomass yield on light can also be expressed as:

$Y_{x,E} = 0.063\ C\text{-}mol\cdot mol_{ph}^{-1}\cdot24\ g\cdot C\text{-}mol^{-1} = 1.5$ g of the biomass of microalgae per mol of PAR photons.

Energy input from the light source can be calculated from previous three parameters:

$E_{in} = M_x(PFE\cdot Y_{x,E})^{-1} = 24\ g\cdot C\text{-}mol^{-1}(1.6\cdot10^{-6}\ mol_{ph}s^{-1}\ W^{-1}\cdot1.5\ g\cdot mol_{ph}^{-1})^{-1} = 10\ MJ\cdot C\text{-}mol^{-1}$

Assuming energy preserved in the biomass of microalgae is equal to combustion enthalpy of algae biomass ($H^C = 0.477\ MJ\cdot C\text{-}mol^{-1}$) [59] the energy from electrical input that is conserved in microalgal biomass can be calculated as $(H^C/E_{in})\cdot100$ which finally gives merely 4.8 % energy from electrical input is conserved in microalgal biomass in the most optimistic calculations setup, which leads to conclusion that for mass cultivation of biomass of microalgae destined for e.g. biodiesel production sunlight is the cheapest and most reasonable solution.

3.4.1.3 Mass cultivation of microalgae and photobioreactor design

Due to the need of large illuminated surfaces and highly diluted cultures, comparing to microbial ones, microalgal bioreactors generally have a different design than classical bioreactors used to cultivate other microorganisms. Supply, distribution and use of light in microalgal cultures are the most important issues in the design of photobioreactors. Mixing, process monitoring and control as well as aeration with oxygen/carbon dioxide mixture are other important issues to be attended [60]. Factors that can limit the microalgae mass productivity in industrial cultures are nutrient concentration, adequate turbulence of the culture, temperature and irradiation (photic volume). Mass cultivation of microalgae can be produced using one of two basic techniques: open (raceway pond system) and closed culture in photobioreactor (usually tubular) which can be further designed as external loop tubular reactor or horizontal tubular system (**Fig. 11**) [61].

In **Tab. 4** are presented cultivation techniques used for mass production of major commercial microalgae [19].

Table 4. Culture techniques of most commercial microalgae species (adapted from [19]).

Microalgal species	Product	Cultivation type
Spirulina platensis	Pigments (Phycocyanin)	Open ponds
C. vulgaris	Biomass	Open ponds, tubular photobioreactors
Dunaliella salina	Pigments (Carotenoids)	Open ponds
Haematococcus pluvialis	Pigments (Astaxanthin)	Open ponds, photobioreactors
Odontella aurita	Lipids, fatty acids	Open ponds
Porphyridium cruentum	Polysaccharides	Tubular photobioreactors
Isochrysis galbana	Lipids, fatty acids	Open ponds
Phaedactylum tricornutum	Lipids, fatty acids	Open ponds
Lyngbya majuscule	Immune modulators	Photobioreactors

Open cultures are cultivated in open air horizontal ponds (10 - 30 cm deep) of different types and sizes (l000 - 5000 m^2) with interconnected units which are paddle stirred (12-30 rpm). This technique combines agriculture features such as climate dependence, solar radiation, water, and nutrients and also the specific problems of industrial cultures such as continuous operation, nutrients supply, and pH control [62,63].

Closed cultures use photobioreactors that can control temperature and irradiation. In general, this system is composed of one or several connected tubes coupled with aeration and cells-harvesting systems. They can be placed on the floor or underwater, thereby making temperature control possible. [64,65]. Closed cultures are basically used for high-value metabolite production, because they are more expensive than open cultures. Raceway is a tubular reactor for mass production of microalgae [65]. It is an airlift reactor where the culture circulates in transparent tubes lying on the ground and interconnected by a manifold. In summer, during the day, temperature is maintained using a water spray. In winter, the temperature in the tubes rises rapidly in the morning as compared with an open raceway even if placed inside a greenhouse, thus the number of hours with optimal temperature prevails in

the culture throughout the year [63].

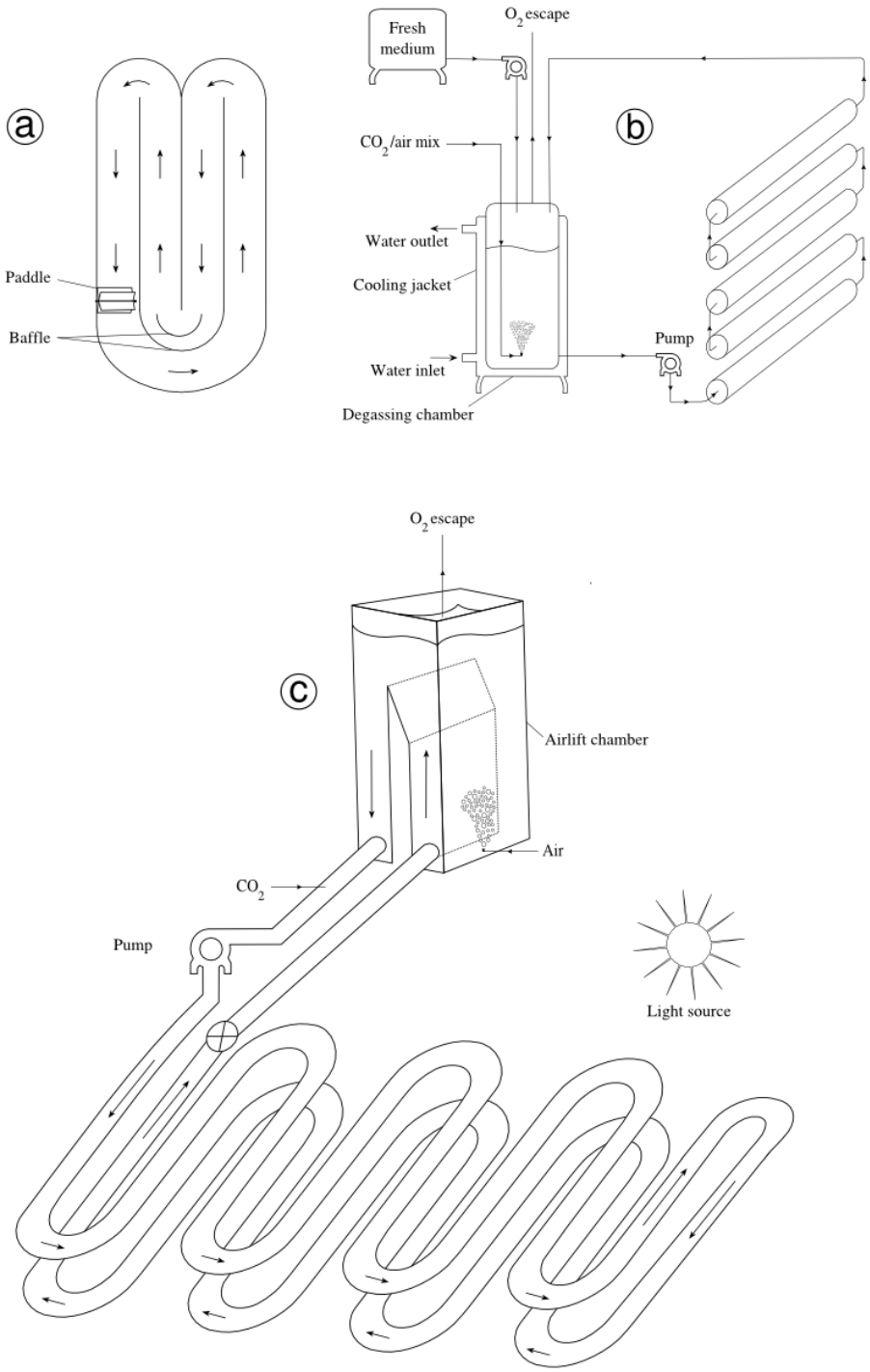

Figure 11. Three typical reactor designs, destined for mass cultivation of microalgae: raceway **(a)**; vertical tubular reactor **(b)**; and horizontal tubular reactor with external loop **(c)** (adapted from [61]).

3.4.1.4 Biomass composition of Chlorella sp. and basic nutrient requirements of culture medium used in medium formulation

The basic nutrient requirement for industrial media depends on many factors. One of them is the composition of the microbial biomass, which is summarized in **Tab. 5**.

Table 5. Approximate biomass composition of different microorganisms groups [30,66].

Component (% dry weight)	**Bacteria**	**Yeast**	**Fungi**	**Microalgae**
Carbon	48 (46-52)	48 (46-52)	50 (45-55)	51.4 – 72.6
Nitrogen	12.5 (10-14)	7.5 (6-8.5)	6 (4-7)	6.2 – 7.7
Protein	55 (50-60)	40 (35-45)	32 (25-40)	54.5 (51-58)
Carbohydrates	9 (6-15)	38 (30-45)	49 (40-55)	14.5 (12-17)
Lipids	7 (5-10)	8 (5-10)	8 (5-10)	18 (14 - 22)
Nucleic Acids	23 (15-25)	8 (5-10)	5 (2-8)	5,5 (3-8)
Ash	6 (4-10)	6 (4-10)	4 (4-10)	7
Minerals (% dry weight) – same content for all organisms				
Phosphorus	1.0 – 2.5			
Sulphur, Magnesium	0.3 -1.0			
Potassium, Sodium	0.1 -0.5			
Iron	0.01 -0.1			
Zinc, Copper, Manganese	0.001 – 0.01			

As a general rule all culture media, for industrial or laboratory use must satisfy the needs of the microorganism in carbon, nitrogen, minerals, growth factors and water. In addition they must not contain materials which inhibit culture growth.

Nitrogen is an essential constituent of all structural and functional proteins as well as nucleic acids and accounts for 7 – 10 % of cells dry weight [67]. Nitrogen sources for microalgae are nitrate and less common ammonium. When growing microalgae on nitrate, the biomass yield will be less than the obtained with ammonium, considering nitrate degree of reduction [25]. In this thesis, nitrate has been used as unique nitrogen source.

Nitrate assimilation in microalgae involves three basic steps: 1) the uptake of nitrate which seems to be mediated by a specific permease and requires metabolic energy, 2) the reduction of nitrate to ammonium which is ATP independent and is catalyzed by the successive action of nitrate reductase and nitrite reductase and 3) the incorporation of ammonium into carbon skeletons which is catalyzed by the enzymes of glutamine/glutamate cycle [63].

Table 6. Composition of M-8 medium for *C. sorokiniana* cultivation (adapted from [66])

Medium component	**Concentration, [g·L^{-1}]**	**Medium component**	**Concentration, [g·L^{-1}]**
KNO_3	3.0	$Na_2EDTA{\cdot}2H_2O$	0.04
KH_2PO_4	0.74	H_3BO_3	$6.18 \cdot 10^{-5}$
$Na_2HPO_4 \cdot 2H_2O$	0.26	$MnCl_2 \cdot 4H_2O$	$1.3 \cdot 10^{-2}$
$MgSO_4 \cdot 7H_2O$	0.4	$ZnSO_4 \cdot 7H_2O$	$3.20 \cdot 10^{-3}$
$CaCl_2 \cdot 2H_2O$	0.01	$CuSO_4 \cdot 5H_2O$	$3.2 \cdot 10^{-3}$

The most suitable medium for all experiments reported hereby is M-8 medium which have been formulated by Mandalam and Palsson [66] in order to fulfill the basic requirements for high cell density photoautotrophic *Chlorella sp.* cultures in enclosed photobioreactors (**Tab. 6**) having in mind basic elemental composition of *Chlorella* (**Tab. 7**).

Medium M-8 for *C. sorokiniana* cultivation has been widely used for production of *Chlorella b*iomass [66,68,69]. This culture medium has a high capacity to maintain long-term and large-scale *Chlorella* cultures and was used to successfully cultivate *Chlorella* for 24 days in 3 L photobioreactor [66]. This medium has also been used for *C. sorokiniana* continuous cultivation in flat panel reactor [69].

Table 7. Elemental composition of *Chlorella sp.*, (adapted from [66]).

Element	Content range , % (w/w)	Element	Content range , % (w/w)
Carbon	51.4 – 72.6	Sulphur	0.28 – 0.39
Nitrogen	11.6 – 28.5	Iron	0.04 – 0.55
Hydrogen	7.0 – 10.0	Calcium	0.005 – 0.08
Nitrogen	6.2 – 7.7	Zinc	0.0006 – 0.005
Phosphorus	1.0 -2.0	Copper	0.001 – 0.004
Potassium	0.85 – 1.62	Magnesium	0.36 -0.80

3.4.2 Selenium effect on green microalgae (Chlorophyta)

Intensive investigation of the past decades assigned selenium (Se) as an important human micronutrient with both antioxidant and chemoprotective function, able of fortifying immune system, increase male fertility and slow down ageing [70-74]. Se can be found in soil in a concentration range of 0.05 – 0.09 $mg \cdot kg^{-1}$ while in most aquatic environments its concentration is nanomolar [75]. Dissolved Se in aquatic ecosystems, usually comes from industrial and agricultural sources and circulates in environment by chemical processes and biological transformation performed by microalgal communities [76-79]. When exposed to dissolved inorganic Se, microalgae will uptake it up to certain level depending on ambient concentrations. If ambient Se concentration is above micromolar, Se uptake can result in growth rate decrease, photosynthesis inhibition and damage to the cell ultrastructure [41,42,44,47]. However, these negative effects are not observed in natural microalgae communities because water Se concentration is normally in a lower range 0.01–0.2 $\mu g \cdot L^{-1}$ (0.13–2.50 nM) [41,44,46]. As in the majority of recent publications dealing with Se, microalgae cultivated in laboratory are exposed to much higher concentrations than naturally occurring [41-49,80], study of the impact of Se on microalgae with practical emphasis on its bioaccumulation in the chemical form of Se-amino acids and proteins, with possible application as human food and animal feed supplements could lead future research to expand the potential of microalgal biotechnology and, consequently, Se-enriched biomass of microalgae production.

The study of Wrench was among the first published reports of the effect of Se focused on two marine microalgae, *Tetraselmis tetrathele* and *Dunaliella minuta* [81]. Further study treated Se effect on six unicellular marine algae including C*hlorella sp.*, *Dunaliella primolecta, Tetraselmis chuii*, two species from genus *Platymonas* as well as one red alga *Porphyridium cruentum* [82]. Bottino et al. published the study on Se-amino acids and proteins in *D. primolecta* and *P. cruentum* [83]. Bennett described Se effect on *Chlorella pyrenoidosa* cultivated continuously in bioreactor [84]. Besser et al. published paper on

separation technique of Se species from Se exposed *C. reinhardtii* [85]. Studies on Se effect on microalgae are available for unicellular calcifying marine algae (coccolithophorids) *Cricosphaera elongata* [86], *Chaetoceros calcitrans* [77] and *Emiliania huxleyi* [87,88]. Z-Y. Li et al. published an extensive study on bioeffects of Se on cyanobacteria *Spirulina platensis* [80]. Recent publications on Se effect on microalgae include studies on *C. reinhardtii* [41-44,46], *S. quadricauda* [45,47], *Dunaliellla salina* [89] as well as macroalga *Ulva sp.* [90]. Several studies about Se effect on algae from genus *Chlorella* include: metabolism of selenate to volatile compounds in *Chlorella sp.* [91], Se effect on *C. zofingiensis* with emphasis on heat-stable proteins [92], phytochelatin induction by selenate in *C. vulgaris* [93], (see **Fig. 12**).

3.4.2.1 Biological role and requirement of Se in living organisms

Se is a chemical element with atomic number of 34, atomic weight of 78.96 that occupies the position between the metal tellurium and the non-metal sulphur in Group VI of the periodic table of elements and has chemical and physical properties of both metal and non-metal (see **Fig. 13** and **Tab. 8**)[75]. In a number of lower organisms including microalgae and bacteria as well as in mammals, birds and fishes, Se is required as an essential micronutrient due to the action of selenoproteins containing Se in the form of selenocysteine (SeCys) in their active site [71, 88]. On the other hand, Se has not been found essential to yeast and land plants, as no selenoproteins are present in their proteomes [95,96]. Environmental selenium is involved in three major transformation paths: oxidation and reduction, mineralization and immobilization, and violatilization in terrestrial plants and some alga (**Fig. 14**) [78].

Se forms part of as many as 30 human selenoenzymes involved in several important metabolic pathways including immune system defence, thyroid hormone metabolism, antioxidant defence systems and reproductive performance (**Fig. 15**) [70-73]. In microalga *C. reinhardtii* it have been identified and characterized at least 12 natural selenoproteins with essential role in maintaining cell viability [95]. Humans require more than 22 mineral elements, including Se, in order to maintain health and right development, which have to be included in an appropriate diet [97]. Se in humans can act both as an essential micronutrient and toxic element depending on the ingested dose [71]. Daily Se requirements are approx. 40 μg for adults, whereas, dose of 200 $\mu g \cdot day^{-1}$ are still considered therapeutic, intake of 5 $\mu g \cdot kg \cdot day^{-1}$ is maximal permitted dose, while levels above 800 $\mu g \cdot day^{-1}$ are considered toxic [70,71,73,98,99]. The fact that toxic dose of Se for humans (800 - 1000 $\mu g \cdot kg^{-1}$) is aprox. 20 times higher than recommended daily intake dose (40 - 50 $\mu g \cdot kg^{-1}$) underlines the importance of understanding Se cycle in nature and its metabolism in living organisms. Detailed information about Se impact on human health and Se supplementation in food is abundant in literature [70-73, 99-102].

Table 8. Chemical and physical properties of elemental selenium [75,94].

Chemical/physical property	Value	Chemical/physical property	Value
Atomic number	34	Atomic radius (nm)	0.12
Atomic mass	78.96	Hardness, relative units	2
Density ($g \cdot cm^{-3}$)	4.79	Electronegativity, relative units (Li = 1)	2.4
Melting point (°C)	217	Heat of vaporization ($J \cdot g^{-1}$)	272.98
Boiling point (°C)	685.4	Thermal conductivity, W (m°C)	0.293 - 0.766

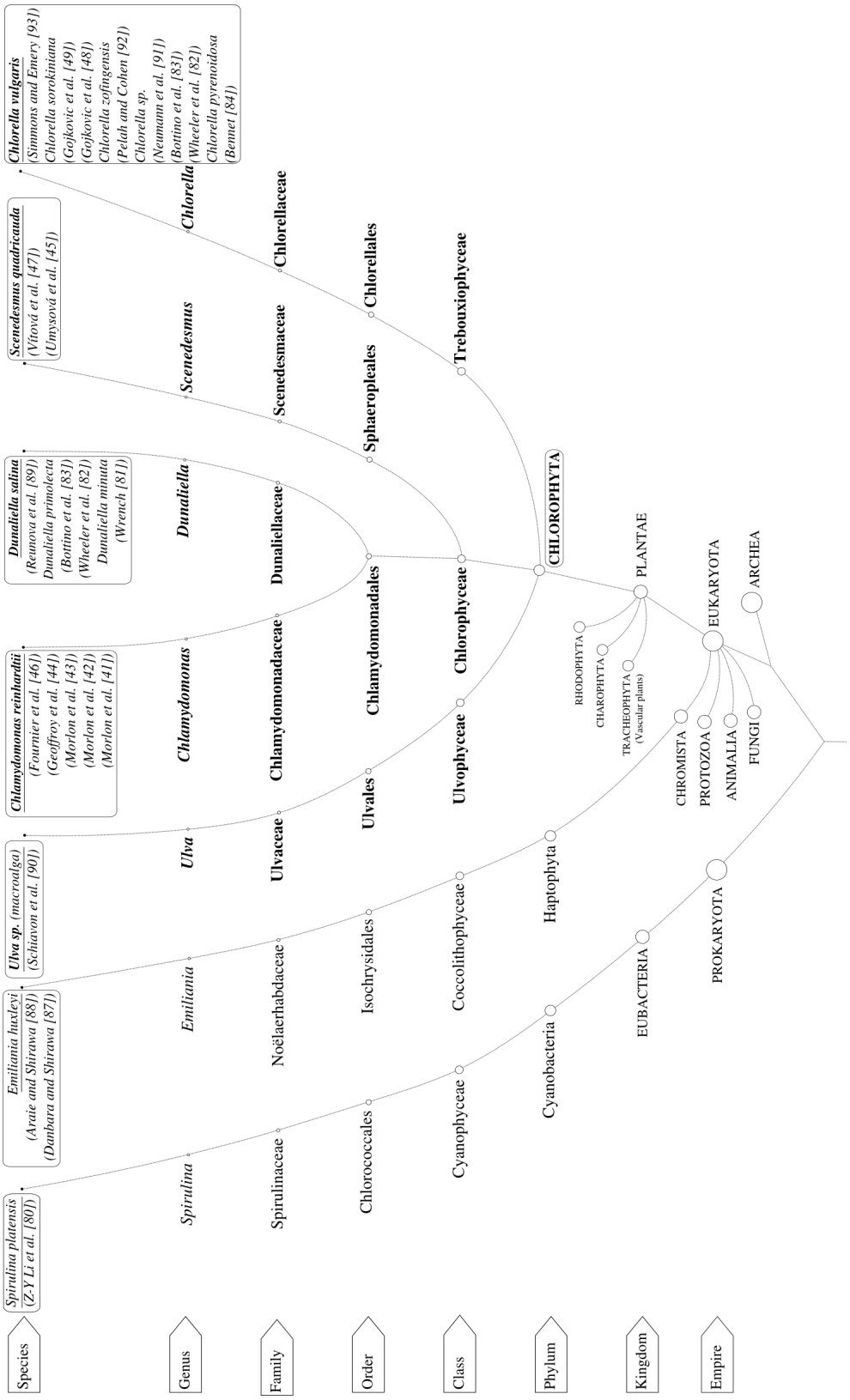

Figure 12. Schematic overview of published literature on selenium, with microalgae as the target organisms, including phylogenetic relationship within Chlorophyta (*sensu* Lewis and McCourt [37]) [26,35-37].

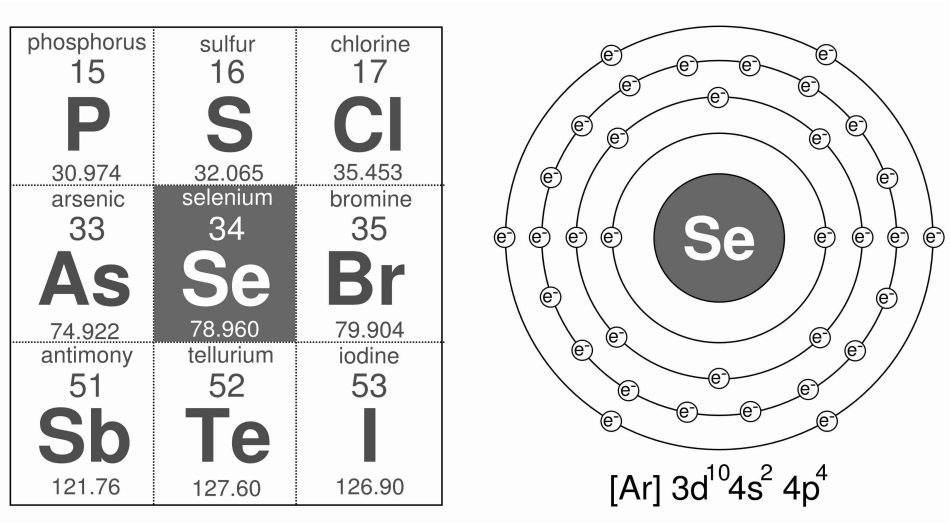

Figure 13. Position in periodic table of elements and atomic configurations of selenium. The average Se concentration in the earth's crust is in range of 0.05 to 0.09 mg·kg^{-1} [75].

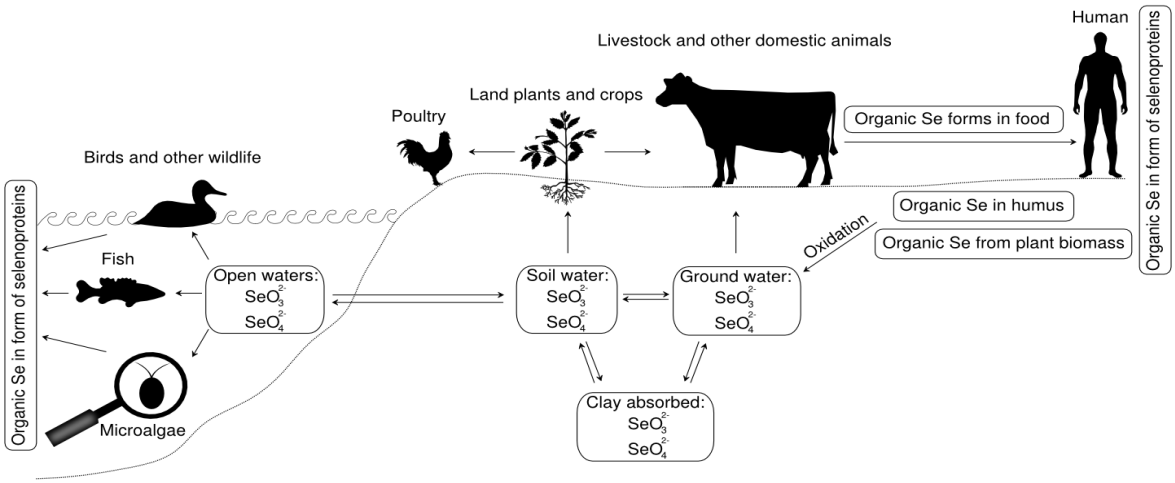

Figure 14. Selenium circulation in food-chain and ecosystem (adapted from [78]). Plant roots take up Se in Se(+IV) or Se(+VI) form from the soil water. Environmental circulation of Se between soil/water to plant and final consumer occurs via chemical transformation of different Se forms from adsorbed to dissolved state and vice-versa and via biological transformation/mineralisation of organic-bound Se to inorganic forms.

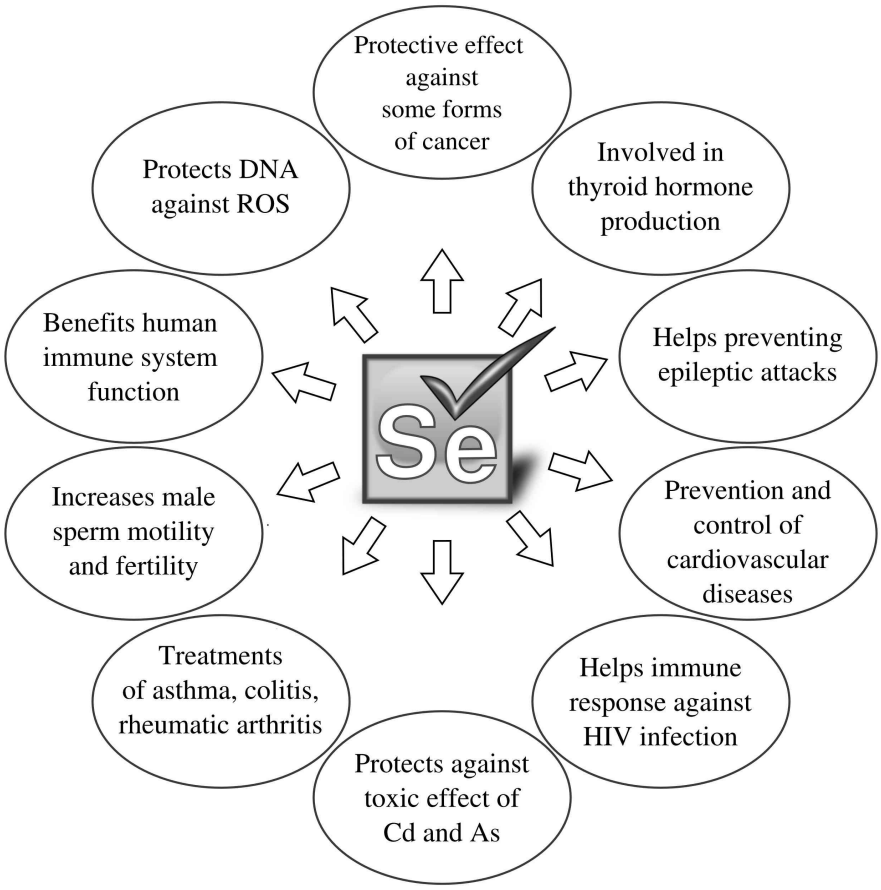

Figure 15. Selenium importance and role in human health [70-73,100].

Dietary Se levels in food are generally low in Europe. In case of inadequate supply from the diet, Se should be supplemented. In **Tab. 9** selenium levels in usual alimentary sources are presented. Natural food supplements such as Se-enriched microalga biomass that contain bioavailable organic Se forms are far more suitable and less toxic then inorganic Se salts [70-73,100].

Table 9. Average selenium content per 100 g of food in usual food sources, (adapted from [71]).

Food	Mean selenium content [µg/100 g]	Food	Mean selenium content [µg/100 g]
Milk	1.5	Kidney	145
Beef	7.6	Fish	16
Pork	14	Fruit	1
Lamb	3.8	Vegetables	2
Liver	42	Cereals	11
Bread	4.5	Brazilian nuts	254

3.4.2.2 Se uptake and metabolism in microalgae

Se can exist in four oxidative states: elemental Se (0), selenide (-2), selenite (+4), and selenate (+6) [75]. In aquatic environments Se is predominantly present in form of water soluble oxyanions - selenite (Se IV) and selenate (Se VI), which are the main Se forms available to microalgae community [43,75]. Bottino et al. proposed Se metabolic pathway based on two assumptions, which are widely accepted ever since: metabolism of Se in higher plants is analogous to that in microalgae and that Se follows sulphur metabolism to be further incorporated into amino acids and proteins [83]. Selenite and selenate are imported in microalgae by different mechanisms, which explains different levels of toxicity of these anions to microalgae cultures [45]. On the other hand, the adsorption of these Se forms to the cell wall is negligible compared to their uptake, as negatively charged functional groups at the cell surface, such as amino and carbonyl groups of structural proteins and carboxyl groups of polysaccharides, tend to repulse oxyanions, as proposed by Morlon et al. [43].

Microalgae do not reduce Se extracellularly either, as no Se forms other then selenate were detected in the culture medium of *C. reinhardtii* during the 96 h of cultivation [46]. It is believed that selenate intake by microalgae is regulated via sulphate transport system and its accumulation is directly proportional to selenate concentration and inversely proportional to sulphate concentration in culture medium [88]. On the other hand, selenite transport into *C. reinhardtii* cells is conducted by two different transporter systems, depending on its concentration in the culture medium [43]. Namely, at low concentrations (<nM) selenite is transported by specific but rapidly saturated transport system, whereas at higher concentrations uptake is conducted by a non-specific transport system and is proportional to a broad range of extracellular selenite concentrations [43]. Using a ^{75}Se isotope tracing technique, Araie and Shiraiwa [88], also identified two selenite intake mechanisms in marine calcifying microalga *Emiliania huxleyi* - an ATP-dependent active transport process with a high affinity for selenite and a passive transport process with a low affinity for selenite. In analogy to algae, both selenate and sulphate are transported across the plasma membrane of plants in roots epidermis, with uptake being driven by the high affinity transporter located exclusively in roots [103]. On the other hand, the low affinity transporters, located in leaves and roots are involved in uptake of sulphate/selenate from the soil solution into roots [103].

Upon intake selenate and selenite may share the same metabolic pathway, although exact Se metabolism is yet unknown [46]. Based on the research on Se uptake in plants and microalgae a schematic overview on Se metabolism in microalgae is proposed (**Fig. 16**).

Upon intake, both ions are gradually reduced to selenide Se^{2-} which can be further:

1) Incorporated specifically into proteins via SeCys insertion machinery [96]
2) Gradually metabolised to SeMet and SeCys

SeMet is further volatilised to dimethylselenide (DMSe) [91], or accumulated intracellularly in some microalgae [45,48,49]. It was demonstrated that *Chlorella sp.* metabolizes selenate to volatile DMSe when transferred from culture medium to water [91]. SeCys can further be methylated to Se-methylselenocysteine (SeMeSeCys) and accumulated [103].

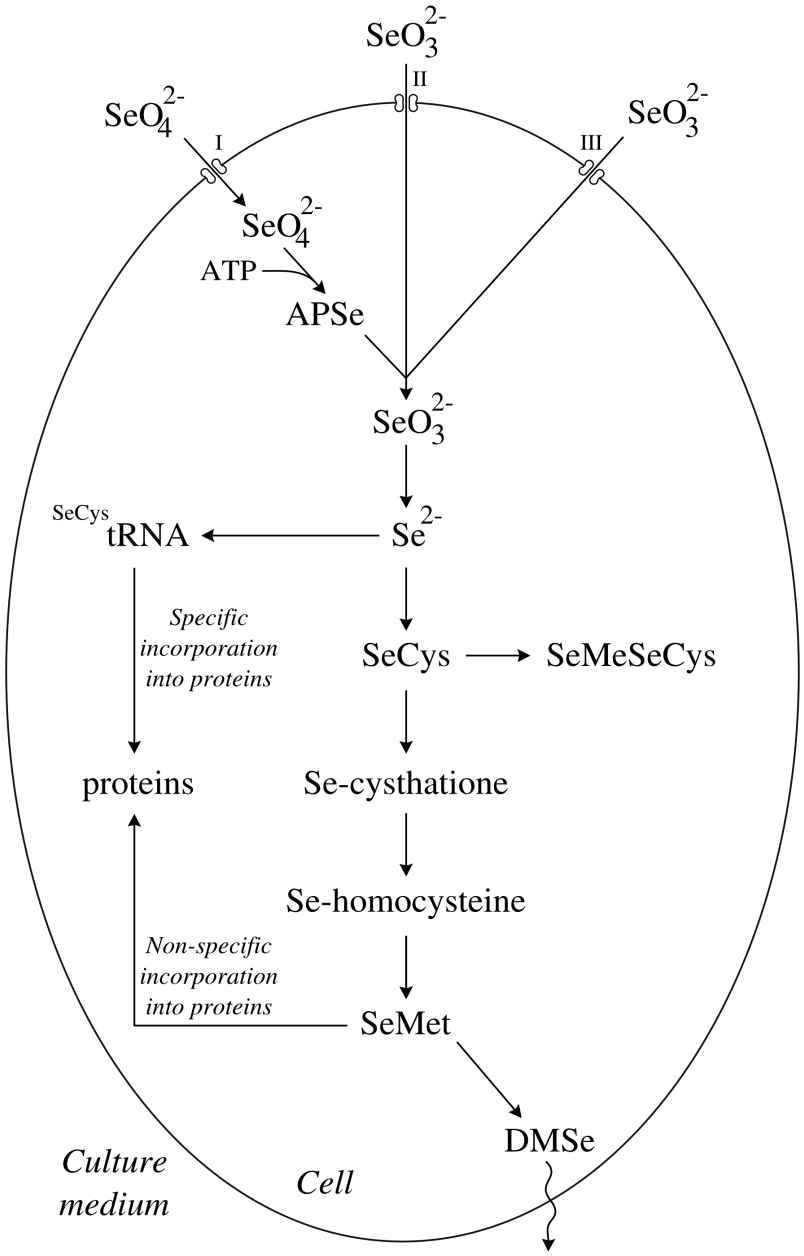

Figure 16. Schematic overview of proposed selenium metabolism in microalgae, based on published work on Se intake of plants and algae, (adapted from [78,103-106]). DMSe- dimethylselenide; ^{SeCys}tRNA – dedicated tRNA of SeCys insertion mechanism in proteins; APSe – adenosinphosphoselenate; SeMeSeCys – Se-methylselenocysteine; I – sulphate/selenate transporter; II – specific selenite transport system involved at low ambient concentrations; III – non-specific, low-affinity selenite transporter, saturated at high ambient concentrations.

4. OBJECTIVES OF THE STUDY

The aim of presented thesis was to study the use of several types of biomass to produce some valuable products.

The objective of the first experimental phase was to test selected animal sources for isolation of collagen. Following partial topics were studied:

- Optimization of isolation procedure of collagen I from several animal tissues
- Characterization of collagen by electrophoresis
- Characterization of isolated collagen by physical chemical methods – viscosimetry and ultrasonic spectroscopy
- Molecular characterization of collagen preparatives – amino acid composition, elemental composition

The objective of the second experimental phase was to study the use of biomass of microalgae as a carrier of valuable seleno-amino acids.

Following partial topics were studied:

- The impact of Se on culture parameters of microalga, was expressed as EC_{50} value
- Effect of Se on cell ultrastructure and photobiochemical performance
- Proposal of schematic overview of biochemical steps involved in the metabolism of uptaken Se
- Characterization of seleno-amino acids and seleno-proteins accumulated by *C. sorokininana* cultivated with selenate in culture medium
- Production of *C. sorokininana* biomass enriched in SeMet using photobioreactor operated in batch and continuous mode

5. MATERIALS AND METHODS

5.1 INVESTIGATION OF ANIMAL SKIN COLLAGEN PROPERTIES

Molecular weight of collagen samples, their thermal stability and denaturation temperatures, amino acid composition, trace elements content, effect of enzyme incubation on properties and protein stability were determined in scope of this research. Thermal and structural stability of collagen isolates was tested using ultrasonic spectroscopy. The denaturation temperature (T_d) was measured using viscosimetry measurements. Results were confirmed by PAGE-SDS electrophoresis and related to amino acid composition.

5.1.1 Chemicals reagents

All reagents were of analytical grade. Type I collagen from bovine achilles tendon was purchased from Sigma Company (Germany). Purified bovine collagen solution was purchased from Advanced BioMatrix (USA). Pepsin from porcine mucose was purchased from Sigma.

5.1.2 Raw materials

Raw chicken, hen, fish, turkey and pork whole parts with meat, skin and bones were purchased locally and originated from farm grown animals. Average age of animals produced by industrial farming is about 4 – 7 weeks for chicken and about 2 – 3 years for hens. Mature hen tissue was obtained from 5 years old animal from home farm to compare characteristics of collagen of different age. Skin tissue samples were extracted after filleting. Samples were placed in polyethylene bags and stored at -18 °C, until needed.

5.1.3 Isolation of skin tissue collagen

Isolation procedure was performed by modified method of Duan et al. [11]. The skins were mixed with 0.1 M NaOH at a sample/alkali solution ratio of 1:8 (w/v) to remove non-collagenous proteins. The mixture was stirred for 6 h. The alkali solution was changed every 3 h. Then the samples were washed with cold distilled water, until neutral pH of washing water was obtained. Deproteinised skins were soaked in 4,0 % detergent Triton X-100 suspended in 5% KCl, at sample/detergent solution ratio of 1:10 (w/v) overnight to extract fat, and then the samples were washed with cold distilled water repeatedly. The treated skins were cut into small pieces by scissor and extracted with 0.5 M acetic acid for 3 days with stirring. The extract was centrifuged at 14 000 rpm for 1 h. The supernatant were salted-out by adding NaCl to a final concentration of 2.5 M in the presence of 0.05 M TRIS (hydroxymethyl) aminomethane, pH 7.0. The resultant precipitate was collected by centrifuging at 12 000 rotations per minute for 30 min. All procedures were conducted below 10 °C to prevent collagen denaturation. Isolation procedure is schematically presented in (**Fig. 17**).

5.1.4 Lyophilization of isolated material

Major part of isolated skin collagen was freeze-dried at -75 °C (Lyophilizator LABCONCO, Freeze Dry Systeme/Freezone 4.5) and used in later experiments as well as the rest of raw material.

5.1.5 Hartree-Lowry assay

Total protein was determined by modified Hartree-Lowry method [107]. Absorbance was measured at 650 nm. Protein concentration in the sample was determined in [mg·mL^{-1}] from the bovine albumin calibration curve. Biuret test was performed simultaneously as a reference method.

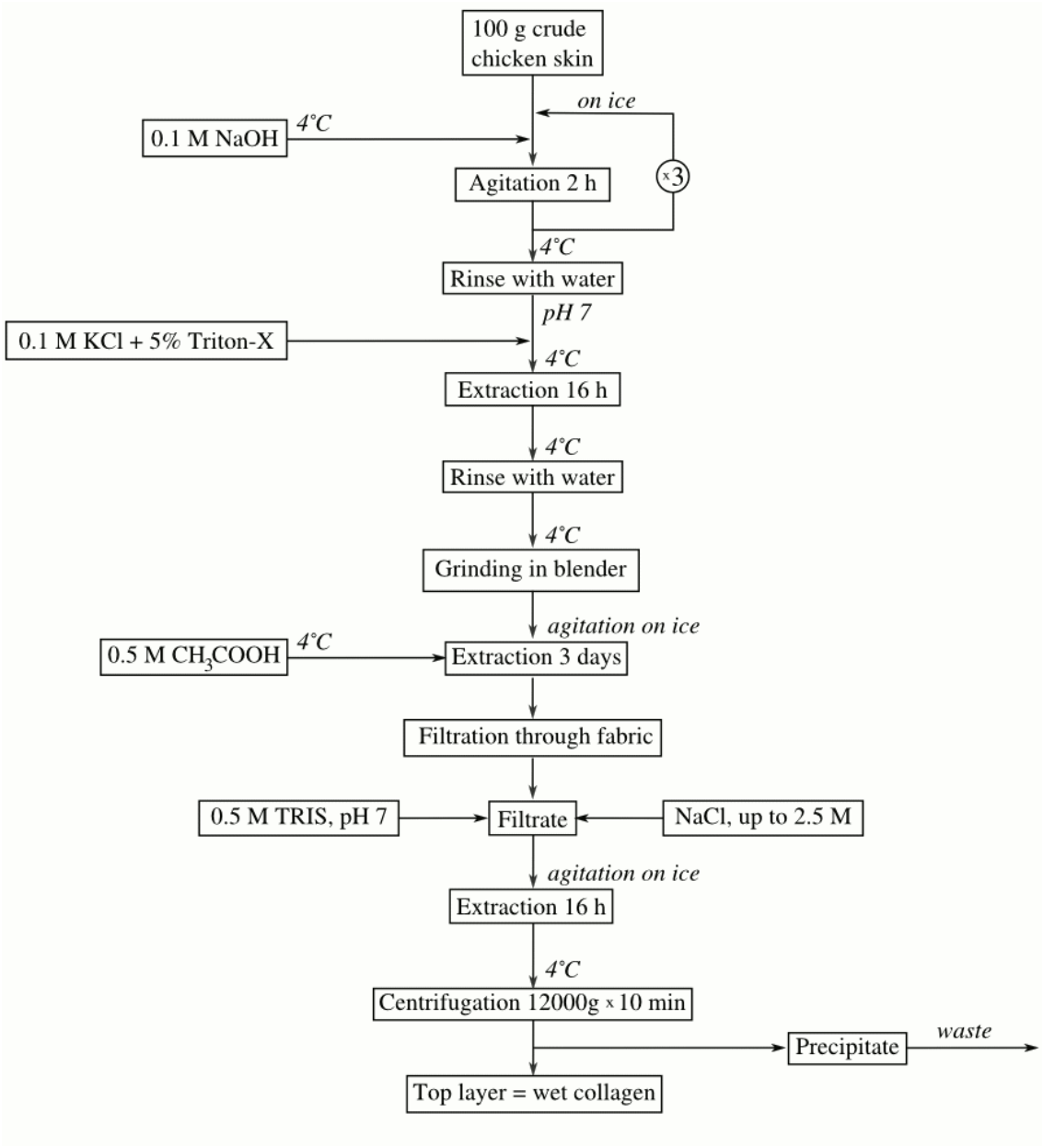

Figure 17. Scheme of animal skin collagen isolation procedure, as described by Duan et al. [11].

5.1.6 Trinitrobenzene sulfonic acid - (TNBS) assay

Quantification of the ε-amino groups of collagen isolates was carried out by a colorimetric method described by Duan et al. [11]. Same method was used to determine free amino acids levels as a part of thermal and biological stability testing. Briefly, volumes from 0.125 ml to 0.5 ml of collagen sample at concentration 0.2 $mg \cdot mL^{-1}$ was incubated with 0.5 mL of 0.1 M $NaHCO_3$ pH 8.5 and 0.25 mL of 0.01 % TNBS in 0.1 M $NaHCO_3$ solution. After 2 h at 37 °C, 0.25 mL of 100 $g \cdot L^{-1}$ sodium dodecyl sulfate (SDS) in distilled water and 0.125 mL of 1 $mol \cdot L^{-1}$ HCl were added to the reaction mixture. Absorbance was then measured at 335 nm. The number of amino groups present in the sample was directly determined from the lysine calibration curve.

5.1.7 Collagen content in isolates - hydroxyproline assay

Collagen content in isolates was determined using a colorimetric-based hydroxyproline assay according to [108]. Concentration of collagen in each isolate was analyzed in triplicate and standard deviation of 6 analysis was counted for each tissue.

5.1.8 Thermal stability testing using SDS–PAGE electrophoresis

SDS-PAGE electrophoresis was used for collagen characterization as well as for thermal stability testing. The collagen samples were dissolved in 0.1 M acetic acid and/or pepsin. Then the samples were mixed with the sample buffer (0.5 M Tris–HCl, pH 6.8 containing 5 % SDS, 20 % glycerol) at 1:2 ratio at the presence of 10 % β-mercaptoethanol. Electrophoresis was performed on 7.5 % gels. High molecular weight markers (Sigma Co, USA) were used to estimate the molecular weight of proteins. Type I collagen from bovine achilles tendon (Sigma Co, Germany) and purified bovine collagen solution (Advanced BioMatrix, USA) were used as control. Volume of 15 µl of sample was loaded in each well. Gel electrophoresis was performed in Mini Protean Tetra Cell Apparatus (Bio-Rad Laboratories, USA). All collagen samples were analyzed simultaneously under the same electrophoresis conditions. Gels were stained by Coomassie Brilliant Blue.

5.1.9 Amino acid analysis

Acid-soluble collagen samples from skin, scale and bones were hydrolyzed respectively in 6 M hydrochloric acid at 110 °C for 24 h in the absence of oxygen [11]. The hydrolyzates were analyzed on a automatic amino acid analyzer.

5.1.10 Ultrasonic spectrophotometry of collagen material

Thermal and structural stability of collagen isolates was tested using ultrasonic spectroscopy. Device used was HRUS 102 Ultrasonic Scientific, frequency was set to 11 950 kHz. One milliliter of samples were measured against deionized water. Temperature increase was 0.16 $°C \cdot min^{-1}$ and changed from 25 °C to 85 °C in 6 hours period and then cooled back to 25 °C in 3 hours period. During experiment time, samples were mechanically mixed at 600 rotations per minute.

5.1.11 Determination of denaturation temperature using viscosimetry measurements

The denaturation temperature (T_d) was measured by the method described by Duan et al. [11]. Ten ml of 0.75 % collagen solution in 0.1 M acetic acid were used for viscosity measurements in rotational rheometer (Model AR-G2 TA Instruments). Collagen solution was heated from 20 to 90 °C in two hours period. Samples from chicken, hen, mature hen and bovine collagen (as a reference) were measured at concentration of 100 $mg \cdot ml^{-1}$. Denaturation temperature was determined as the temperature on which the change in viscosity was half completed. The course of dependence of shear viscosity on temperature was monitored. Each measurement was performed in duplicate, average values of two measurement were evaluated.

5.1.12 Elemental trace analysis

Determination of certain trace elements was conducted using mass spectrometry with inductively coupled plasma (ICP-MS) on samples of chicken and hen skin and bone tissue. Previously lyophilized samples were disrupted using microwave energy. Digestion was conducted in microwave type Digestion Drying Module Milestone MLS 1200 under these conditions: 6 ml of 65% HNO_3, power 189 W, pressure 2.7 bar for 15 minutes. The ICP-MS was Thermo X-Series (with collision cell) operated under normal operating conditions [109]. Operating conditions were set as follow: forward power 1.35 kW, intermediate gas flow rate 1 $L \cdot min^{-1}$, outer gas flow rate 14 $L \cdot min^{-1}$, injector gas flow rate 0,86 $L \cdot min^{-1}$, solution delivery rate 0.8 $ml \cdot min^{-1}$, nebulizer type: Meinhard concentric, Petier cooling 5˚C, expansion stage 2.2 mbar, intermediate stage 10^{-7} bar, analyser stage $1.6 \cdot 10^{-10}$ bar, internal standard (^{115}In) 50 $\mu g \cdot L^{-1}$. Levels of Se, Pb, Sr, Zn, Hg, Cd, Co, Ni, Cr, Cu in tissues were determined.

5.2 INVESTIGATION OF *C. sorokiniana* CULTIVATION AND GROWTH WITH SELENATE

This experimental part of the thesis was performed at the laboratory of Biotechnology of Algae from the Faculty of Experimental Sciences at the University of Huelva in Spain. Experimental work was partially financed by a Spanish grant from Agrifood Campus of International Excellence (ceiA3) for foreign PhD-students.

5.2.1 Microalga and growth medium

C. sorokiniana CCAP 211/8K was obtained from the UTEX culture collection. It was maintained in modified M-8 medium [66] in Erlenmeyer flasks at 25°C and 165 $\mu mol_{ph}\ m^{-2}s^{-1}$. The culture medium was prepared as stated in chapter 3.5.4. Chemicals were purchased from Sigma-Aldrich (Germany), unless otherwise indicated. During chemostat experiments in the photobioreactor threefold concentrated medium was used to avoid nutrient limitation. In the prepared fresh medium pre-calculated amount of selenium was added in form of aqueous stock solutions of Na-selenate (Na_2SeO_4). The final concentration of selenate in fresh medium ranged from 5 $mg \cdot L^{-1}$ to 50 $mg \cdot L^{-1}$ in the first experimental phase where optimal selenate concentration for SeMet productivity and culture viability was determined. In the next

experimental phase where influence of dilution rate on SeMet productivity and culture viability was determined, selenate concentration in culture medium was fixed to 40 $mg \cdot L^{-1}$. Photobioreactor was inoculated with microalga cells in the exponential growth phase in order to obtain an initial concentration of 20 $mg \cdot L^{-1}$ of total chlorophyll. The pH was adjusted to 6.7 with concentrated solution of NaOH and controlled daily over the course of the experiment.

5.2.2 Experimental conditions for continuous cultivation experiments

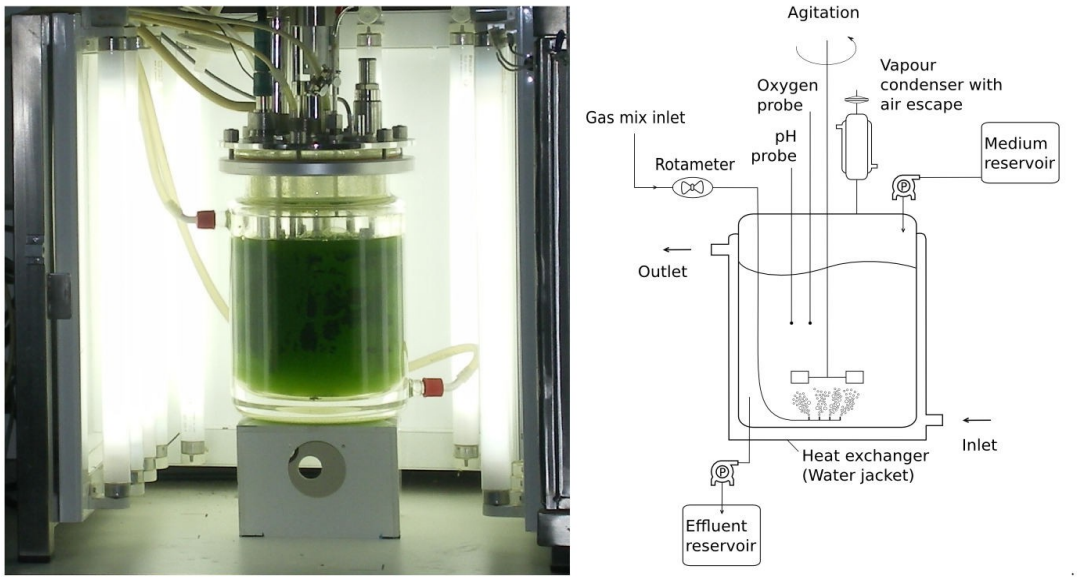

Figure 18. Commercial Applikon bioreactor used in continuous cultivation experiments: Total volume 2.2 L; Working volume 1.7 L; Photosynthetic active radiation (PAR) up to 500 $\mu mol \cdot m^{-2}s^{-1}$; pH range 6.8 - 7.2; Agitation speed 350 rpm; Aeration mix: air + 5 % CO_2; Temperature 25 °C;

Cultivation vessel used in microalga continuous cultivation experiments was commercial 2.2 L jacketed glass reactor produced by Applikon, The Netherlands (**Fig. 18**). It has inner diameter of 115 mm with average liquid height of 150 mm and working volume of 1.7 L giving a surface to volume ratio of 38 m^{-1}. It belongs to a group of the most applied reactor types in biotechnology [30]. Due to its modular design it can be used for a variety of cultivations including microbial and yeast fermentations, cell cultures and because it is made of glass and thus transparent as a cultivation vessel for photoautotrophic microorganisms. Taking in account that in microalga culture with total chlorophyll content in range of 1 to 300 $mg_{CHL} \cdot L^{-1}$ light penetration in the chlorophyll a main absorption region (600 – 700 nm wavelenght) is approximately in range of 2 to 8 mm [110] it can be calculated for a cilindrical bioreactor of 115 mm diameter with entire outer surface illuminated uniformly that a photic volume comprises from 7 % to 25 % of the total reactor volume, depending on culture chlorophyll content. Both intense aeration and mixing by mechanical stirrer minimize light limitations. Penetration depth was calculated [110] as the distance from the irradiated reactor surface where light intensity decreases tenfold (see **Fig. 19**).

The culture suspension was mixed both by mechanical stirrer at 350 rpm and bubbling air containing 5 % (v/v) CO_2, as unique carbon source through built-in gas spargler. Cultivation

vessel was placed into a cubic illumination chamber with dimensions 50 x 50 x 50 cm (W x D x H). Each side of the illumination chamber had four Philips 15 W white fluorescent lamps 9 cm apart one from another, which makes total of 16 symmetrically distributed lamps in the chamber. To ensure reactor was uniformly illuminated, it was placed on 10 cm high wooden stand so that its vertical axis of symmetry coincides with illumination chamber's vertical axis.

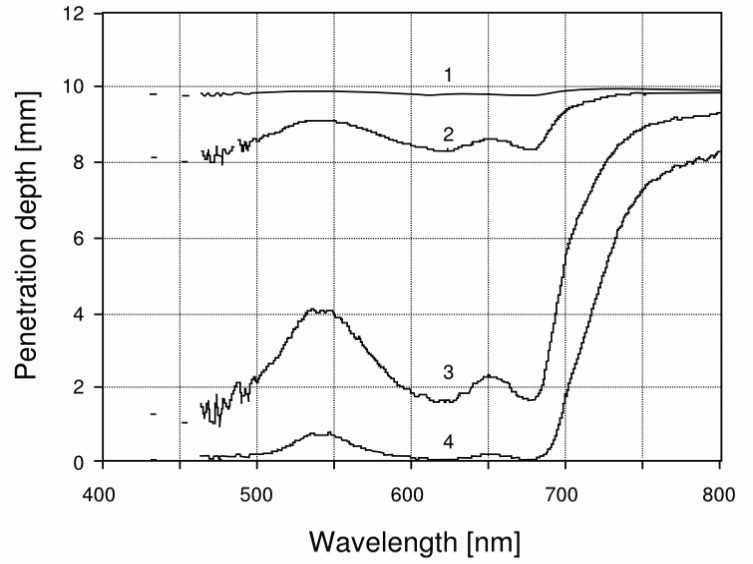

Figure 19. Penetration depth of light in the photosynthetically active radiation range, determined as the depth at which light intensity is decreases tenfold compared to incident value. Numbers 1,2,3,4 represent chlorophyll content of examined cultures of 1, 10, 100 and 300 $mg_{CHL} \cdot L^{-1}$ respectively, (adapted from [110]).

Light intensity at the reactor surface was measured with a photoradiometer Delta OHM (model HD 9021 - Italy) and expressed as a mean value of the light intensity at 16 points radially located on the reactor surface in the height of vertical axis of symmetry. The average value of the light intensity on the reactor surface was found to be 500 $\mu mol_{ph}\ m^{-2}s^{-1}$ in the PAR range (400–700 nm). Repeated equivalent measurements of light intensity for top and bottom part of the reactor had the same light intensity mean value. Cultures were grown at 25 ºC. The photobioreactor was equipped with a thermostatic water bath (Lauda, Konigshofen, Germany) connected to the 1.3 L cooling jacket keeping reactor temperature constant. Water-cooled metal condenser prevented water evaporation from the reactor. The pH and temperature inside the culture broth, were measured using reactor's Applisens sensors (Applisens, The Netherlands) connected to Applikon control modules, all together connected to computer running dedicated BioXpert virtual instrument software providing data acquisition. For chemostat experiments, two calibrated peristaltic pumps (Watson Marlow 101R, Cheltenham, UK) were used to maintain continuous cultivation. One pump provided input of fresh medium (influent) while the other pumped out culture (effluent), keeping working volume constant. The volume of fresh medium delivered to system as well as the volume of the reactor content pumped out were adjusted daily in order for reactor to operate in the steady state according to theoretical assumptions. When pump delivers fresh medium at the dilution rate lower than the maximal specific growth rate (μ_m) cell population will grow although not indefinitely because environmental changes cause growth rate to decrease [111]. If the dilution rate that is lower than the maximal specific growth rate the cells can be

maintained at a constant specific growth rate for a prolonged time called steady state [69]. While reactor operates in steady state, (also known as chemostat), the optimal biomass concentration in culture is determined by the dilution rate because the only limiting growth factor is light intensity [69]. In this condition, the specific growth rate μ equals the dilution rate D which is culture flow rate to volume ratio (μ = D) [68].

The theoretical value of the starting dilution (D_0) rate was calculated based on separate batch cultivation without any Se, from the theoretical growth rate curve during exponential growth phase using this formula:

$$\mu = (\ln N_2 - \ln N_1) \cdot (t_2 - t_1)^{-1}$$

where N_1 and N_2 represent cell numbers in two different times during culture experimental growth [111]. The number of cells was determined by microscopy Olympus CX41 in a Neubauer chamber. The experiment had two phases with two different continual cultivations performed.

Prior to continuous cultivation, a batch cultivation with a starting light intensity of 200 $\mu mol_{ph} m^{-2} s^{-1}$ was performed until a sufficient biomass density was reached. Intensity was gradually increased to 500 $\mu mol_{ph} m^{-2} s^{-1}$. As OD_{680} reached 3.2 the continuous cultivation started in absence of selenate with dilution rate D_0 value of 0.89 day^{-1}. The OD_{680} was adjusted by dilution rate change until the cell system reached steady state, which was confirmed if optical density (OD_{680}) values were constant for three consecutive times (adapted from [112]). In total, eight different Na-selenate concentrations were applied: 5, 10, 15, 20, 25, 35, 40 and 50 $mg \cdot L^{-1}$.

Based on the data obtained in the first experimental phase, 40 $mg \cdot L^{-1}$ selenate was determined as the optimal selenate concentration and applied in the next continuous cultivation. It was necessary to acclimate culture prior to continuous cultivation start, by batch cultivation that lasted two weeks at 40 $mg \cdot L^{-1}$ selenate. When OD_{680} reached 15 continuous cultivation started. Cultivations were performed in non-aseptic conditions without any contamination.

5.2.3 Biomass concentration, productivity and yield on light energy calculations

Biomass concentration inside the reactor was determined by dry weight and optical density measurements. Dry weight was determined by filtration of the culture broth over glass fiber filters with a pore size of 0.47 μm (Whatman GF/F, Kent, UK). The filter weight was determined on a 0.01 mg precision balance. Aliquots of 5 ml of culture broth, diluted 10 times with prefiltered demineralized water in order to remove balast inorganic salts, were filtered through prewashed, predried, and preweighed filters. Filters were dried at 80 °C during at least 16 h and cooled down in a dessicator for 2 hours. Dry weight, expressed as [$g \cdot L^{-1}$] of culture broth, was calculated by differential weight. Optical density was determined spectrophotometrically at 680 nm in UV/Visible spectrophotometer (Ultrospec 3100 pro, Amersham Pharmacia Biotech, Uppsala, Sweden). The dilution rate was determined on daily measurements of the effluent flow. The volumetric productivity (P_v) was expressed per total culture volume (V) in the reactor as product of the dilution rate (D) and biomass density (C_X):

$$P_v = D \cdot C_X \qquad [g \cdot L^{-1} day^{-1}];$$

The volumetric productivity was calculated during the steady state for every chemostat experiment. The efficiency of light utilization for photoautotrophic growth can be expressed in several ways. Biomass yield on light energy $Y_{x,E}$ [$g \cdot mol_{ph}^{-1}$] expressed as dry weight

produced per amount of quanta (photons) absorbed in the photosynthetic active radiation (PAR) range can be easily measured and compared to the theoretical yield. For each experiment both biomass yield and volumetric productivity were calculated during the steady state on an average of al least three measurements, unless otherwise indicated.

Biomass yield on light energy is a cultivation parameter that represents dry weight produced per amount of photons absorbed in the PAR range, expressed as [69]:

$$Y_{x,E} = 277.78 \cdot C_X \cdot \mu \cdot V \cdot PFD^{-1} \cdot A^{-1} \quad [g \cdot mol^{-1}_{ph}];$$

where: C_X represents biomass concentration [$g \cdot L^{-1}$]; μ is growth rate [h^{-1}]; V working volume [L]; A – irradiated surface [m^2]. PFD is photon flux density [$\mu mol_{ph} m^{-2} s^{-1}$]; $Y_{x,E}$ is the biomass yield on light energy [$g \cdot mol_{ph}^{-1}$]. Theoretical biomass yield on light energy can be calculated based on the stoichiometric reaction equations for the formation of biomass on carbon dioxide, water, and the nitrogen source used in the cultivation. For growth on nitrate as a sole nitrogen source theoretical biomass yield has value of 1.5 $g \cdot mol_{ph}^{-1}$ [25,69].

5.2.4 Population density, microalgae growth and statistical analysis

Population density was determined by counting the number of cells using a Neubauer chamber and light microscopy (Olympus CX41), then calculated based on equation: $N = 0.25 \cdot 10^4 \cdot (\Sigma N_i) \cdot D$; and expressed in 10^6 $cell \cdot ml^{-1}$. Where: N is population density ($cell \cdot ml^{-1}$); ΣN_i is the sum of the counted cell numbers on Neubauer chamber (i=1,2,3,4); D is applied dilution of the culture [h^{-1}].

The simplest model of exponential growth can be presented by equation: $\mu \cdot dt = dN/N$; where N is a population density [$cells \cdot ml^{-1}$]; t [h] is time; and μ [h^{-1}] is a culture growth rate which is equal to maximal growth rate ($\mu = \mu_m$) during exponential growth [84]. This equation has a solution: $N(t) = N_0 \cdot e^{\mu m \cdot t}$, where N(t) is a population density in time t, N_0 is a starting population density (t = 0), N_{max} is a maximal population density reached in indefinite time ($t = \infty$), and μ_m [h^{-1}] is the maximal growth rate [113]. To estimate Se effect on culture growth in this stufy was used more complex logistic model as it is more realistic mathematical model of microalgae growth [113]. This model uses three key parameters: initial cell density at time zero (N_0, $cell \cdot ml^{-1}$), maximal density that cell population can theoretically reach in the indefinite time (N_{max}, $cell \cdot ml^{-1}$), and the maximal culture growth rate (μ_m, h^{-1}). Logistic model gives cell density N(t) at the moment of time (t) in the equation:

$$N(t) = N_{max} \cdot N_0 \cdot (N_0 + (N_{max} - N_0) \cdot e^{-\mu t})^{-1}$$

The maximal cell density and the growth rate of selenate culture and control, were estimated using logistic curve estimation function of SPSS Statistical Package software (v.19). Model curve was fitted to mean values of population density data [114], so every model gives single maximal growth rate parameter, instead of μ_m mean value. This model was previously successfully used to describe growth kinetics of microalga in general [115] and species such as *C. reinhardtii* [41,42,46] and *Chlorella minutissima* [116].

Another important toxicity parameter - EC_{50} presents selenate concentration that results in 50 % of maximal growth rate (μ_m) inhibition in *C. sorokiniana* culture. In order to calculate EC_{50} value, maximal growth rates obtained from growth curves previously fitted to logistic model, were used to construct dose-response curve. Culture growth data for one selenate concentration are enough to fairly predict EC_{50} value, as demonstrated in work of Vítová et al. [47] for *S. cuadriculada* at 100 $mg \cdot L^{-1}$ selenate. In order to predict 50 % effect concentration (EC_{50}), growth rates data were fitted to the two parameter log-logistic model (also known as

Hill's model) using the open source software "R statistical package" [117], according to instructions on fitting a single dose-response curve [118]. The Hill model is characterized by two parameters, the Hill number (n) and the 50 % effect concentration EC_{50} and is described by the following mathematical function: $f(x) = x^n \cdot (x^n + EC_{50}^n)^{-1}$; where f(x) has value of 0.5 in case of EC_{50} [41,46]. R statistical package has been previously used by Geoffroy et al. for statistical analysis of data on selenate effect on *C. reinhardtii* [44].

5.2.5 Chlorophyll and carotenoids

The chlorophyll and carotenoids content was determined by methanol extraction and spectrophotometry. After centrifugation (5 min at 4400 rpm), biomass was mixed with methanol and the mixture was placed in an ultrasound bath for 5 min to disrupt the pellet. Subsequently, mixture was incubated at 60°C first and then cooled at 0°C to break the cells. After centrifugation, supernatant was collected and analyzed by UV/Visible spectrophotometry. Modified Arnon's equations [119] were used to calculate the chlorophyll and carotenoid concentrations in the extracts (DF - *dilution factor)*:

$$Chl_a = (16.72 \cdot A_{665} - 9.16 \cdot A_{652}) \cdot DF \quad [mg \cdot L^{-1}]$$
$$Chl_b = (34.09 \cdot A_{652} - 15.28 \cdot A_{665}) \cdot DF \quad [mg \cdot L^{-1}]$$
$$Chl_{total} = Chl_a + Chl_b \quad [mg \cdot L^{-1}]$$
$$Car_{total} = 4.52 \cdot 10^{-3} \cdot (DF \cdot 1000 \cdot A_{470} - 1.63 \cdot Chl_a - 104.96 \cdot Chl_b) \quad [mg \cdot L^{-1}]$$

The cell content of chlorophyll and carotenoids were expressed per gram of biomass, calculated based on the dry weight of the samples [120].

5.2.6 PSII Maximum quantum yield as an estimation of biomass viability

Maximum fluorescence yield (Y_{op}) was determined by pulse amplitude modulation (PAM) fluorometry with the saturating-pulse technique (**Fig. 20**). A chlorophyll fluorometer (PAM-210, Walz, Germany) was used. The samples were first adapted to dark for 15 min in order to open all reaction centers. The measuring light of 0.04 $\mu mol_{ph} m^{-2} s^{-1}$ was used to measure the zero fluorescence level (F_0). Saturating light pulse (1850 $\mu mol_{ph}\, m^{-2} s^{-1}$) was used to measure the maximum fluorescence (F_m). Then the sample was illuminated with actinic light and series of saturating pulses in order to reach steady (light-adapted) state fluorescence (F') and steady state maximum fluorescence F'_m level. Finally, the actinic light and saturating pulses were switched off to measure F'_0 level. The maximum photochemical yield and effective photochemical yield of photosystem II were calculated using equations [120-122]:

$$Y_{op} = (F_m - F_0)/F_m$$
$$\Phi_{PSII} = (F'_m - F')/F'_m$$

Both Y_{op} and Φ_{PSII} were determined in *C. sorokiniana* cultures with different selenate concentrations in medium.

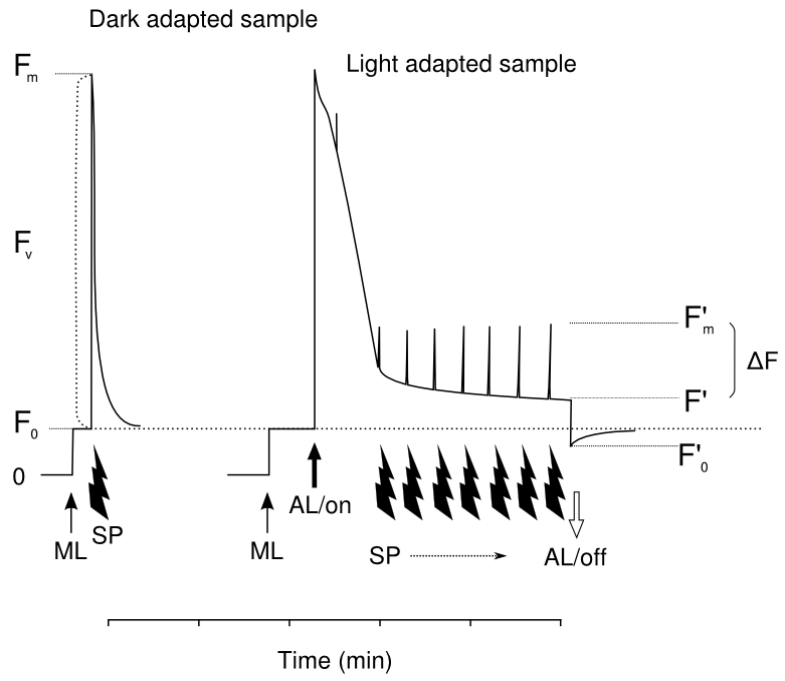

Figure 20. Pulse amplitude modulation (PAM) method schematically represented (adapted from [55]). Maximum fluorescence level (F_m) and zero fluorescence level (F_0) are measured in the dark adapted sample using modulated measuring lightand saturating light pulse. Then the sample is illuminated with actinic light and series of saturating pulses in order to reach steady (light-adapted) state fluorescence (F') and steady state maximum fluorescence F'_m level. Finally, the actinic light and saturating pulses are switched off to measure F'_0 level.

5.2.7 Cell protein isolation and fractionation with ammonium sulfate

Cultures containing 40 mg·L^{-1} as well as untreated culture, were grown in batch for 240 h. One liter of each culture was sampled on time zero, 120 h of cultivation as well as at the end of the experiment (240 h). Cells from sampled culture were collected by centrifugation (4400 rpm for 5 min) and resuspended in 20 mM phosphate buffer (pH 7) to a final concentration of 0.67 g·ml^{-1}. Cell disruption was performed on ice with an ultrasonic probe (Lab Sonic) at 40 % of power for 10 seconds, followed by a 50 second pause to avoid heat denaturation. This procedure was repeated 10 times. Extracts were centrifuged (13 000 rpm for 20 min at 4°C), cell debris was discarded and supernatant was collected. Prior to ammonium sulfate fractionation, non-protein materials were precipitated with 0.1 M streptomycin sulfate solution in phosphate buffer (pH 7). Ammonium sulfate fractionation procedure was performed using pre-calculated salt weights (**Tab. 10**) according to protocol described by Harris (**Fig. 21)** [123]. All solid fractions were resuspended in 20 mM P-buffer (pH 7) and kept frozen until electrophoresis was performed.

Table 10. Pre-calculated weights of solid ammonium sulfate to be added to a solution to give the desired final saturation at 0°C [123].

	Final concentration of ammonium sulphate [% of saturation at 0°C]																
	20	25	30	35	40	45	50	55	60	65	70	75	80	85	90	95	100
Initial concentration of ammonium sulphate																	
	Mass of solid ammonium sulphate to add to 100 ml of solution [g]																
0	10.7	13.6	16.6	19.7	22.9	26.2	29.5	33.1	36.6	40.4	44.2	48.3	52.3	56.7	61.1	65.9	70.7
5	8.0	10.9	13.9	16.8	20.0	23.2	26.6	30.0	33.6	37.3	41.1	45.0	49.1	53.3	57.8	62.4	67.1
10	5.4	8.2	11.1	14.1	17.1	20.3	23.6	27.0	30.5	34.2	37.9	41.8	45.8	50.0	54.5	58.9	63.6
15	2.6	5.5	8.3	11.3	14.3	17.4	20.7	24.0	27.5	31.0	34.8	38.6	42.6	46.6	51.0	55.5	60.0
20	0	2.7	5.6	8.4	11.5	14.5	17.7	21.0	24.4	28.0	31.6	35.4	39.2	43.3	47.6	51.9	56.5
25		0	2.7	2.7	8.5	11.7	14.8	18.2	21.4	24.8	28.4	32.1	36.0	40.1	44.2	48.5	52.9
30			0	2.8	5.7	8.7	11.9	15.0	18.4	21.7	25.3	28.9	32.8	36.7	40.8	45.1	49.5
35				0	2.8	5.8	8.8	12.0	15.3	18.7	22.1	25.8	29.5	33.4	37.4	41.6	45.9
40					0	0.9	5.9	9.0	12.2	15.5	19.0	22.5	26.2	30.0	34.0	38.1	42.4
45						0	2.9	6.0	9.1	12.5	15.8	19.3	22.9	26.7	30.6	34.7	38.8
50							0	3.0	6.1	9.3	12.7	16.1	19.7	23.3	27.2	31.2	35.3
55								0	3.0	6.2	9.4	12.9	16.3	20.0	23.8	27.7	31.7
60									0	3.1	6.3	9.6	13.1	16.6	20.4	24.2	28.3
65										0	0.1	6.4	9.8	13.4	17.0	20.8	24.7
70											0	3.2	6.6	10.0	13.6	17.3	21.2
75												0	3.2	6.7	10.2	13.9	17.6
80													0	3.3	6.8	10.4	14.1
85														0	3.4	6.9	10.6
90															0	3.4	7.1
95																0	3.5
100																	0

5.2.8 Total protein determination using Bradford protein assay

Coomassie Brilliant Blue dye forms complex with proteins to give an absorption maximum at 595 nm [124]. This simple method is sensitive down to protein concentration of 20 $\mu g \cdot ml^{-1}$. Protein concentrations were determined spectrophotometrically [125]. Twenty ml of protein sample previously dissolved in phosphate buffer (pH 7) were pipetted into 1 ml disposable Eppendorf cuvettes and 1 ml of the dye reagent was added, mixed, and incubated for 15 min at room temperature. The absorbance was measured at 595 nm. The concentration of the sample was obtained from a standard curve obtained by using known concentration of standard protein - bovine albumin (Sigma).

5.2.9 SDS–polyacrylamide gel electrophoresis (SDS–PAGE) of seleno-proteins

Protein samples were mixed with the sample buffer (0.5 M Tris–HCl, pH 6,8 containing 5 % SDS, 20 % glycerol) at 1:2 ratio at the presence of 10% β-mercaptoethanol. Electrophoresis was performed on 10 % resolving gels with 4 % stacking gels. Molecular weight marker 14.2 – 66 kDa (Sigma) was used to estimate the molecular weight of proteins. Volume of 20 µl of sample was loaded in each well containing 15 µg of proteins. Protein concentration was determined by spectrophotometry using BioRad Bradford reagent at 595 nm, with bovine serum albumin as the standard [125]. Electrophoresis run at 180 V for 75 min. Gels were washed three times with distilled water, stained with Coomassie-Blue stain for 180 min, and de-stained overnight with 10 % acetic acid /30 % ethanol aqueous solution.

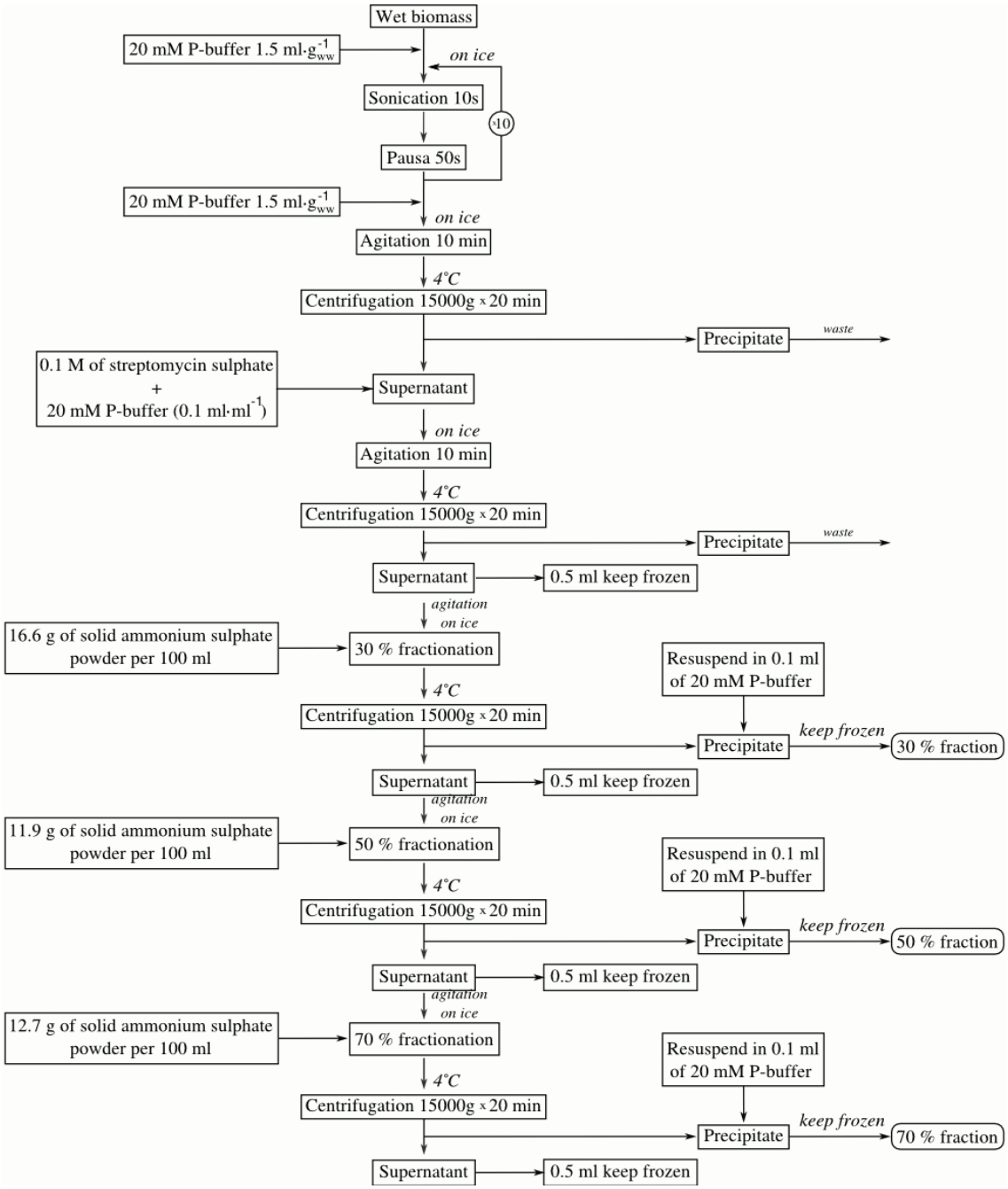

Figure 21. Scheme of protein isolation procedure from biomass of microalgae and subsequent fractionation with ammonium sulphate (as described in [123]).

5.2.10 Transmission electron microscopy (TEM)

Intracellular structure examination was performed using transmission electron microscopy (TEM). For observations in electron microscopy, cultures containing 50 mg·L^{-1} and 100 mg·L^{-1} of selenate, as well as untreated culture, were cultivated in batch for 240 h. The microalgae cells were then collected from each culture, washed with culture medium, and collected by centrifugation (2500 rpm, 5 min). The microalgae cells were fixed with 1% glutaraldehyde in 0.1 M sodium cacodylate buffer (pH 7.4) for 2 h at 4ºC. The cells were then washed three times (5 min each one) using the same buffer. The samples were fixed with 1% osmium

tetroxide in 0.2 M cacodylate buffer at 4ºC for 1 h. Samples were washed with the same buffer, dehydrated in a graded ethanol series, and embedded in Epon 812 (EMbed 812 Kit; Electron Microscopy Science, Hatfield, PA, USA). Ultrathin sections of 80–90 nm obtained by an ultramicrotome (UCT, Leica, Wetzlar, Germany) and placed on nickel grids, were stained with aqueous 1% (w⁄v) uranyl acetate and lead citrate (**Fig. 22**). Transmission electron micrographs were observed with a JEM 1011 (JEOL Ltd., Tokyo, Japan) electron microscope using an accelerating voltage of 80 kV. Several photographs of entire cells and of local detailed structures were taken at random, analyzed, and compared to investigate selenium effect in the different subcellular structures of *C. sorokiniana*. All chemicals used for histological preparation were purchased from Electron Microscopy Sciences.

5.2.11 Extraction and determination of selenium species

For the determination of selenium species the cultures of *C. sorokiniana* were centrifuged to separate the pellet. Cells were disrupted with liquid nitrogen and 20 mg of sample was weighted in a centrifuge tube, then 20 mg of Protease XIV was added. The extraction was performed with the assistance of a ultrasonic probe at 25% power during 2 minutes. After the extraction, the sample was centrifuged for 5 minutes at 6000 rpm and the supernatant was collected. Finally the supernatant was filtered through 0.45 μm and injected in the HPLC-ICP-MS. Se was measured by ICP-MS using the following operational conditions: Forward power 1500W; Sampling depth 7-8 mm; Auxiliary gas flow rate 0.10-0.15 $mLmin^{-1}$; Extract I: 0-3V; Extract II: -137,5V; Omega Bias-ce -20V; Omega Lens-ce -1.6 V; Cell entrance -40V; QP Focus -15V; Cell Exit -44V; OctP RF 190V; OctP Bias -18V; H_2 flow 3.8 $mLmin^{-1}$; QP Bias -16V; Discriminator 8 mV; Analog HV 1840V; The instrumental approach for the determination of selenium species is based on reverse phase chromatographic separation coupled to ICP-MS detection. The ^{77}Se, ^{80}Se and ^{82}Se were monitored for analysis, but only isotope ^{80}Se was used for quantification. A solution containing Li, Y, Tl and Ce (1 $\mu g \cdot L^{-1}$ each) prepared in the mobile phase was used to tune the ICP-MS for sensitivity, resolution, percentage of oxides and doubly charged ions. The chromatographic separation was performed on the basis of a previously described instrumental coupling [126,127]. Briefly: (a) when chiral species are not separated the sample is loaded in the first Rheoyne valve at the inject position which allows mobile phase flowing through the C18 column and then enter the second valve that is maintained in the load position, therefore the mobile phase get the ICP-MS detector; (b) when chiral species are separated, the chiral column is activated after SeCys and Se-MeSeCys (seleno-methylcysteine) elution (5 min), changing the valve 2 to the inject position which allows both columns to work in series, therefore L- and D-SeMet enter the chiral column where are retained. After 6.7 min, valve 2 is moved again to the load position and Se (VI) elutes from the C18 column. Finally, from 9 to 16 min, the chiral column is again activated allowing L and D-SeMet separation. The retention times for selenium species when chiral column is not activated are: 3.0 min (SeCys), 4.3 min (SeMeSeCys), 7.2 min (SeMet) and 8.3 min (Se(VI)), these values changes when two columns work in series and chiral forms are separated, as follows: 3.0 min (SeCys), 4.3 min (SeMeSeCys), 8.1 min (Se(VI), 13.8 (L-SeMet), 14.8 min (D-SeMet). Se(VI) is allowed to elute before than SeMet in the second chromatographic approach to avoid peak broadening. Chromatographic performance was checked regularly by measuring control standards to ensure a suitable separation between species and sensitivity of the method after a considerable number of samples.

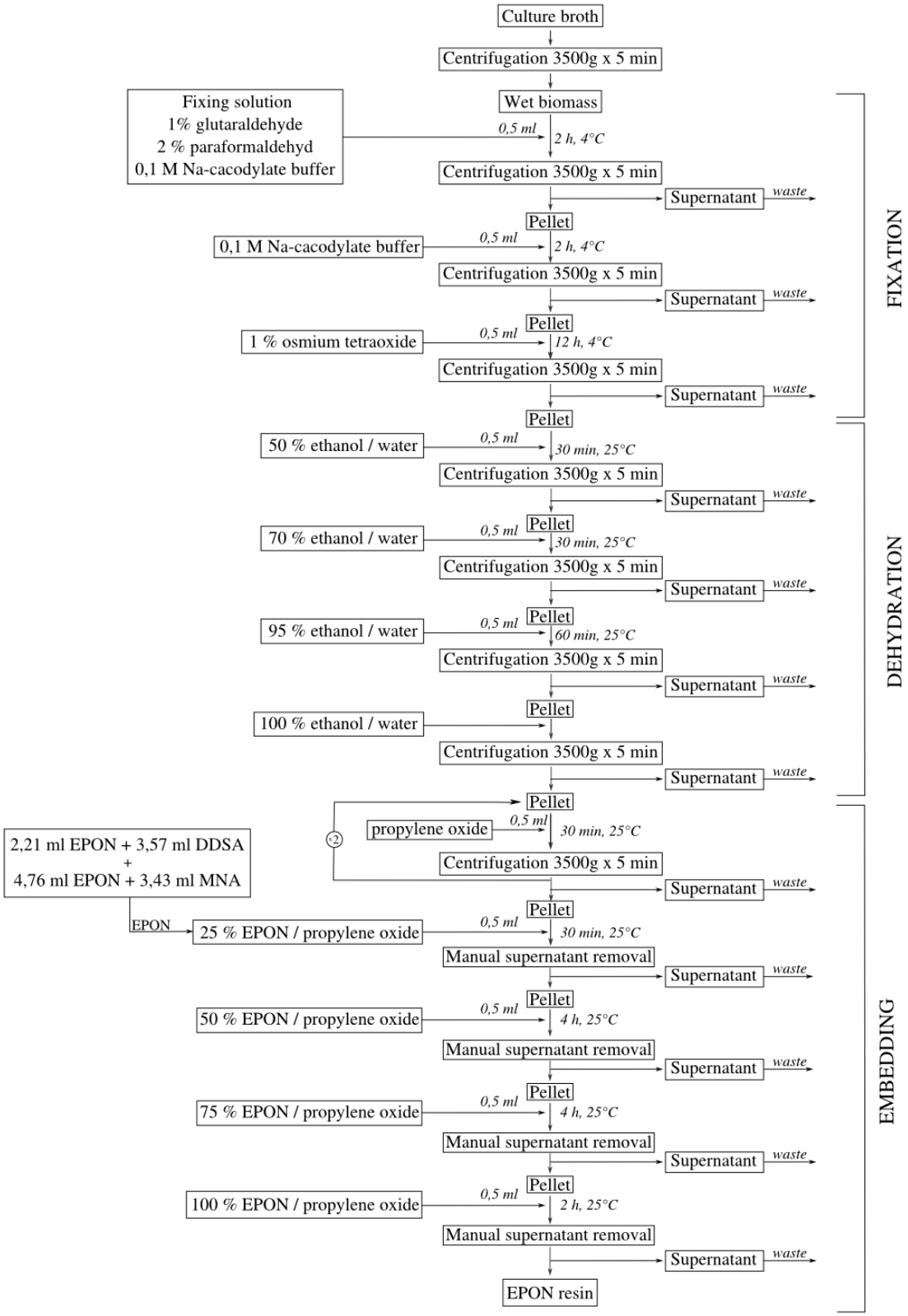

Figure 22. Scheme de TEM sample preparation using standard procedure including steps of fixation, dehydration and embedding in resin as preparation for cutting by microtome. DDSA - Dodecenyl succinic anhydrid; MNA - Nadic methyl anhydride; EPON 812 - Bisphenol/Epichlorohydrin Epoxy.

5.3 STATISTICS

Collagen from each animal tissue was isolated twice. Data of yield, water as well as total protein content (%) were evaluated as average value of these two isolation procedures. Concentration of proteins in each isolate was analyzed in triplicate and standard deviation of 6 analyses was reported for each tissue. Collagen content in isolates (determined using a hydroxyproline assay) was analyzed in triplicate and standard deviation of 6 analyses was calculated for each skin tissue. Total number of amino groups in isolates was evaluated as average value of two isolation procedures. Each measurement of denaturation temperature was performed in duplicate and average values of two measurements were calculated.

All experiments involving *C. sorokiniana* were triplicates. Mean values have been reported with standard deviations (SD). Correlations between selenate concentrations in culture medium for continuous cultivation and its effect on culture parameters were calculated with Spearman's rank correlation test. Test indicated a moderate negative linear relationship between selenate level and all measured parameters, with p value of 0.001. Statistical analyses were performed using the Statistical Package for Social Sciences, SPSS version 9.0 (SPSS Inc. USA) and open source software "R statistical package" propriety of R Development Core Team [117].

6. RESULTS AND DISCUSSION

6.1 INVESTIGATION OF ANIMAL SKIN TISSUE COLLAGEN

In this part of the thesis molecular weight of collagen samples, their thermal stability, amino acid composition and trace elements content, have been determinated. Thermal and structural stability of collagen isolates was tested using ultrasonic spectroscopy and denaturation temperature (T_d) was measured using viscosimetry measurements. Results were confirmed by PAGE-SDS electrophoresis and related to amino acid composition.

6.1.1 Collagen characterization using PAGE-SDS electrophoresis

Results of PAGE-SDS electrophoresis showed ubiquitous presence of two α chains both between 115 kDa and 130 kDa, ($\alpha_2 < \alpha_1$ with ratio $\alpha_2 : \alpha_1 = 1:2$), with visible fraction β (most probably α chains dimer) with molecular weight of 220 kDa (**Fig. 23**). These findings correspond to literature data [128]. Based on such subunits presence it was confirmed that collagens from chicken skin and all other tested animals were of type I.

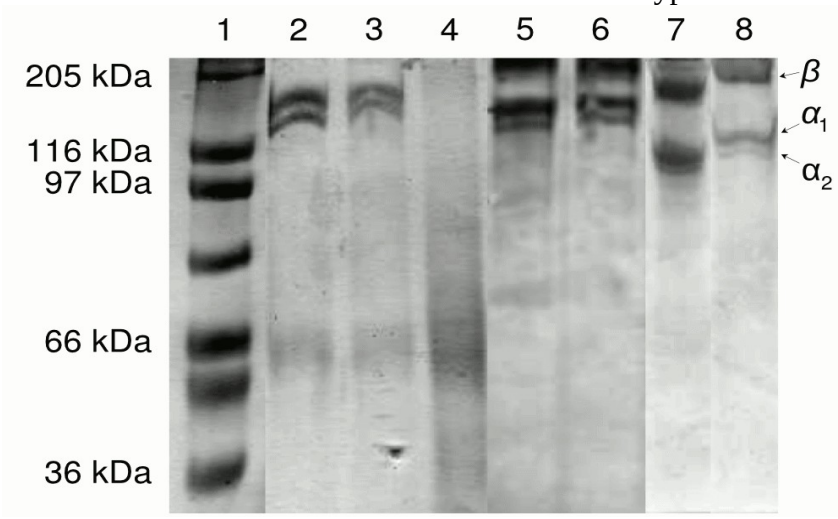

Figure 23. SDS–polyacrylamide gel electrophoresis of collagens from animal skins on 7.5 % gels (90 V, 120 mA, 4 hours). Lane 1: Sigma high molecular weight marker (36 kDa - 205 kDa); lane 2: chicken; lane 3: hen; lane 4: mature hen (5 yrs); lane 7: carp; lane 8: pork; lane 5: Purified Bovine Collagen Solution (Advanced BioMatrix, USA); lane 6: bovine collagen in 0,1 M acetic acid; lane 7: carp; lane 8: pork.

Basic properties of collagen isolates are shown in **Tab. 11**. Yield was calculated on raw isolate weight basis. Water content was determined after freeze-drying for 48 hours at -75 °C.

Highest total protein yield was obtained in chicken skin, almost 25 % while pork and fish had lower values and lowest yields were measured in case of turkey and mature hen. Chicken skin collagen had highest protein content, as well as lowest water content of all samples.

Free amino acid residues in raw collagen isolates showed highest levels in bovine and fish samples and lower content in chicken which increased with the growth of the animal. This parameter is particularly important in application of biomaterials as primary amino groups are important for molecular interactions with artificial surfaces.

Table 11. The extractability of acid soluble collagen isolated from animal skin tissues, water and total protein content.

Skin tissue	Yield (% w/w)	Water (% w/w)	Protein content (% w/w)	Protein conc. ($mg \cdot g^{-1}_{dw}$)	Collagen conc. ($mg \cdot g^{-1}_{dw}$)	Collagen purity (% of protein)	Free amino residues ($10^3 \cdot pg^{-1}_{prot.}$)
Chicken	24.25	67	27	65.6 ± 7.15	28.2 ± 1.85	40.6	2 840
Hen	10.1	73.5	26.2	26.5 ± 2.11	10.4 ± 1.02	39.1	2 890
Mature hen	7.7	68	17.4	13.4 ± 1.04	5.85 ± 0.82	43.8	3 620
Carp	21.8	65.2	19.2	41.4 ± 2.85	19.4 ± 1.58	46.8	27 695
Porkey	24.3	68.5	69.9	72.7 ± 5.16	18.2 ± 2.41	25	8 743
Turkey	7.6	80.2	27.9	21.2 ± 3.11	5.12 ± 1.11	24.1	17 512
Bovine	-	90.1	28.1	52.8	40.6	76.9	17 400

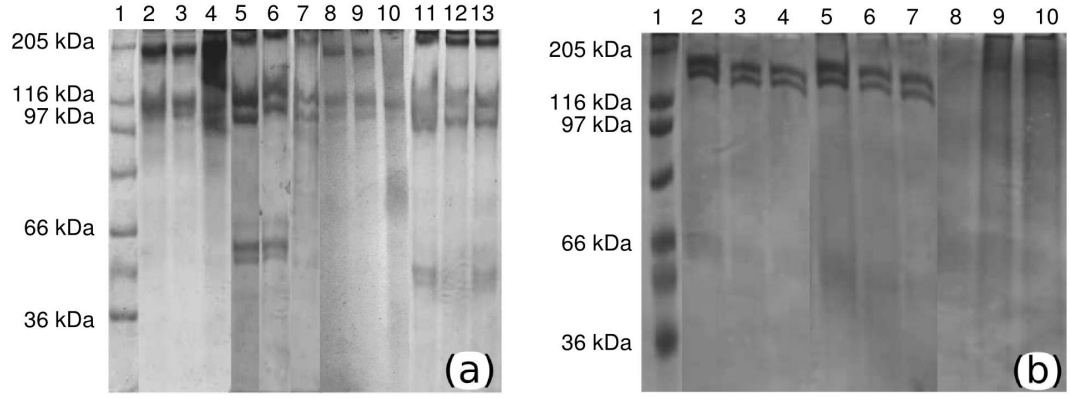

Figure 24. SDS–PAGE electrophoresis of temperature pretreated collagens from animal skins on 7,5% gels (90 V, 120 mA, 4 hours): **a)** lane 1: Sigma high molecular weight marker (36 kDa - 205 kDa) ; lane 2: fish (55 °C); lane 3: fish (60 °C); lane 4: fish (70 °C); lane 5: chicken (30 °C); lane 6: chicken (50 °C); lane 7: chicken (80 °C); lane 8: bovine (40 °C); lane 9: bovine (45 °C); lane 10: bovine (50 °C); lane 11: turkey (20 °C); lane 12: turkey (30 °C); lane 13: turkey (35 °C); **b)** lane 1: Sigma high molecular weight marker (36 kDa - 205 kDa) ; lane 2: chicken (25 °C); lane 3: chicken (40 °C); lane 4: chicken (80 °C); lane 5: hen (25 °C); lane 6: hen (40 °C); lane 7: hen (80 °C); lane 8: mature hen (5 yrs.) (25 °C); lane 9: mature hen (5 yrs.) (40 °C); lane 10: mature hen (5 yrs.) (80 °C).

Chicken collagen was stable up to 50 °C, when reaching 70 °C, denaturation (line 7a, **Fig. 24**) occurs rapidly due to triple-helix structure breakdown. Electrophoresis patterns of chicken collagen (discrete bands of native collagen) reveal that it resists higher temperatures than turkey, fish and bovine (line 10 a, **Fig. 24**). Denaturation temperature of chicken skin collagen is proved to be 30 % higher than that of carp skin collagen which is reported to be at 35 °C [128].

6.1.2 Amino acid analysis

The amino acid composition of collagen is highly specific due to its high hydroxyproline

content and to the fact that every third amino acid in triple helix is glycine. Comparing amino acid composition of particular collagen samples (**Tab. 12**) and bearing in mind amino acids with key role such as glycine, proline and lysin and total nitrogen count, the conclusion that can be made is that chicken collagen has two times higher levels of lysine than bovine, which provides thermal stability as (Lys-Gly-Y) units are energetically favorable in macromolecular structure, and are also involved in side chain interactions. On the other hand, bovine collagen has higher content of glycine and proline, which contributes to its coils rigidity and stabilize units of fibril strength (Gly-Pro-Y) [5]. Total nitrogen level in chicken is 14,29 % which is significantly lower than that obtained in bovine collagen and it corresponds with same levels obtained in carp skin [128]. In poultry samples, both proline and glycine content increased with age of the animal and the highest levels were obtained in mature hen (Pro 10,48 %, Gly 18,05 %) because age was accompanied by decrease of natural turnover of collagen molecules and higher degree of collagen cross-linking described in aging tissues [5,11,128].

Table 12. Amino acid content in collagen samples from different sources.

Amino acid code	**Amino acid content in sample ($g \cdot kg^{-1}_{material}$)**				
	Chicken skin	Hen skin	Skin of 5 yrs. old hen	Turkey	Bovine tendon
Asp	12.1	13.7	16.3	9.7	59.4
Thr	5.2	6.4	6.8	4.2	17.9
Ser	5.6	6.5	8.8	4.3	32.5
Glu	16.0	18.4	23.8	14.5	95.8
Pro	8.4 (5.88 %)	10.9 (6.8 %)	24.1 (10.48 %)	9.5	147.4 (14.98 %)
Gly	14.4 (10.07 %)	16.6 (10.41 %)	41.5 (18.05 %)	14.7	195.6 (19.88 %)
Ala	9.4	10.9	18.8	8.0	86.2
Val	6.6	7.5	7.9	4.8	24.1
Met	1.9	2.8	2.7	2.5	5.4
Iso	5.2	5.9	5.2	4.2	15.3
Leu	9.8	11.0	11.1	7.6	29.9
Tyr	3.3	4.2	3.9	3.0	4.9
Phe	5.1	5.6	6.9	3.9	19.5
His	3.4	4.0	4.2	2.4	10.8
Lys	10.1 (7.07 %)	11.7 (7.34 %)	12.1 (5.26 %)	7.5	37.4 (3.80 %)
Arg	12.6	14.2	22.3	9.2	81.8
Total nitrogen ($g \cdot kg^{-1}$)	142.9 (38.6)*	159.5	229.9	136.8	984.0 (68.9)

** amount of amino acid expressed in grams per kilogram of protein*

6.1.3 Elemental trace analysis

Trace elements content in different animal skin samples is shown in **Tab. 13**. Data of analysis shows a significant higher level of heavy metals in bone tissue than in the skin, particularly in Zn and Sr. Levels of elements depend on age of the animal. Heavy metal concentration in the hen skin is significantly higher than that obtained in chicken (Co, Ni, Cu, Se, Cd).

Table 13. Analysis of trace elements in different chicken skin samples.

Sample	Content level (in bpm of sample dry weight)								
	Cr	Co	Ni	Cu	Zn	Se	Sr	Cd	Pb
Chicken skin	946	8	127	447	2 662	197	220	3	53
Chicken bone	905	25	320	674	13 300	259	5 834	10	150
Hen skin	287	10	185	555	2 270	97	61	8	179
Hen bone	624	112	1 618	921	69 425	131	22 350	11	259
Skin of 5 yrs. old hen	922	28	502	754	3 137	212	212	83	132

6.1.4 Thermal stability testing using ultrasonic spectroscopy

Heating induces the denaturation of native proteins. These denatured proteins tend to aggregate and if aggregation is long enough, a gel is formed [129]. Ultrasonic attenuation measurement are presented in **Fig. 25** It seems that pre-aggregation occurs at lower temperatures and is indicated by a decrease in temperature interval from 20 °C to 27 °C, which is proof of disaggregation and liquefaction of samples. Signal afterwards peaks in temperature interval from 30 °C to 40 °C, with two separate consecutive peaks, except bovine where single peak appears. From 40 °C upwards second phase occurs as signal constantly increases while liquefaction process finishes and aggregation continues. In bovine this phenomenon starts at 40°C, in fish at 50°C and continues till 70 °C. When compared with electrophoresis of heat pretreated samples, obtained results confirmed that bovine collagen denaturation starts at 40 °C and finalizes at 70 °C. According to results in chicken samples actual denaturation is not visible till 50 °C, and ends at 70 °C which could explain high thermal stability of chicken collagen.

6.1.4 Determination of denaturation temperatures using viscosimetry measurements

In addition to ultrasonic spectrophotometry measurement, viscosity measurements of chicken samples were conducted (**Fig. 26, Tab. 14**). In case of bovine and chicken collagen viscosity increased until 35 °C due to samples liquefaction, afterwards it decreases till 40 °C for bovine and 50 °C for chicken, when liquefaction process ends and viscosity steeply grows. The denaturation temperature was determined as the mid-point temperature where viscosity changes reached 50 % e.g. viscosity decreased to one half of its maximum value and aggregation (in this case equivalent to denaturation) started [130]. In bovine this point would be around 40 °C, which corresponds with 37.5 °C from literature [130]. In chicken collagen this temperature is approx. 50 °C, which confirmed previous findings of its thermal stability. In hen, viscosity increased rapidly from approx. 60°C, while in mature hen there is a single viscosity increase at 78 °C, which corresponds with its total denaturation [131].

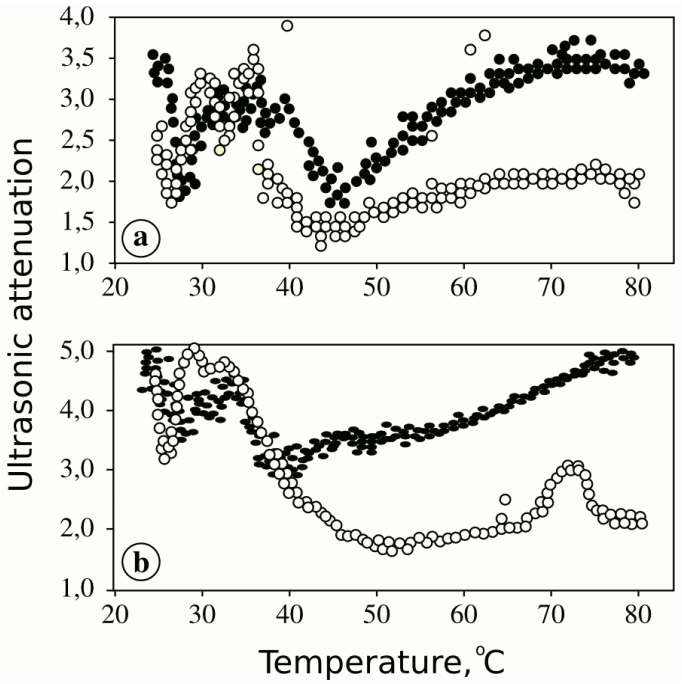

Figure 25. Ultrasonic attenuation profile in the process of thermal denaturation of collagen from: **a)** chicken (•) and turkey (◦); **b)** bovine tendon (•) and carp (◦).

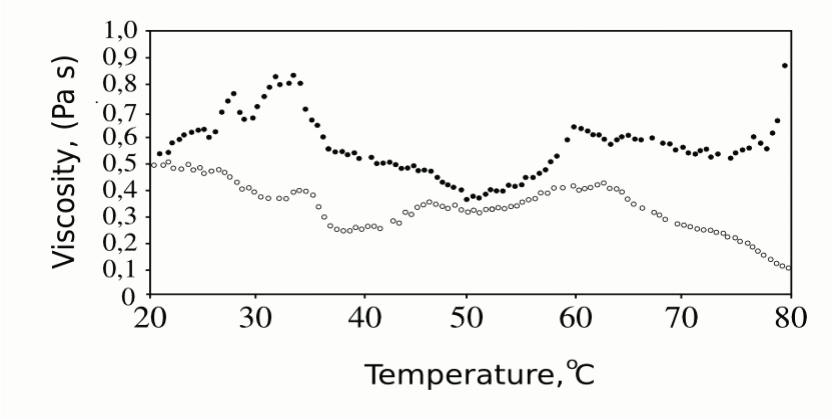

Figure 26. Dependence of shear viscosity on temperature for collagen isolated from: chicken (•) and bovine tendon (◦).

Table 14. Changes of viscosity in temperature range 20 – 90 °C in different types of collagen. Bold values represent denaturation points.

T(°C)	20	25	30	35	40	45	50	55	60	65	70	75	80	85
Skin tissue	Viscosity, Pa·s													
Chicken	0.50	0.63	0.68	0.83	0.54	0.50	**0.40**	0.50	0.65	0.58	0.56	0.88	1.92	0.05
Hen	0.47	0.55	0.66	0.52	**0.22**	0.09	0.11	0.44	0.48	0.78	1.39	1.28	1.68	2.25
Mature hen	0.51	0.50	0.38	0.52	**0.09**	0.08	0.41	0.54	0.52	0.10	3.22	0.45	0.82	2.58
Bovine	0.48	0.35	0.35	0.38	**0.24**	0.29	0.34	0.30	0.39	0.25	0.18	0.08	0.10	0.16

6.2 INVESTIGATION OF SELENATE EFFECT ON MICROALGA CULTURES VIABILITY AND SELENOMETHIONINE ACCUMULATION

6.2.1 Selenate effect and bioaccumulation in *C. sorokiniana* batch culture

Green unicellular microalga *C. sorokiniana* was selected for this second part of the experimental phase as an ideal target microorganism which is ubiquitous, has positive effects on human health and biotransforms selenate in Se-amino acids such as SeMet [132,133]. Study of the effect of selenate on *C. sorokiniana* was focused on several levels: monitoring various culture parameters and comparing results with those of unexposed cultures (control cultures); ultrastructure examination by transmission electron microscopy (TEM); isolation and identification of Se-affected proteins, and Se biotransformation to SeMet and other Se-amino acids. The objective was to investigate the production of SeMet-enriched *C. sorokiniana* biomass in batch cultures exposed to sub-lethal Se concentrations and demonstrate that SeMet-enriched biomass of microalgae production is feasible in batch systems keeping both cell viability and structural stability intact.

Experimental work was performed at the laboratory of Biotechnology of Algae from the Faculty of Experimental Sciences at the University of Huelva, Spain. Experimental work was partially financed by a Spanish grant from Agrifood Campus of International Excellence (ceiA3) for foreign PhD-students.

6.2.1.1 Effect of selenate on culture growth

In microalgae, Se toxicity is usually assessed in terms of exponential growth rate decrease often expressed in [day^{-1}] units [84]. Maximal culture growth rate (μ_m, [h^{-1}]) is a fundamental growth parameter that will decrease if any key metabolic process of the cell is affected by toxins. That makes it a relevant indicator for Se toxicity on microalgal cultures [84].

A logistic mathematical model was used to fit data of population density changes in function of time (**Fig. 27**). Correlation coefficients (R^2) of the fitted models were 0.977 for selenate exposed cultures and 0.974 for control cultures. Values of the parameters used in this model are presented in **Tab. 15**. Experimental data of cell numbers and calculated data are graphically presented in **Fig. 27**.

Table 15. Growth parameters N_{max} (10^6 cell·ml^{-1}) and μ_{max} (day^{-1}) obtained by fitting logistic model equation to experimental data of population density in function of time from selenium exposed culture and control. Model curve was fitted to mean values of population density data hence fitted models give single parameters values, instead of N_{max} and μ_m mean values ±S.D.

Selenate concentration (mg·L^{-1})	**0**	**40**
N_{max} (10^6 cell·ml^{-1})	252	145
μ_{max} (day^{-1})	1.72	1.31
Correlation coefficients (R^2)	0.977	0.974

Maximal growth rate in 40 mg·L^{-1} selenate exposed *C. sorokiniana* culture (μ_{max}=1.72 day^{-1}) accounted for 76 % of the control value, which is comparable to literature data (**Tab. 16**).

Both growth rate and maximal population density of *C. reinhardtii* decreased with increasing selenate concentrations in medium [44,46]. On the contrary, selenite in higher concentrations range did not affect *C. reinhardtii* growth rate while population density decreased [41,42].

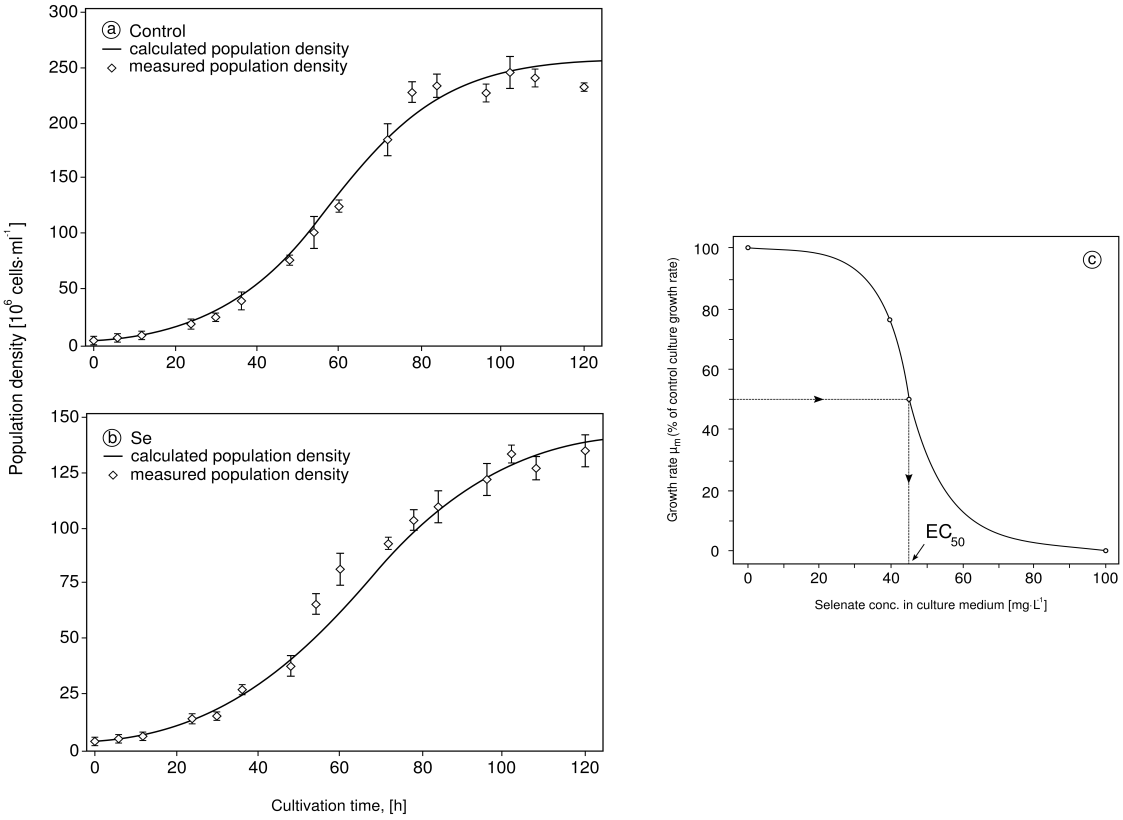

Figure 27. Growth curves of *C. sorokiniana* culture grown with 40 mg·L^{-1} of selenate **(b)**; and control culture **(a)**. Data are given as mean values ±S.D. of the means. Both experimental data of population numbers and data calculated from logistic mathematical model fit are presented**.** Concentration-response relationship between maximal growth rates from logistic growth models and selenate concentrations in medium **(c)**; Concentration-response curve was fitted to the 2 parameter log-logistic model (Hill's model) [41,46]. To predict EC_{50} presumption that concentration of 100 mg·L^{-1} selenate corresponds to the maximal (100 %) growth inhibition was made, while zero inhibition corresponds to Se free culture growth rate.

Cultivation with 10 mg·L^{-1} of selenite had no effect on growth rate of *S. quadricauda* when grown with 40 and 400 mM of sulphate in a culture medium, but at lower sulphate concentration (4 mM and 0.4 mM), growth rate of the culture progressively decreased [45]. It is obvious that with sulphur deficiency, Se toxicity in *S. quadricauda* increases, as demonstrated in other microalgae [45,46]. Microalga *S. quadricauda* cultivated with 100 mg·L^{-1} selenate had a very low growth rate and no cell division occurred, suggesting that this Se concentration was lethal to microalga [47]. Concentrations of 0.01 and 0.5 mg·L^{-1} of selenite had a stimulating effect on population density of *D. salina* [89]. On the contrary, population density of *D. salina* cultivated with 5 and 10 mg·L^{-1} of selenite decreased

compared to control, whereas upon 7 days of cultivation both cultures turned yellow with bleached chloroplasts and visible biomass precipitations, suggesting that selenite was lethal to microalga for the applied exposure time [89].

Effect concentration, (EC_{50}) is a toxicity parameter which can be used to express Se toxicity on microalgae culture representing concentration of Se resulting in 50% decrease of maximal culture growth rate (μ_m, [day^{-1}]), and is usually determined during the exponential growth phase using the dose-response curve [41,42,44,46,47]. In our experiments with *C. sorokiniana*, having in mind that 100 $mg \cdot L^{-1}$ selenate strongly inhibited cell growth and provoked severe cell deformation and death, as proven by ultrastructure microscopy, maximal (100%) growth inhibition was set for 100 $mg \cdot L^{-1}$, and the obtained EC_{50} value from the log-logistic model curve was 45 $mg \cdot L^{-1}$ (**Figure 27c**). In **Tab. 17** are presented EC_{50} values for selenate and selenite growth reduction effect on microalgae. Fournier et al. (2010) and Geoffroy et al. (2007) determined similar EC_{50} values of 3.1 and 4.5 μM respectively, for selenate and 80 μM of sulphate in *C. reinhardtii* cultures [44,46]. Corresponding EC_{50} values for selenite were 14 and 80 μM, determined using the same microorganism, culture medium and sulphate concentration [41,42]. As both values are much higher than EC_{50} values of selenate, it indicates the greater toxicity of selenate over selenite on *C. reinhardtii*. As the average levels of Se in unpolluted aquatic environments ranges from 0.01–0.2 $\mu g \cdot L^{-1}$ (0.13–2.50 nM) [41,44,46], and form 1 to 10 $\mu g \cdot L^{-1}$ (7–10 nM) [93] in contaminated areas, it was suggested, based on the obtained EC_{50} value, that selenate could affect the growth of *C. reinhardtii* in its natural habitat [46]. According to EC_{50} values, toxic effect of selenate in *S. quadricauda* culture (EC_{50} =418 μM) is comparable to our results obtained in *C. sorokiniana* (EC_{50} =238.2 μM), while *C. reinhardtii* is less resistant to this Se form (EC_{50}=0.4–4.5 μM) [44,46,47,49]. Based on EC_{50} values it can be concluded that both selenate and selenite are significantly less toxic to *S. quadricauda* and *C. sorokiniana* than to *C. reinhardtii* [41,42,46,49].

In order to obtain SeMet enriched biomass while maintaining cell viability, a sub-lethal selenate concentration of 40 $mg \cdot L^{-1}$ was used. Time-course evolution of biomass concentration and optical density for control culture and Se-added cultures are presented in **Fig. 28**. Data show that both optical density and biomass concentration decreased for about 50 % compared to control culture values, and cultures were viable up to 120 h of cultivation.

In literature, Se concentration range used in experiments varies significantly depending on microalgae species. It has been reported that *C. zofingiensis* was resistant to selenite concentrations up to 100 $mg \cdot L^{-1}$[92]. Li et al. found selenium to be an essential trace element at low concentrations, and toxic at high levels in cyanobacterium *Spirulina platensis*, for which growth was enhanced when cultivated on 0.5 to 40 $mg \cdot L^{-1}$ selenate [80].

Umysová et al. observed that most of *S. quadricauda* wild-type strain cells died within one or two days of cultivation if Se was added (both selenate and selenite forms) at concentrations higher than 50 $mg \cdot L^{-1}$[45]. Related studies on *S. quadricauda* revealed that 50 $mg \cdot L^{-1}$ selenate in medium was not lethal to microalga cultures as cells grew and divided normally [47]. In our case, a selenate concentration of 40 $mg \cdot L^{-1}$ (212 μM) in the culture medium was selected based on experiments as a sub-lethal concentration suitable for biomass enrichment in SeMet.

Table 16. Values of maximal growth rates μ_m [day^{-1}], and maximal population densities N_{max} [$10^6 cell \cdot ml^{-1}$] for Se exposed microalgal cultures. Data of Se concentration in medium that are presented bold are in originally published units.

Microalga							
Se form	Se conc. in medium		μ_m [day^{-1}]		N_{max} [$10^6 cell \cdot ml^{-1}$]		Reference
	$mg \cdot L^{-1}$	µM	Control	Se exposed	Control	Se exposed	
C. reinhardtii							
Se(IV)	0.79	**10**	2.23 ± 0.05	2.42 ± 0.19	2.05 ± 0.07	1.25 ± 0.04	[42]
	1.58	**20**		2.56 ± 0.14		0.90 ± 0.04	
	2.37	**30**		2.48 ± 0.30		0.38 ± 0.10	
	3.16	**40**		2.64 ± 0.00		0.42 ± 0.13	
	3.95	**50**		2.64 ± 0.00		0.55 ± 0.10	
Se(IV)	0.79	**10**	2.35 ± 0.03	2.53 ± 0.01	2.21 ± 0.06	1.98 ± 0.05	[41]
	3.95	**50**		2.79 ± 0.04		1.42 ± 0.08	
	7.9	**100**		2.86 ± 0.11		0.93 ± 0.02	
	39.5	**500**		2.68 ± 0.04		0.22 ± 0.06	
Se(VI)	$7.9 \cdot 10^{-3}$	**0.1**	2.04 ± 0.08 (8 µM SO_4^{2-})	2.05 ± 0.05	1.58 ± 0.51	1.67 ± 0.03	[46]
	$4.7 \cdot 10^{-2}$	**0.6**		1.62 ± 0.18		0.4 ± 0.14	
	0.2	**2.5**		1.65 ± 0.32		0.04 ± 0.002	
	0.2	**2.5**	2.14 ± 0.24 (80 µM SO_4^{2-})	2.06 ± 0.15	1.35 ± 0.54	0.78 ± 0.08	
	0.47	**6**		2.05 ± 0.14		0.40 ± 0.04	
	0.91	**11.5**		2.03 ± 0.11		0.14 ± 0.01	
C. sorokiniana							
Se(VI)	**40**	212	1.72	1.31	252	145	[49]
C. pyrenoidosa							
Se(VI)	**0.53**	6.71	1.76 ± 0.024	1.46 ± 0.024	1.64 ± 0.10	1.32 ± 0.12	[84]
	0.90	11.4		0.60 ± 0.024		0.97 ± 0.04	
	1.37	17.3		0.29 ± 0.024		0.98 ± 0.11	
	1.41	17.9		0.94 ± 0.024		1.48 ± 0.03	

Table 17. Published values of EC_{50} parameter, (Se concentration at which 50% of the maximum growth inhibition effect was observed), in [μM], for Se exposed microalgae. Part of the table adapted from [47].

Microalga					
Se form	**EC_{50}, [μM]**	**Reference**	**Se form**	**EC_{50}, [μM]**	**Reference**
S. quadricauda			*C. reinhardtii*		
Se(IV)	50	[47]	Se(VI)	3.1	[46]
	64	[79]		0.4	[46]
Se(VI)	418	[47]	*C. sorokiniana*		
C. reinhardtii			Se(VI)	238.2	[49]
Se(IV)	80	[41]	*C. pyrenoidosa*		
	14	[42]	Se(VI)	10	[84]

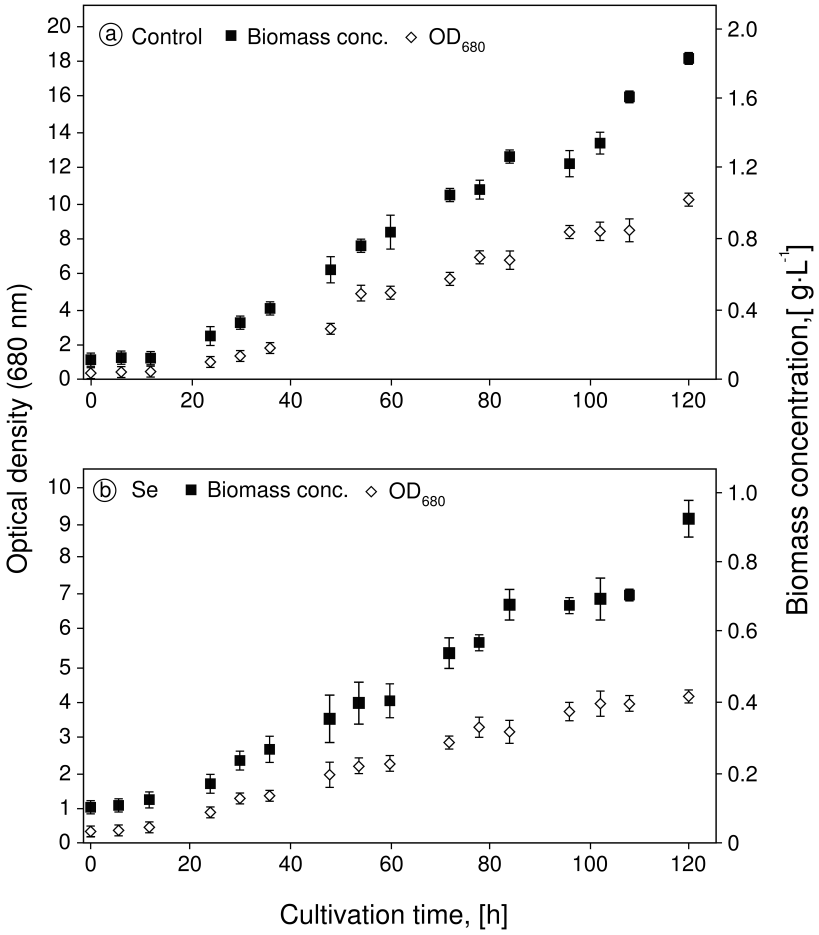

Figure 28. The optical density and biomass concentration of *C. sorokiniana* as a function of cultivation time for: **(a)** control (no selenate); **(b)** culture with 40 $mg \cdot L^{-1}$ of selenate in culture medium. Data are given as mean values ± S.D. of the means.

6.2.1.3 *Se effect on the cell ultrastructure*

Electron microscopy studies on the ultrastructure of C. sorokiniana were carried out at the end of the experiment. **Fig. 29** shows longitudinal and cross-sections through control cells (Se-free culture). This alga is about 3 µm length and 2 µm wide. The nucleus is about 1 µm length and 1µm wide located in the central portion of the microalga. The cell has a prominent cup-shaped chloroplast that partially surrounds the nucleus, and the thylakoids inside are compressed and very dense which makes them indistinguishable.

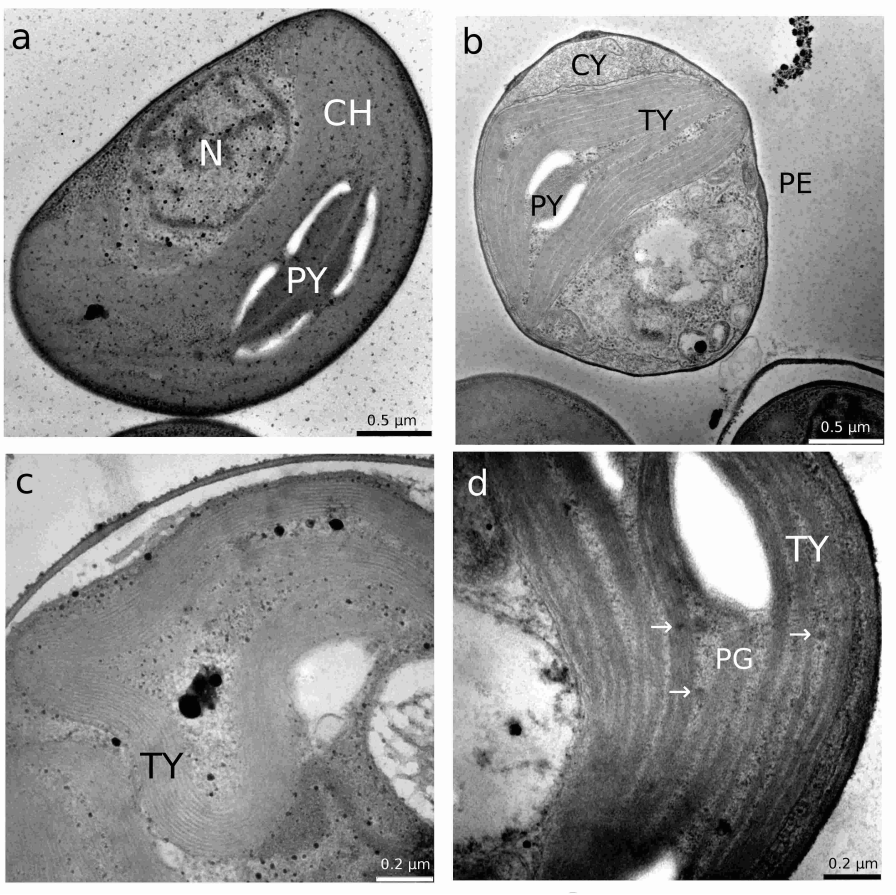

Figure 29. Ultrastructure images made by transmission electron microscopy of: Se-free single cell (**a**); and cell exposed to 40 mg·L^{-1} selenate (**b**); fingerprint-like thylakoids (**c**) and plastoglobules (indicated by arrows) (**d**) in cell exposed to 100 mg·L^{-1} selenate; Abbreviations: CH chloroplast; CY cytoplasm; CW cell wall; N nucleus; PE periplasm; PG plastoglobules; PY pyrenoid; TY thylakoids; VA autophagic vacuole; V vacuole.

The pyrenoid (PY) is surrounded by four layers of starch. At 40 and 100 mg·L^{-1} of selenate in the culture medium, the stroma of the chloroplast became granule and less dense, and the thylakoids had a fingerprint-like appearance (**Fig. 29b**,**c**). Fingerprint-like appearance of the chloroplast in Se-exposed microalga cultures was previously observed and reported in related literature [44,47]. Analysis of chloroplast ultrastructure by electron microscopy in cultures incubated with selenate 40 and 100 mg·L^{-1}, revealed the presence of lipoprotein particles called “plastoglobules” in the stroma of chloroplasts that appeared as small black globules in close proximity to thylakoids (**Fig. 29b**,**d**). Plastoglobules are involved in stress responses.

Several studies have reported their presence in chloroplasts from plants grown under diverse stress conditions [134,135]. Plastoglobules observed in cells treated with Se (**Fig. 30a**), are plastid-localized lipoprotein particles that contain tocopherols and other lipid isoprenoid derived metabolites of commercial value, as well as structural proteins [136,137]. In addition to vascular plants, plastoglobules are found in non-vascular species such as moss [138] and algae [139]. At the highest Se concentration added to the culture medium (100 $mg \cdot L^{-1}$), some of the Se-exposed cells had large vacuoles (V) (**Fig. 30b**) indicating a process of autophagy, a housekeeping mechanism, in which damaged or unwanted cellular components get degraded in vacuoles.

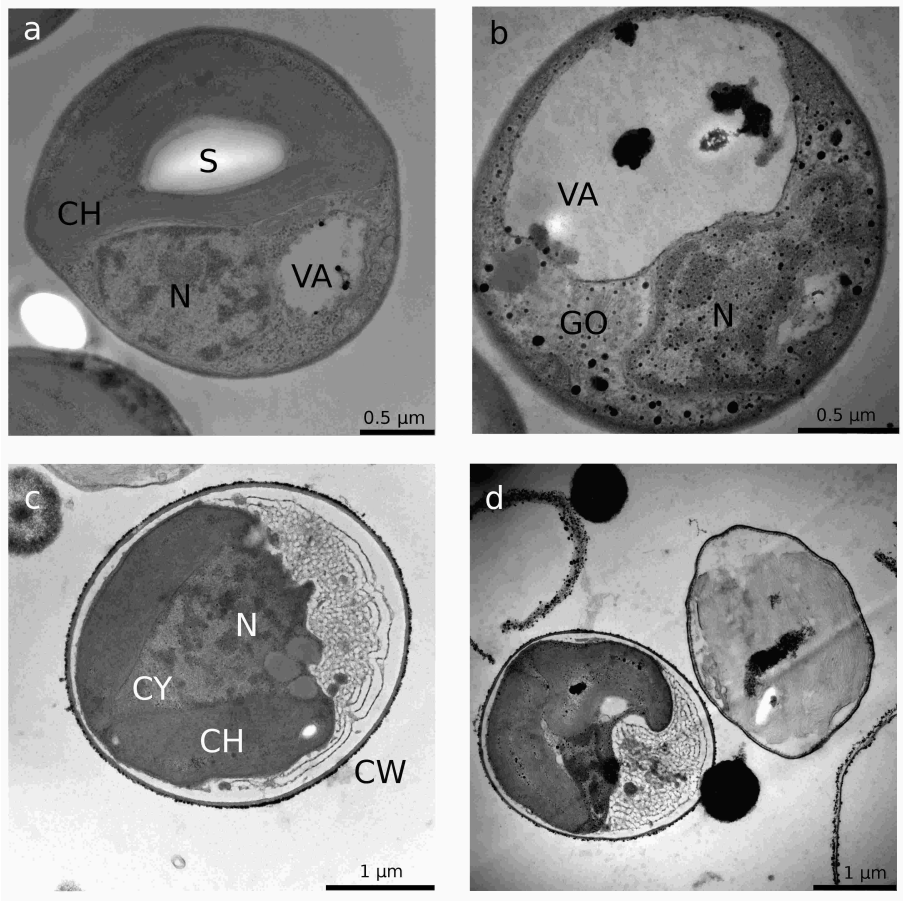

Figure 30. Ultrastructure images made by transmission electron microscopy of: autophagy in cell exposed to 40 $mg \cdot L^{-1}$ selenate (**a,b**); necrotic cell (**c**) and pair of cell in different stages of necrosis (**d**). Abbreviations: CH chloroplast; CY cytoplasm; CW cell wall; N nucleus; PE periplasm; PG plastoglobules; PY pyrenoid; TY thylakoids; VA autophagic vacuole; V vacuole.

Autophagic vacuole (VA) and its compounds get recycled [140]. Structure of the cells exposed to 100 $mg \cdot L^{-1}$ became severely disrupted and normal cell organelles were often hardly distinguishable at the end of the experiment. Therefore, from the results in can be inferred that 100 $mg \cdot L^{-1}$ selenate, or higher concentrations, are not compatible with cell viability.

Ultrastructural damages to the chloroplast of *C. reinhardtii* have been observed at selenite concentrations above 50 µM in culture medium, and involved granular and less dense stroma, thylakoids with a fingerprint-like appearance and increased number of starch grains [41]. In

culture exposed to 500 μM of selenite starch nodules occupied most of the cell volume, cell structures were severely disrupted and normal cell organelles were indistinguishable [41]. In *C. reinhardtii* exposed to 9.3 μM of selenate, ultrastructural damage to the chloroplast was almost identical to damage after selenite exposure in [41] - granular, dense cytosol, granular and less dense stroma, and the thylakoids with a fingerprint-like appearance with reduction of stacked thylakoid membrane domains, but without increase in starch accumulation [44]. Exposure of *S. quadricauda* to 50 $mg \cdot L^{-1}$ selenite, had similar ultrastructural effects as in *C. reinhardtii* [41], resulting in the chloroplast with typical fingerprint-like appearance, less dense stroma and increased starch production [47]. Authors suggested that starch overproduction during Se exposure in microalgae could be caused by retardation of cell division since starch serves as energy reserve for cell division and maintenance during the dark period [47]. Exposure to 100 $mg \cdot L^{-1}$ of Se in *S. quadricauda* caused bleaching of chloroplasts, cell malformations, and abnormal spine number and position [45,47]. Ultrastructural damage to the *Dunaliella salina* cultivated with 5 and 10 $mg \cdot L^{-1}$ selenite in culture medium included structural alterations to the chloroplasts and mitochondria with chloroplast lacking thylakoids, mitochondria with signs of destruction, vacuoles with autophagic activity [140], fusion of vacuoles and a number of completely destroyed cells [89].

6.2.1.2 *Effects of selenate on photosynthesis and pigment production*

Chlorophyll fluorescence measurement is used as an economic and sensitive method for rapid detection of photoinhibition on microalgae cultures [121,122]. In **Fig. 31** can be observed that for *C. sorokiniana* cultures, 40 $mg \cdot L^{-1}$ (212 μM) of selenate affected maximum quantum yield of PSII (Y_{op}). Even though Y_{op} for Se-exposed cultures was approx. 20% lower than those obtained in control culture, the Y_{op} was within the typical range for microalgae cells, therefore cultures were accordingly considered viable throughout the experiment [55]. During the first 24 h of cultivation, values of Y_{op} for Se-exposed and control cultures decreased in approx. 15 and 10 % , respectively, compared to initial values, due to culture adaptation phase. Nevertheless, this decrease was only temporary and Y_{op} values stabilized after 24 h.

During the experiment, effective photochemical yield (Φ_{PSII}) values for control remained within the 0.33 - 0.42 range, while Φ_{PSII} of Se-exposed cultures remained within the 0.27 - 0.34 range (**Fig. 31b**). Throughout the experiment, 25 % decrease in Φ_{PSII} was found for Se-exposed cultures compared to control cultures.

Geoffroy et al. reported a decrease of 22 % in Y_{op} after 24 h of cultivation of *C. reinhardtii* cells growing in 9.3 μM of selenite [44]. After 96 h the decrease was 66 % compared to control culture values. Effective photochemical yield (Φ_{PSII}) decreased 52% after 24 h and 18 % after 48 h exposure. These results evidence strong inhibition of the photosynthetic electron transport [44]. According to our results, photosynthetic activity of *C. sorokiniana* was less affected.

Oxygen evolution rates decreased 50 % in cells exposed to 40 $mg \cdot L^{-1}$ Se compared to control cells after 48 h cultivation (**Fig. 32**). That difference is similar to reported values [90]. During the 10 days of cultivation with up to 100 μM of selenate, oxygen evolution rate decreased in 44–72 % range, compared to control. Nevertheless, Se-treated *Ulva sp.* recovered its full capacity to produce photosynthetic O_2 when transferred to a fresh culture medium. Authors suggested, that possible resistance mechanism of *Ulva sp.* to selenate toxicity lays in its capacity to keep intracellular Se at low level [90].

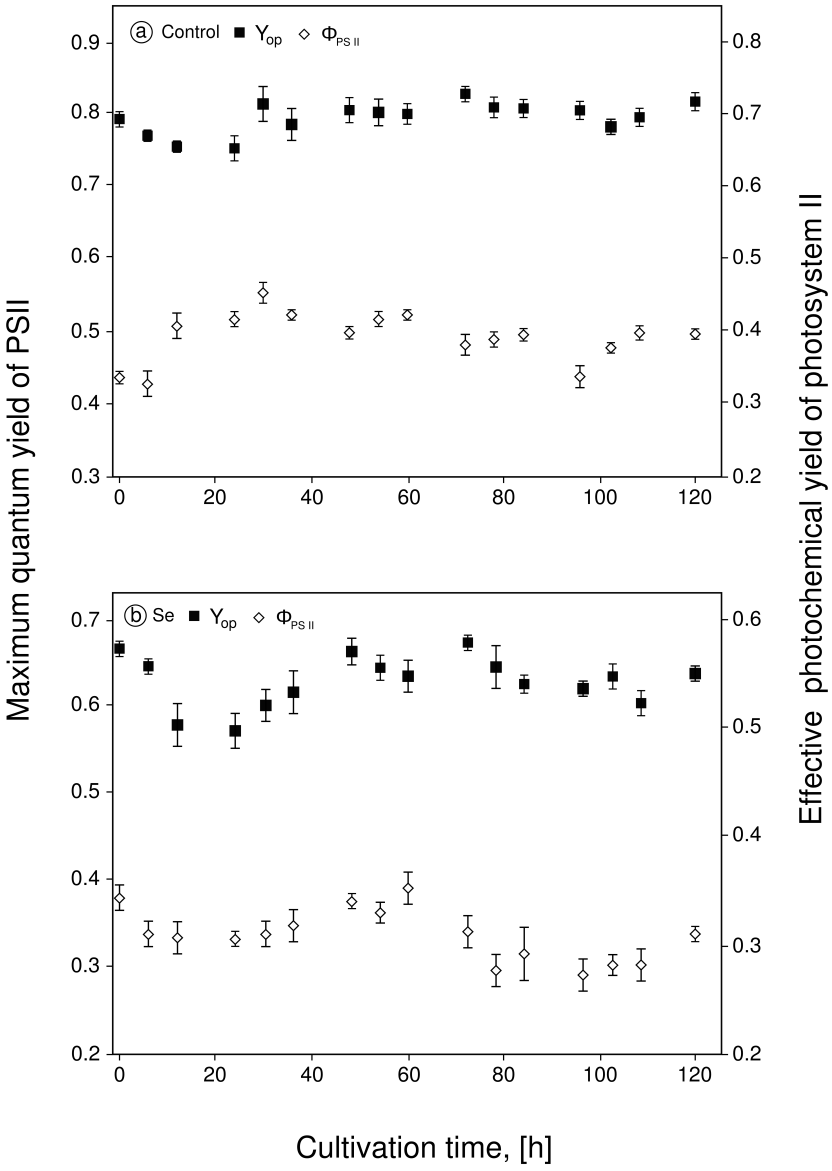

Figure 31. Maximum quantum yield of PSII (Y_{op}) and effective photochemical yield of PSII (Φ_{PSII}) in function of cultivation time for culture exposed to 40 mg·L^{-1} selenate in culture medium (**a**); and Se-free culture (**b**). Data are given as mean values ± S.D. of the means.

Total chlorophyll and carotenoid content of control culture (**Fig. 33**) increased during the first 48 h of batch cultivation up to values of 60 mg·g^{-1} and 20 mg·g^{-1}, respectively, and remained almost constant until 96 h of the experiment. From then on, total pigments content of control culture decreased due to self-shading effect [120,141]. No significant differences in total pigment content were found for Se-exposed cultures. Based on PSII fluorescence, oxygen evolution and pigment production data, it can be concluded that 40 mg·L^{-1} of selenate was a sub-lethal concentration for *C. sorokiniana* culture and can therefore be used for SeMet accumulation studies.

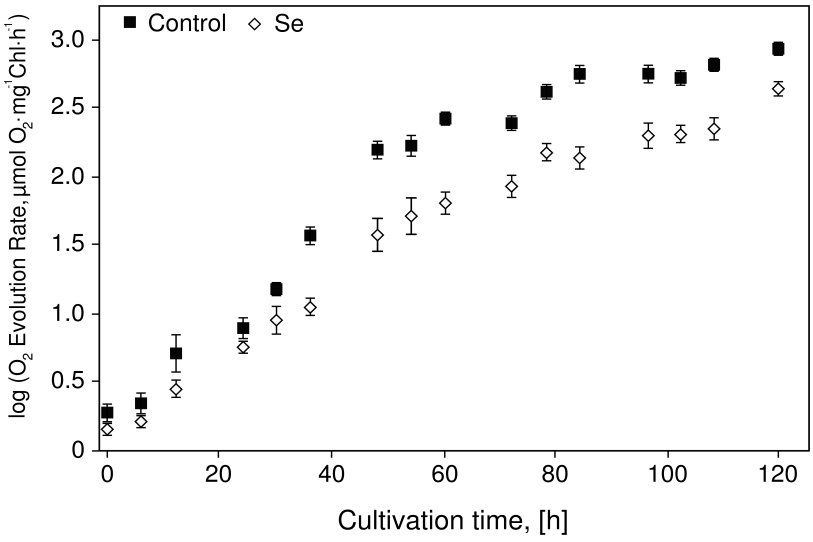

Figure 32. Photosynthetic oxygen evolution (µmol O_2 mg^{-1}_{Chl} h^{-1}) by *C. sorokiniana* in function of time for culture with 40 mg·L^{-1} of selenate and control culture. Data are given as mean values ± S.D. of the means.

The content of total chlorophyll in *Ulva sp.* cultivated for 10 days in the presence of 2.5 – 100 µM selenate have not changed compared to control, while the content of carotenoids in alga increased at Se concentration above 50 µM [90]. Increase of accessory pigments content in this alga was attributed to carotenoids protective role on chloroplast from oxidative damage [90]. In cultures of *C. vulgaris* cultivated with 7 - 70 nM of selenate for 48 h on two different sulphate concentrations (31.2 µM and 312 µM), chlorophyll content was not significantly affected by exposure to Se, regardless of sulphate concentration [93]. It seems that although Se interferes with photosynthetic electron transport it does not significantly affect pigment production in green microalgae, as it does in macroalgae, and there is no definitive evidence to establish link between pigment content and Se exposure in microalgae.

In order to understand Se mode of action on chloroplast, which results inhibitory on photosynthesis and damages cell ultrastructure it is necessary to take a closer look into a thylakoid membrane where photosynthetic electron transport actually occurs (see **Fig. 6**). Based on chlorophyll fluorescence measurements and the overall photosynthesis inhibition in Se exposed *C. reinhardtii* cells it has been suggested that Se affects photosynthetic electron transfer due to possible modification of Cyt b_6f complex [44]. Because of their chemical similarity, Se can substitute sulphur in iron-sulphur protein that is a part of Cyt b_6f complex, which can eventually lead to disruption of photosynthetic electron transfer as Cyt b_6f transfers excitation from PS II to PS I [44]. As a result, chlorophyll fluorescence parameters Y_{op} and Φ_{PSII} decrease in value upon Se exposure of microalgal culture. Se interference of photosynthetic electron transfer indirectly affects O_2 evolution rate as the water-splitting complex is also associated to PS II, and in order to form one molecule of oxygen, four electrons need to be transferred from water molecule to $NADP^+$ [6].

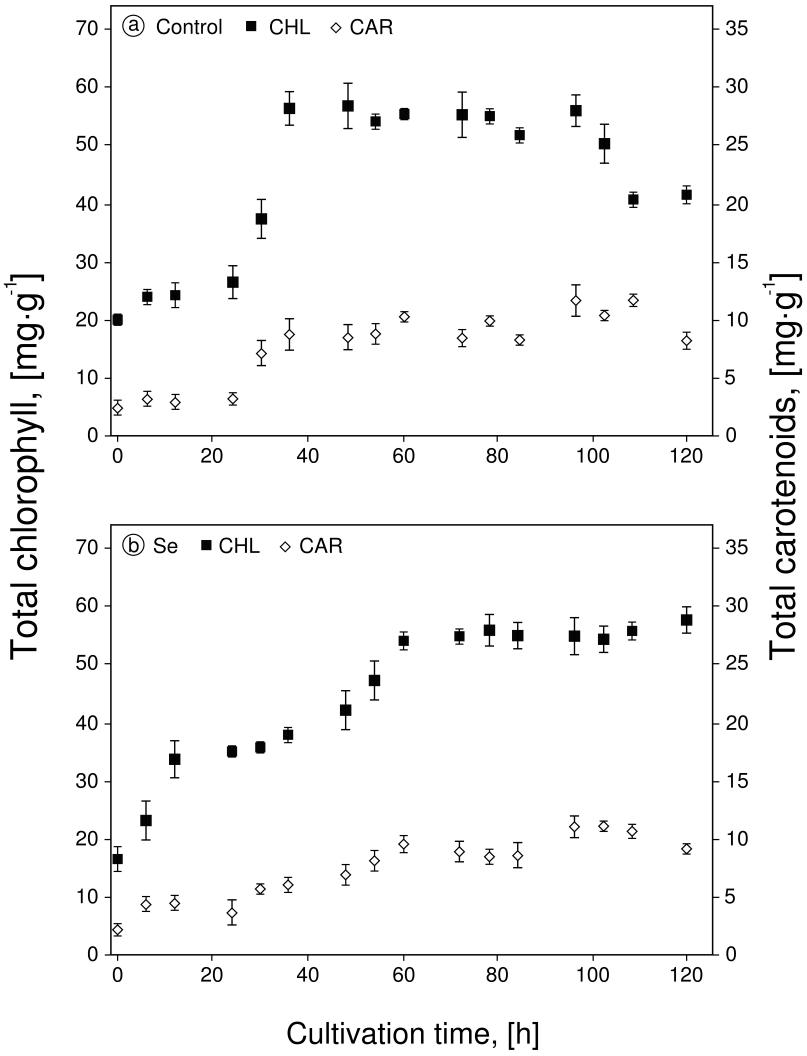

Figure 33. Total chlorophyll ($mg \cdot g^{-1}$) and total carotenoids ($mg \cdot g^{-1}$) content per biomass weight as a function of time for: (**a**) control (no selenate); (**b**) culture with 40 $mg \cdot L^{-1}$ of selenate in culture medium. Data are given as mean values ± S.D. of the means.

6.2.1.4 *Impact of selenate on C. sorokiniana proteins*

Electrophoresis of total protein isolate fractions revealed a band of approx. 50 kDa present in 50% ammonium sulfate fraction of Se-exposed cells while the same band was absent in control culture fractions (**Figure 34** – lanes 1,2). In order to locate in a more precise way that fraction where such a protein band appears, the experiment was repeated and the results confirmed (**Figure 34** – lanes 3,4). Total protein extract was fractionated with ammonium sulfate in the range of 30% - 70%. After SDS PAGE electrophoresis, protein band of Se-exposed culture appeared in 60% ammonium sulfate fraction while the same band was absent again in Se free culture (**Figure 34** – lanes 5,6). To identify proteins in Se-treated culture, bands were cut from SDS PAGE gels, and analyzed by MS-TOF-TOF mass spectrometry. Proteins from these bands were identified as 53 kDa large subunit of *C. sorokiniana* Rubisco enzyme, suggesting that Se may interfere with proteins located in the chloroplast. Rubisco (ribulose 1,5-bisphosphate carboxylase/oxygenase), the most abundant enzyme in nature and

responsible for CO_2 fixation by photosynthetic organisms, is a complex protein composed from eight identical large subunits (M_r 53 000) that are encoded in the chloroplast genome, each one with catalytic site, and eight identical small subunits (M_r 14 000) that are encoded in the nuclear genome [6]. Having in mind that selenate strongly affects chloroplast morphology and function [44,47] these results open the possibility that Se exposure could modify large subunit of *C. sorokiniana* Rubisco by incorporation or association to it, as it is encoded in the chloroplast DNA. Se enters the microalga cell by competing with sulphur metabolism, finally getting incorporated into seleno-amino acids (SeMet and SeCys) [91]. Therefore, Se-aminoacids biosynthesis and its further incorporation into proteins might be among the biochemical reasons that explain the appearance of that probable Se-protein band.

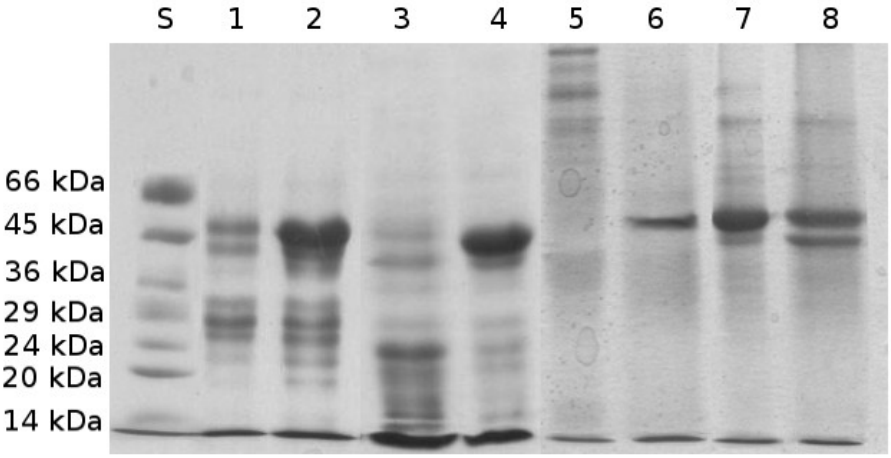

Figure 34. SDS-PAGE analysis of proteins extracted from biomass of *C. sorokiniana:* 50 % ammonium sulfate fractions of control (lane 1 and 3) and 40 mg·L^{-1} selenate exposed (lane 2 and 4) cultures; 60 % ammonium sulfate fractions of control (lane 5) and 40 mg·L^{-1} selenate exposed (lane 6) cultures; 40 % ammonium sulfate fractions of control (lane 7) and 40 mg·L^{-1} selenate exposed (lane 7) cultures. All lanes were extracted from cells of *C. sorokiniana* after 120 h of cultivation. Lanes 1 to 4 origin from initial cultivation while lanes 5 to 8 belong to repeated cultivation. Lanes 1 and 2 were loaded with 15 µg of proteins, lane 3 with 20 µg, lane 4 with 10 µg, while lanes 5 to 8 contained 7.5 µg of proteins each. S = protein ladder (molecular weight marker).

Binding of Se on microalga proteins is reported by various authors [83,92,95,132]. An increase of cytosolic selenium and total cell protein of the marine microalga *Cricosphaera elongate* with increasing selenium concentrations, was reported [86], suggesting that these proteins take part in detoxifying process. *S. platensis* could accumulate 85% of selenium in organic form of which 25% was integrated with proteins [80]. Novoselov et al. (2002) identified selenoproteins present in a 20 to 80% ammonium sulfate fraction of *C. reinhardtii* with molecular weight of 7 to 52 kDa [95]. In spite of the results mentioned above, the mechanism of interaction between Se and large subunits of Rubisco is still unknown and merits further investigation.

6.2.1.5 Se *bioaccumulation and effect on cell proteins in C. sorokiniana batch culture*

*M*icroalgae, due to their reductive metabolism preferentially accumulate selenite and selenate in form of selenoproteins and various Se-amino acids, particularly SeMet and SeCys [91]. Wrench et al. was among the first studies that used radiolabeled selenite to investigate the metabolic transformation of Se. Particularly, the Se-amino acids Se-methylcysteine, selenocystine ($(SeCys)_2$) and SeMet were detected by this procedure in biomass of microalgae of *Tetraselmis tetrathele* and *D. minuta* [81]. Bottino et al. identified Se-methyl selenocysteine (SeMeSeCys), $(SeCys)_2$ and SeMet in biomass of *Chlorella sp*. cultivated in artificial sea water [83]. Marine calcifying microalga, *E. huxleyi* after 16 h of cultivation with radiolabeled selenite, incorporated 17 % of ^{75}Se as as the protein fraction and up to 70 % as low molecular fraction of Se, which contained SeMeSeCys but no SeCys and SeMet, suggesting that these seleno-amino acids were rapidly metabolized in *E. huxleyi* which requires Se for normal growth [87,88].

As can be seen in **Fig. 35** microalga *C. sorokiniana* was able to accumulate up to 140 $mg \cdot kg_{DW}^{-1}$ of SeMet in 120 h of batch cultivation at 40 $mg \cdot L^{-1}$ of selenate. After the first 24 h of cultivation *C. sorokiniana* accumulated 60 $mg \cdot kg_{DW}^{-1}$ of SeMet and 40 $mg \cdot kg_{DW}^{-1}$ of intracellular selenate, suggesting both rapid intake and biotransformation of Se. Intracellular selenate concentration decreased during the cultivation due to its transformation to SeMet and SeMeSeCys and $(SeCys)_2$ which have been identified as minor intermediates [127], and their content was below 20 $mg \cdot kg_{DW}^{-1}$ throughout the experiment. Metabolites, SeMeSeCys, γ-glutamyl-SeMeSeCys and Se-cystathionine have also been found in biosynthesis of SeMet in land plants that can tolerate Se [103]. In *Chlorella sp.* SeMet comprised 39 % and 24 % of the of total Se accumulated, when cultivated with 20 μM of selenate and selenite, respectively [91]. In *S. quadricauda* up to 41 % of total Se was was in form of SeMet in the case of selenate and 29 % of Se as SeMet in the case of selenite [45]. Maximal SeMet content in *S. quadricauda* biomass reached 300 $mg \cdot kg_{DW}^{-1}$, when cultivated with 50 $mg \cdot L^{-1}$ selenate in culture medium [45]. Higher toxicity of selenite compared to selenate on *S. quadricauda* was attributed to lower accumulation of Se in form of SeMet in case of selenite, which resulted in less detoxification [45].

SeMet is as well, the main Se form accumulated by Se-enriched yeast, where it accounts for 54–74 % of total accumulated Se [73]. This fact is of great importance because SeMet is highly suitable for nutritional supplementation as it is more bioavailable, less toxic and can provide greater tissue Se concentrations than inorganic Se [73, 100]. SeMet is also one of the precursors of methylselenol - a potent anticarcinogen which inhibits tumor invasion and angiogenesis [142].

6.2.2 Continuous production of SeMet-enriched *C. sorokiniana* biomass

Primary goal of this research phase was to determine optimal selenate concentrations for continuous operation, aiming at maximized volumetric productivity of biomass and SeMet bioaccumulation. The microalga was grown in a bioreactor on a conventional culture medium containing 5 $mg \cdot L^{-1}$ selenate. Selenate level in inlet medium was increased every time culture reached the steady-state phase. Se species in the biomass were analytically measured from the accumulated effluent of the culture broth. In the second experimental phase, the effect of dilution rate on productivity with previously determined optimal selenate concentrations was investigated.

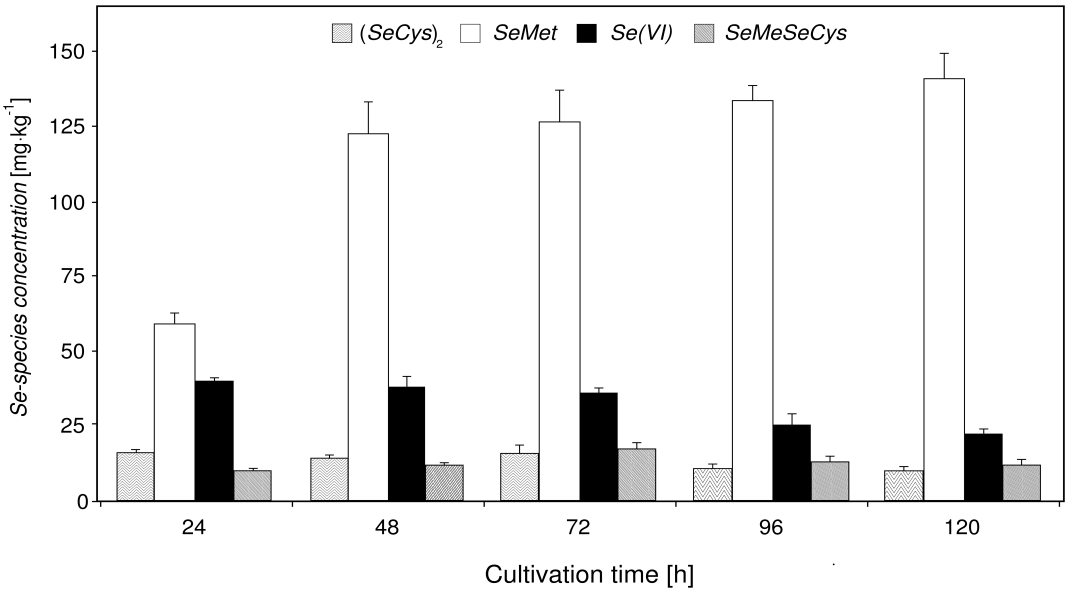

Figure 35. Selenium species concentration in *C. sorokiniana* dry biomass [mg·kg^{-1}] in function of cultivation time for culture exposed to 40 mg·L^{-1} selenate in culture medium. During cultivation 750 ml of culture volume was collected daily from each replicate bottle and centrifuged to obtain sufficient biomass to perform the necessary analyses. Data are given as mean values ± S.D. of the means. SeMet = selenomethionine; $(SeCys)_2$ = selenocystine; SeMeSeCys = Se-methylselenocysteine; Se (+VI) = selenate (SeO_4^{2-});

6.2.2.1 Effect of selenate on growth and photosynthesis in continuous cultivation

Continuous cultivation of *C. sorokiniana* in the air-bubbled stirred photobioreactor was performed using selenate concentration range of 5 – 50 mg·L^{-1} in the culture medium. Dilution rate was constantly adjusted in order to allow *C. sorokiniana* culture for reaching the steady state at each one of the selenium concentrations added in the influent. Time course of optical density in the continuous culture is shown in **Fig. 36**. Increase of selenate concentration in the culture medium above 25 mg·L^{-1} had a significant impact on cell density and biomass concentration of *C. sorokiniana* grown in the photobioreactor. Mean values of dilution rates decreased with increasing selenate concentrations.

Although, apparently, biomass productivity at 50 mg·L^{-1} seemed to be higher than at 40 mg·L^{-1}, steady state at 50 mg·L^{-1} selenate could not be maintained due to rapid culture viability loss, which is in agreement with the work of Umysová et al. (2009) in batch systems [45]. Productivity decreased (**Fig. 37**) as selenate concentration increased, from a maximum value of 1.15 g·L^{-1}day^{-1} at 5 mg·L^{-1} selenate to 0.44 g·L^{-1}day^{-1} at 35 mg·L^{-1} selenate. At the 40 mg·L^{-1} selenate, productivity slightly increased and finally it reached 0.67 g·L^{-1}day^{-1} at 50 mg·L^{-1} selenate. The photosynthetic efficiency values followed the same trend as productivity. Increased selenate concentrations resulted in decreased biomass yield on light energy, from a maximum value of 0.83 g·mol$_{ph}^{-1}$ at 5 mg·L^{-1} selenate. Biomass yield reached the minimum value in cultures with selenate concentrations higher than 35 mg·L^{-1}.

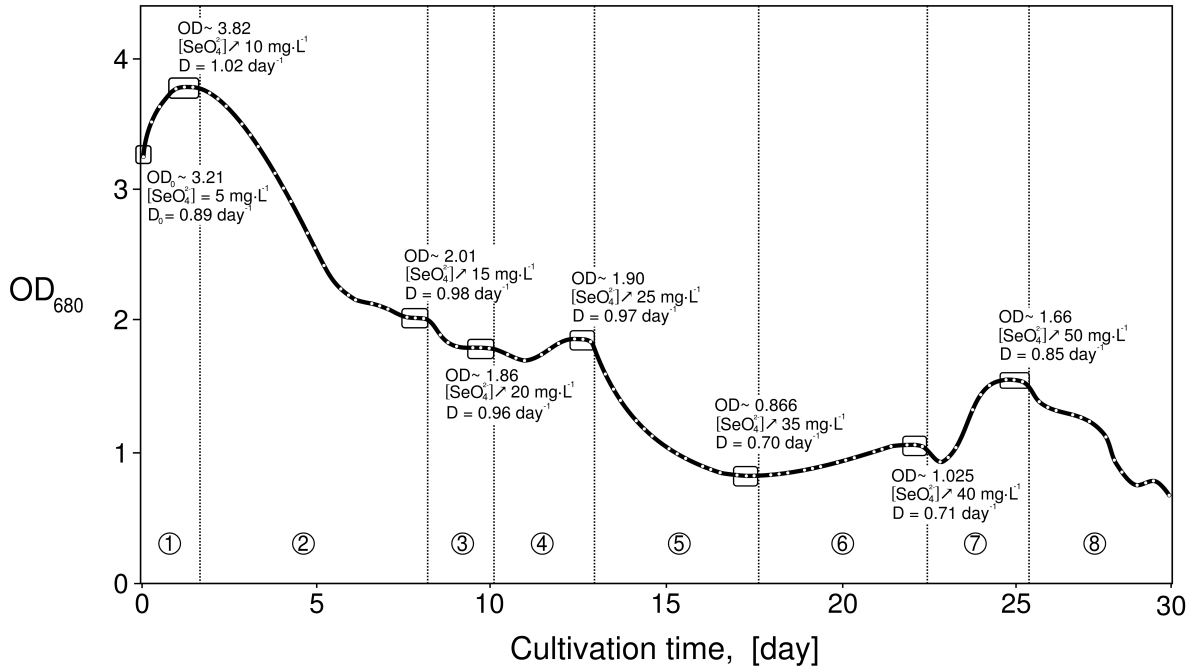

Figure 36. Optical density of *C. sorokiniana* (OD_{680}) as a function of time of cultivation in 2.2 L photobioreactor with different selenate concentration in culture medium. Every steady-state is indicated with bar and respective values of optical density and dilution rate. Selenium concentrations are the initial selenium concentrations in the fresh culture medium pumped to the reactor. Once steady state was reached and productivity calculated, selenium concentration was increased (as indicated by arrows). For that reason selenium level is different depending on culture time. Encircled numbers present selenate concentrations in fresh culture medium: 1–5 mg·L^{-1}; 2–10 mg·L^{-1}; 3–15 mg L^{-1}; 4–20 mg·L^{-1}; 5–25 mg·L^{-1}; 6–35 mg·L^{-1}; 7–40 mg·L^{-1}; 8–50 mg·L^{-1}.

There is strong evidence that selenate affects photosynthesis by damaging the thylakoid membrane structure both by impairing PS II function and limiting electron transport between PSII and PSI [44]. Damage on PSII function can be observed as Y_{op} drop, therefore affecting photosynthetic electron transport negatively. Consequently, a decrease of the effective photochemical yield of PSII (Φ_{PSII}) should also be observed. In our experiments, reduced photosynthetic efficiency of *C. sorokiniana* grown in selenate-added culture medium is observed, which resulted in lower values of the PSII maximum quantum yield. The damaging effect of selenate, was dose dependent, and also depended on cultivation time. After the first 24 hours of cultivation Y_{op} decreased proportionally to selenate concentration (**Tab. 18**).

In the next 24 hours Y_{op} values remained constant. From that cultivation time on and for the assayed selenate concentrations, no significant daily Y_{op} differences were observed, suggesting that photosynthetic viability is preserved in the long-term continuous process in selenate presence. After 24 hours of cultivation, effective photochemical yield, Φ_{PSII}, decreased when compared to control cultures, remaining constant until process end. Interestingly, Φ_{PSII} decreased less than Y_{op}, suggesting the impact of the selected selenate concentration range on effective PSII photochemical activity to be slightly attenuated in continuous cultivation. For control cultures, a Φ_{PSII} value of 0.43 was calculated and remained constant throughout the experiment. At 10 mg·L^{-1} selenate, Φ_{PSII} was even higher than that value of control cultures.

The 40 mg·L^{-1} selenate culture showed a lower Φ_{PSII} value of 0.34, as expected. At moderate selenate level, maximum quantum yield of PSII is close to the theoretical value for healthy microalga cultures (Y_{op} of 0.7) [55,143]. As Se concentration in the medium increased, Y_{op} decreases down to 0.57 for the 40 mg·L^{-1} selenate culture. Such decrease in Y_{op} resulted in lower biomass yield and productivity values (**Fig. 37**), though still keeping continuous cultures stable and productive, as inferred from the results.

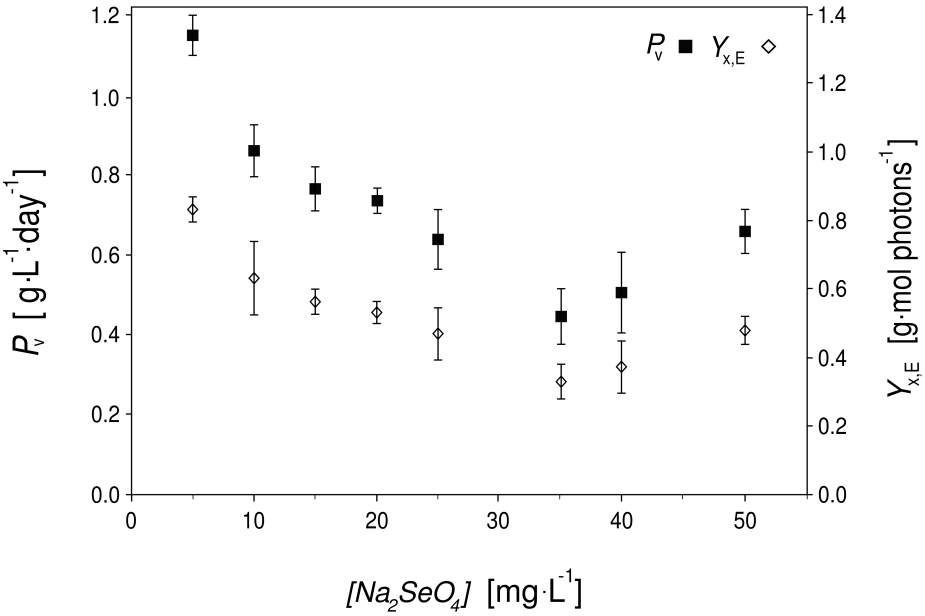

Figure 37. Influence of different selenate concentration on volumetric productivity (P_v) and yield on light energy ($Y_{x,E}$) during *C.sorokiniana* continuous cultivation process.

Table 18. Maximum quantum yield of PSII (Y_{op}) and effective photochemical yield of PSII (Φ_{PSII}) in function of four different concentrations of selenate in culture medium. All results are the mean value of at least seven measurements, presented with respective standard deviation (±SD) values.

Selenate conc. [mg·L^{-1}]	**PSII yields** % of decrease in the first 24h of exposure		**PSII yields** Mean values from 2nd - 10th day of cultivation	
	$\Delta Y_{op}/(Y_{op})_{control}$	$\Delta\Phi_{PSII}/(\Phi_{PSII})_{control}$	Y_{op}	Φ_{PSII}
0	0	0	0.70 ± 0.024	0.43 ± 0.014
10	9.5	5.8	0.68 ± 0.026	0.44 ± 0.022
20	10.3	4.6	0.67 ± 0.025	0.42 ± 0.018
30	6.4	5.8	0.64 ± 0.008	0.40 ± 0.017
40	15.1	18.6	0.56 ± 0.013	0.34 ± 0.021

6.2.2.2 Effect of selenate on seleno-amino acids accumulation in continuous cultivation

Accumulation of some Se-amino acids was determined in Se-added *C. sorokiniana*

continuous cultures. Accumulation of SeMet and other Se metabolites increased almost linearly with the increase of selenate in the culture medium (**Fig. 38**) which is in good agreement with those conclusions reported for batch cultivation of *Ulva sp* selenate supplemented cultures [90]. These results confirmed that selenate tolerance mechanism in selenate-adapted cells lies on assimilation and biotransformation process of selenate to less-toxic organic forms, as proposed by [45]. In our experience, maximum concentration of SeMet was 72 mg·kg^{-1} for 50 mg·L^{-1} selenate in the culture medium. The same authors, [55] reported higher concentration of intracellular SeMet for the microalga *S. quadricauda* cultivated in 50 mg·L^{-1} selenate batch cultures. Probable cause for lower intracellular SeMet levels obtained with *C. sorokiniana* lies in the fact that cultivation was run in continuous mode and therefore retention times were insufficient for *C. sorokiniana* to metabolize most of available Se. However, *Chlorella* growth rates are much higher than those reported for *Scenedemus* [144] and in addition to that continuous cultivation provided SeMet enriched biomass constantly –adapted a cells- so that continuous cultivation mode appears as a more advantageous tool for massive production at large scale.

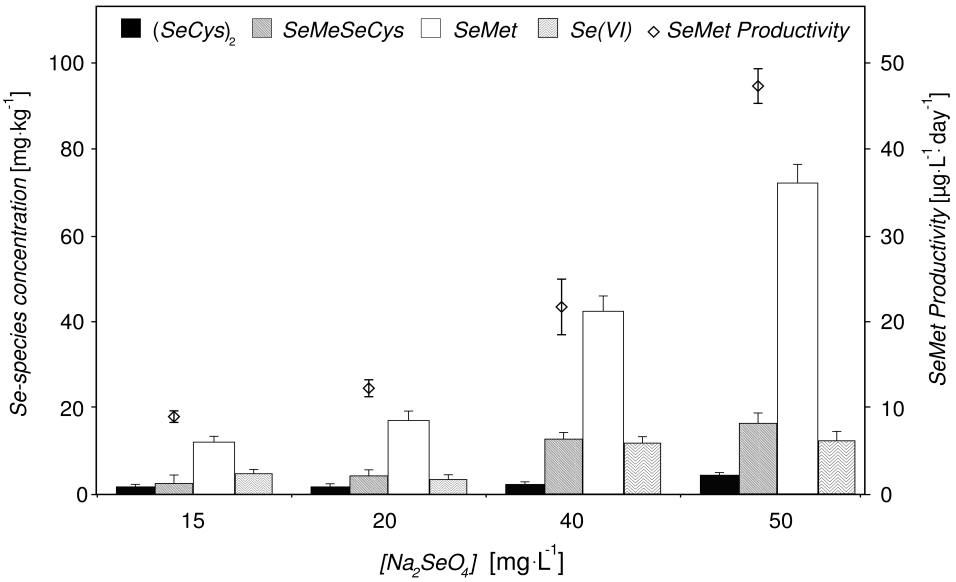

Figure 38. Selenium species concentration in microalga dry biomass and SeMet productivity (µg·L^{-1}·day^{-1}) in function of selenate concentration in culture medium (Na_2SeO_4). During continuous cultivation the entire outflow was collected and centrifuged to obtain sufficient biomass to perform the necessary analysis.

6.2.2.3 Accumulation of selenomethionine in C. sorokiniana biomass during continuous cultivation

Maximum intracellular SeMet accumulation occurred in those cultures of *C. sorokiniana* added with 50 mg·L^{-1}. However, these cultures were not stable at steady-state, apparently due to selenium toxicity effects. Therefore, even though maximum SeMet productivity was higher (**Fig. 38**), a selenate concentration of 40 mg·L^{-1} was taken as most suitable to perform a continuous process for SeMet accumulation. The next experiment consisted of continuous cultivation of *C. sorokiniana* on a fixed selenate concentration of 40 mg·L^{-1} in the culture

medium. Cultivation was first performed in batch mode at 40 mg·L^{-1} selenate for 2 weeks, in order to acclimate C. *sorokiniana* culture, after which continuous cultivation was started at a low dilution rate of 0.22 day^{-1}. During 36 days of cultivation, dilution rate was step by step increased until the cell system reached steady state of constant biomass concentration and volumetric productivity at each one of the dilution rates applied. In total, nine dilution rates were applied: 0.22, 0.30, 0.36, 0.43, 0.49, 0.57, 0.63, 0.82 and 0.97 day^{-1}. Continuous cultivation stopped when biomass concentration dropped below 0.9 g·L^{-1}. Optical density and biomass concentration data as a function of dilution rate are shown in **Fig. 39**.

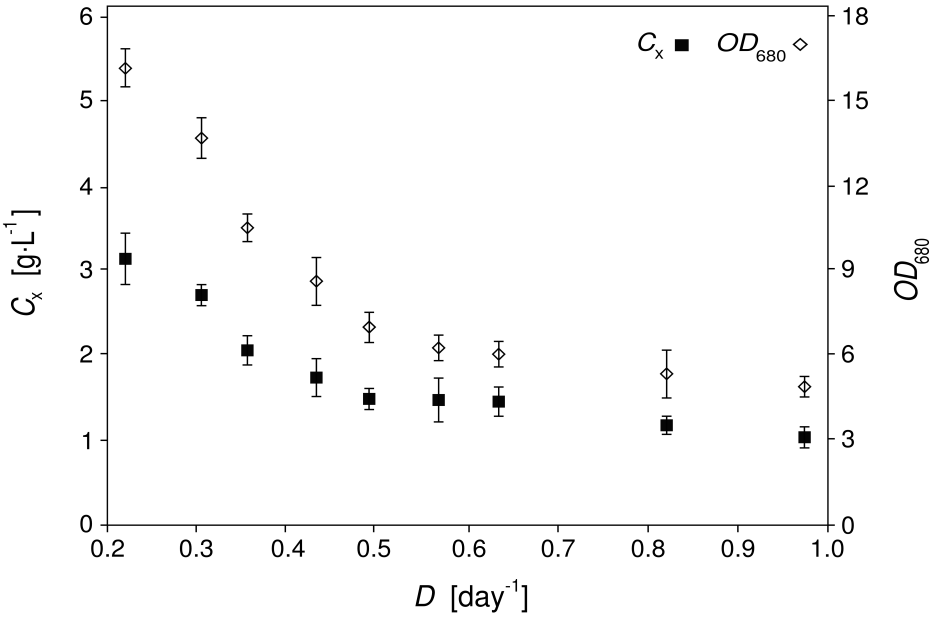

Figure 39. Influence of dilution rate (D) on the mean value of biomass concentration (C_x) and optical density (OD_{680}) of *C.sorokiniana* culture for 40 mg·L^{-1} of selenate in culture medium.

As expected, increased dilution rates reduced optical density and biomass concentration at the steady state phase. In this experiment, dilution rate was gradually increased in order to investigate the optimal biomass concentration and productivity of *C. sorokiniana* with 40 mg·L^{-1} selenate in the influent (**Fig. 40**). At low dilution rates, biomass productivity remained almost constant and around 0.75 g·L^{-1}day^{-1}. When the dilution rate increased up to 0.6 day^{-1}, biomass productivity raised and remained around 0.95 g·L^{-1}day^{-1}. At dilution rate of 0.97 day^{-1} system reached the highest productivity (0.98 g·L^{-1}day^{-1}) and maximal biomass yield on light energy (0.72 g biomass per mol$_{ph}^{-1}$) values. This value accounts for 48% of the theoretical maximum, which is a similar result to that reported for continuous culture of *C. sorokiniana* stressed by intense light [69].

In the experiment at 40 mg·L^{-1} selenate (**Fig. 41**), both total chlorophyll and carotenoids content per unit of biomass decreased with increasing dilution rate. At increased dilution rates, cells experienced higher irradiance due to the lower biomass concentration, therefore chlorophyll requirements for light transduction into chemical energy decreases, as also shown in results of continuous *Chlorella* cultivation under high irradiance [69].

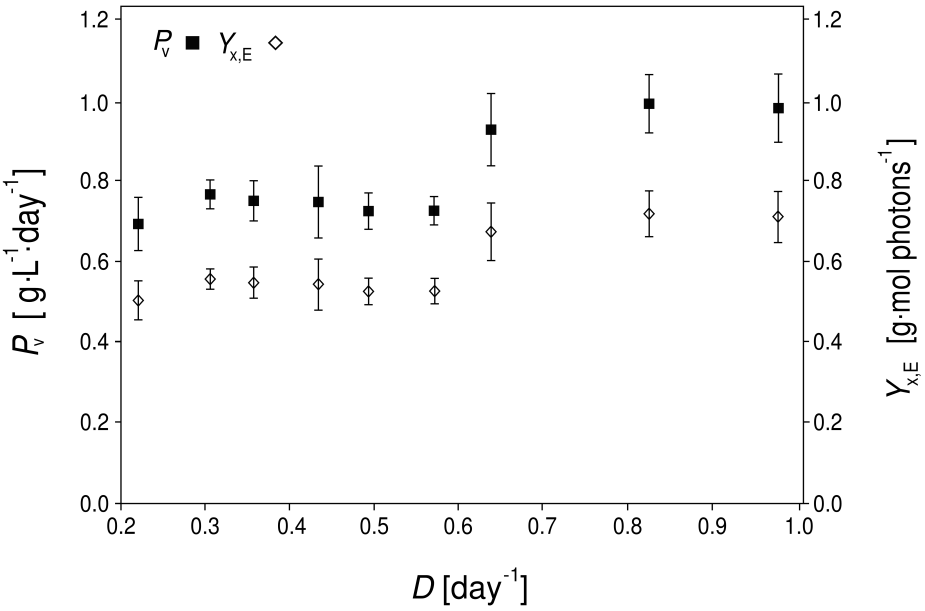

Figure 40. Influence of dilution rate (D) on volumetric productivity (P_v) and yield on light energy ($Y_{x,E}$) during continuous cultivation of *C.sorokiniana* for 40 mg·L^{-1} of selenate in culture medium.

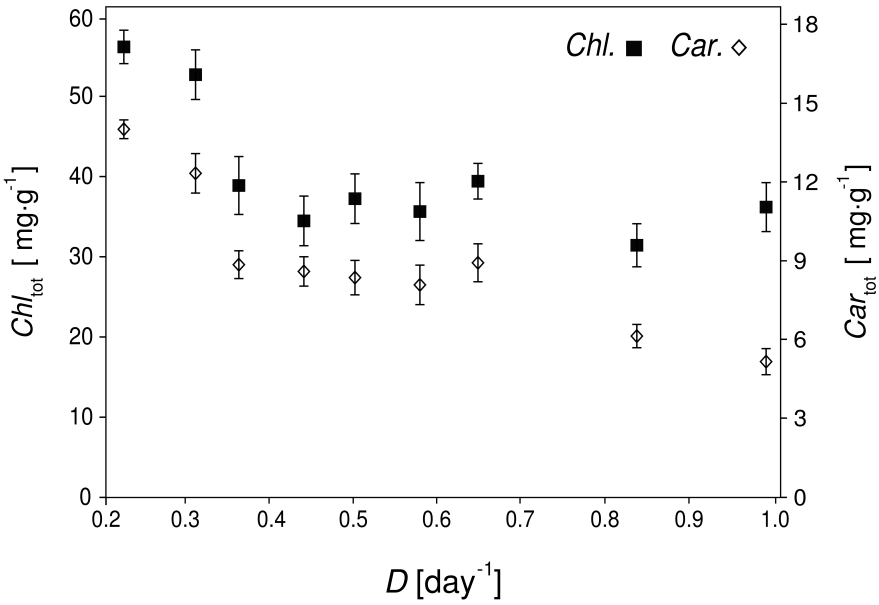

Figure 41. Influence of dilution rate on total chlorophyll (Chl_{tot}) and total carotenoids (Car_{tot}) content of *C. sorokiniana* biomass for 40 mg·L^{-1} of selenate in culture medium.

In the experiment at 40 mg·L^{-1} selenate (**Fig. 42**), intracellular SeMet levels were higher than in the first experiment and values decreased with increasing dilution rate. The most efficient dilution to sustain high intracellular SeMet productivity was 0.49 day^{-1} with an averaged productivity of 246 µg·L^{-1}·day^{-1} calculated on daily effluent volume.

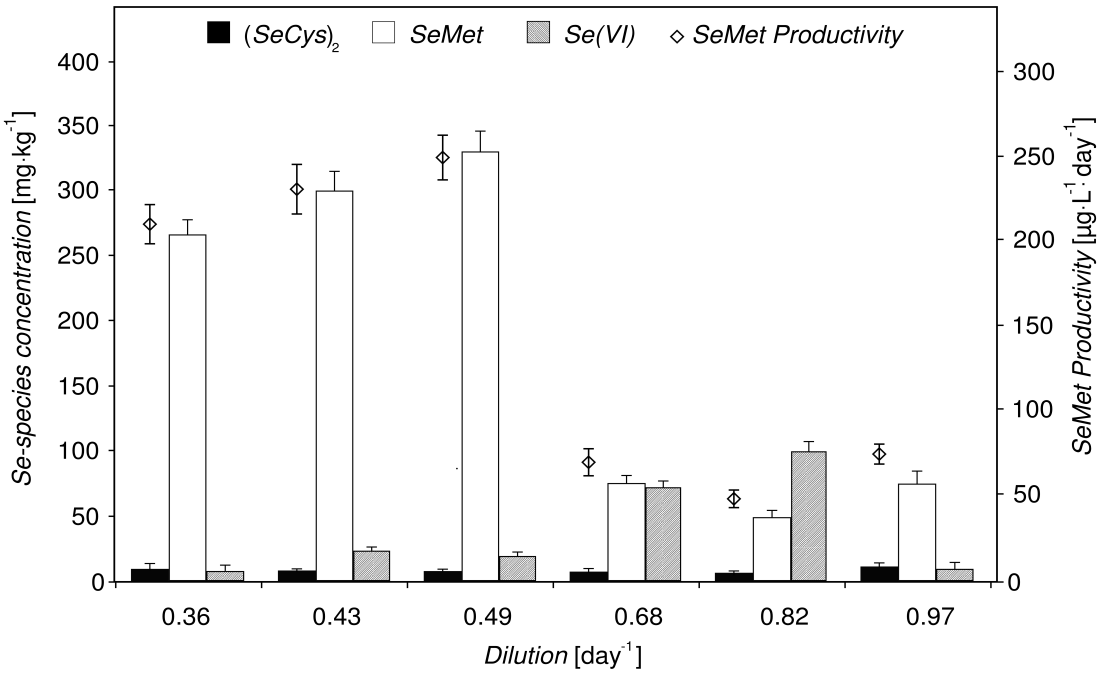

Figure 42. Selenium species concentration in microalga dry biomass and SeMet productivity, [µg·L^{-1}·day^{-1}], in function of dilution rate for 40 mg·L^{-1} selenate in culture medium. During continuous cultivation at 40 mg·L^{-1} selenate in culture medium the entire outflow of every particular dilution rate was collected and centrifuged to obtain sufficient biomass to perform the necessary analyses.

7. CONCLUSIONS

The main objective of this work was to characterize biomass from various natural sources and to investigate its production and possible utilization in biotechnology and food industry. As biomass represents basically all living biosystems, this vast area was narrowed down to two particular biomass sources of interest: 1) chicken skin as a source of collagen type I with application as biomaterial, 2) biomass of microalgae enriched in Se-methionine with possible application in nutraceutics and food industry. Investigation, accordingly, had two main phases.

7.1 CONCLUSIONS OF THE FIRST PART OF THE THESIS

Objective of the first phase of this investigation has been isolation and determination of physical, chemical and molecular properties of collagen type I derived from chicken skin tissue, as an interesting and cheap alternative source. The study of animal skin tissue as a potential source of collagen had demonstrated that waste skins from slaughtering and processing of poultry, are the potential vast source of type I collagen with characteristics comparable to those of commercial bovine tendon collagen.

- Gathered data showed no significant difference between chicken collagen properties and quality and those of commercial bovine tendon collagen. In fact, there are some major advantages of chicken collagen in comparison with bovine tendon and carp skin collagen.
- Chicken skin has denaturation temperature 10 °C higher than bovine collagen as well as higher lysine content which explains its excellent thermal stability and possibility for side chains reactions (cross-linking).
- Chicken skin collagen presents no potential health hazard neither from bovine serum albumin, as in bovine tendon collagen, nor IgE-mediated food hypersensitivity, as in carp skin collagen. Furthermore, it is less expensive and relatively easy to isolate, has high yield and dry matter content, excellent thermal stability and suitable ratio of important amino acids. These facts make this source of collagen an interesting alternative for food industry as well as a potential biomaterial in biomedicine.
- As demonstrated by results, waste chicken skin has a real potential to be an excellent source of raw collagen type I, which could find its application not only in food industry but also, as a component of various collagen based biomaterials.

7.2 CONCLUSIONS OF THE SECOND PART OF THE THESIS

The aim of the second experimental phase was to describe enrichment in Se-amino acids of green microalga *C. sorokiniana* cultured in laboratory conditions. Se uptake, accumulation, biotransformation and effects on culture parameters were investigated in batch and continuous conditions. This experimental part was performed at the laboratory of Biotechnology of Algae from the Faculty of Experimental Sciences at the University of Huelva in Spain. This work was partially financed by a Spanish grant from Agrifood Campus of International Excellence (ceiA3) for foreign PhD-students.

- Microalga *C. sorokiniana* was cultivated in batch culture with sub-lethal selenate concentration of 40 $mg \cdot L^{-1}$ in order to study the effect of selenate on culture growth, photosynthetic efficiency, cell ultrastructure, protein expression and SeMet accumulation. Exposure of *C. sorokiniana* to selenate decreased culture growth and oxygen evolution rates but had no effect on pigment content.
- Se toxicity in *C. sorokiniana* cell was confirmed by ultrastructural alterations of

chloroplast, like: fingerprint-like thylakoids, granular stroma, autophagic vacuoles, plastoglobules and overproduction of starch.

- Selenate can affects the expression of the chloroplast located gene encoding Rubisco resulting in the overproduction of this enzyme. Selenoproteins which appeared in the protein pool of Se-treated cells, but not in Se-free cells, were identified as 53 kDa large subunit of *C. sorokiniana* Rubisco enzyme, suggesting that Se interferes with proteins located in chloroplast and might be incorporated into proteins as Se-amino acids.
- Microalga *C. sorokiniana* exposed to 40 $mg \cdot L^{-1}$ selenate accumulated up to 140 $mg \cdot kg^{-1}$ of SeMet after 120 h of cultivation in batch conditions. Based on growth rate inhibition, toxicity of selenate was expressed as EC_{50} with a value of 238 μM.
- Continuous biomass production of *C. sorokiniana* in selenate-added culture medium was feasible by carefully selecting sub-lethal selenate concentrations which allowed both cell viability and high growth rates. Based on productivity and yield on light energy, optimal selenate concentration for long-term continuous cultivation of *C. sorokiniana* was 40 $mg \cdot L^{-1}$. In a 2.2 L glass bioreactor up to 0.246 $mg \cdot L^{-1} day^{-1}$ of SeMet could be produced in continuous conditions.
- Production of Se-enriched biomass as a secondary product of algae farming could in future represent one of the possible factors contributing to cost reduction of microalgae fuel production if Se-enriched biomass of microalgae became sufficiently attractive for the health food supplement market.

8. CONCLUSIONES

El principal objetivo de esta tesis ha sido caracterizar la biomasa de distintos orígenes naturales, su producción y posible aplicación en el campo de la Biotecnología y la Industria de la Alimentación. El trabajo se centró en el estudio de dos tipos concretos de biomasa:

1) Piel de pollo como fuente de colágeno tipo I y con aplicaciones en la elaboración de biomateriales.

2) Biomasa de microalgas enriquecida en selenometionina con posibles aplicaciones como alimento nutracéutico en el campo de la alimentación.

8.1. CONCLUSIONES DE LA PRIMERA PARTE DE LA TESIS:

El objetivo de esta primera parte fue aislar y determinar las propiedades físicas, químicas y moleculares del colágeno tipo I obtenido de los despojos de la piel del pollo como una alternativa interesante y barata a las actuales fuentes comerciales de colágeno. El estudios de los tejidos de la piel de animales como fuente alternativa de colágeno ha demostrado que los despojos de piel obtenidos en el proceso de sacrificio y procesamiento de aves de corral, son una fuente importante de colágeno tipo I con propiedades comparables a las del colágeno comercial obtenido de los tendones del ganado bovino.

1- Los datos obtenidos muestran que no existen grandes diferencias entre las propiedades del colágeno obtenido de la piel de pollo y las del colágeno de uso comercial obtenido de los tendones del ganado bovino o de la piel de las carpas (peces de agua dulce).
2- La temperatura de desnaturalización del colágeno de la piel de pollo es 10º C más elevada que la del colágeno bovino, además de tener un contenido mayor del aminoácido lisina lo que explicaría su buena estabilidad térmica y la posibilidad de que se produzcan reacciones en las cadenas laterales que aumentarían su estabilidad.
3- El colágeno de la piel de pollo no representa ningún peligro para la salud como si

puede ocurrir con el colágeno bovino y el obtenido de la piel de las carpas que pueden producir problemas de hipersensibilidad. Además es más barato y fácil de aislar, con un alto rendimiento y elevado contenido en peso seco, una excelente estabilidad térmica y una ratio adecuada de aminoácidos.

4- Todos estos factores hacen del colágeno obtenido de los despojos de la piel de pollo, una alternativa interesante tanto en la industria de la alimentación como en su posible uso como biomaterial en medicina. Se puede concluir que la piel de pollo es una fuente excelente de colágeno tipo I con aplicaciones no solo en la industria de la alimentación sino también en el diseño de nuevos biomateriales en el campo de la Medicina.

8.2. CONCLUSIONES DE LA SEGUNDA PARTE DE LA TESIS*:*

El objetivo de la segunda parte de esta tesis ha sido describir el procedimiento de enriquecimiento en selenoaminoácidos de la microalga *C. sorokiniana* en condiciones de laboratorio. Se estudió el consumo de selenio, su transformación y bioacumulación en las células de la microalga en condiciones tanto de baño y como de cultivo en continuo. Esta parte experimental se realizó en el laboratorio de Biotecnología de Algas de la Facultad de Experimentales de la Universidad de Huelva en España y el trabajo fue parcialmente financiado con una ayuda del Campus Internacional de Excelencia (CEIA3) para estudiantes de doctorado extranjeros.

Las conclusiones de esta 2º parte de la tesis fueron:

5- En condiciones de cultivo “en baño” y sometiendo a las células de *C. sorokiniana* a concentraciones crecientes de selenio, la concentración subletal máxima obtenida fue de 40 $mg \cdot l^{-1}$. La exposición a concentraciones crecientes de selenio produjo una disminución en el crecimiento del cultivo y en las tasas de producción de oxígeno pero no tuvo efectos en el contenido intracelular de pigmentos.

6- Los efectos tóxicos del selenio se observaron con técnicas de microscopía electrónica a nivel de la ultraestructura celular de *C. sorokiniana* y los daños observados ron: apariencia de huella dactilar en los tilacoides, estroma con consistencia granular y aparición de vacuolas autofágicas, plastoglobulos y un aumento en la producción de almidón.

7- El selenio afecta a la expresión de los genes que codifican a la enzima Rubisco dando lugar a un aumento en la producción de esta enzima. En células tratadas con selenio se observó presencia de selenoproteinas que no aparecían en el caso de células no tratadas y que fueron identificadas como subunidades cloroplásticas de 53 kDa de la ez Rubsico de *C. sorokiniana*, sugiriendo así que el selenio es incorporado a estas proteínas en forma de selenoaminoácidos.

8- Células de *C. sorokiniana* crecidas durante 120h en condiciones de baño y sometidas a la presencia de 40 $mg \cdot l^{-1}$ de selenato acumularon hasta 140 $mg \cdot kg^{-1}$ de selenometionina. Basándonos en la tasa de inhibición del crecimiento, la toxicidad del selenato expresada como EC_{50} tuvo un valor de 238 µM.

9- La producción de biomasa en continuo de *C. sorokiniana* enriquecida en selenometionina fue posible seleccionando cuidadosamente las concentraciones subletales. Se obtuvieron tasas de crecimiento elevadas y una buena viabilidad celular. Basándonos en la productividad y en el rendimiento fotosintético, se determinó que con una concentración de selenio (en foma de selenato) de 40 $mg \cdot L^{-1}$ en un cultivo en continuo en un reactor de 2.2 litros, las células podían bioacumular hasta 0.246 $mg \cdot L^{-1} dia^{-1}$ de selenometionina.

9. REFERENCES

[1] Kimball, R. N.: *Glossary of Biotechnology Terms.* CRC Press LLC, 2002. 288 p. ISBN 1-58716-122-2.

[2] Chaplin, M. F, Bucke, C.: *Enzyme Technology.* Cambridge University Press, 1990, ISBN 9-78052-134884-3.

[3] Liese, A., Seelbach, K., Wandrey, C.: *Industrial Biotransformations*. WILEY-VCH Verlag GmbH & Co. KgaA, Weinheim, 2000. ISBN 3-527-30094-5.

[4] Aehle, W.: *Enzymes in Industry. Production and Applications.* WILEY-VCH Verlag GmbH & Co. KgaA, Weinheim, 2007. ISBN 978-3-527-31689-2.

[5] Brodsky, B., Persikov, A.V.: Molecular Structure of the Collagen Triple Helix. In *Fibrous Proteins: Coiled-Coils, Collagen and Elastomers. Advances in Protein Chemistry.* Eds. D.A.D. Parry, J.M. Squire. San Diego, Elsevier Academic Press. 2005, vol. 70, p. 301–339. ISBN 0-12-034270-7.

[6] Nelson, D.L., Cox, M.M.: *Lehninger's Principles of Biochemistr*y. 5th ed. Freeman Publishing, 2008, 1294 p. ISBN 978-0-7167-7108-1.

[7] Zeugolis, D.I., Paul, R.G., Attenburrow, G.: Reformed Collagen Fibres. In *Medical Textiles and Biomaterials for Healthcare.* Ed. S.C. Anand et al. England: Woodhead Publishing Limited, 2004. ISBN 1-85573-683-7.

[8] Tsai, S. P., Hsieh, C, Y., Wang, D. M., Huang, L. L. H., Lai, J. Y., Hsieh, H. J.: Preparation and Cell Compatibility Evaluation of Chitosan/Collagen Composite Scaffolds Using Amino Acids as Crosslinking Bridges. *Journal of Applied Polymer Science*, 2007, vol. 105, pp. 1774–1785.

[9] Jančář, J., Vojtová, L., Nečas, A., Srnec, R, Urbanová, L., Crha, M.: Stability of collagen scaffold implants for animals with articular cartilage defects. *Acta Veterinaria Brno*, 2009, vol. 78, pp. 643-648.

[10] Wang, L., Yang, B., Wang, R., Xiuqiao, D.: Extraction of pepsin-soluble collagen from grass carp *(Ctenopharyngodon idella)* skin using an artificial neural network. *Food Chemistry*, 2008, vol. 111, pp. 683–686.

[11] Duan, R., Junjie Z., Xiuqiao D., Xingcun Y., Kunihiko K.: Properties of collagen from skin, scale and bone of carp (*Cyprinus carpio*). *Food Chemistry*, 2009, vol. 112, pp. 702–706.

[12] Swoboda, I., Bugajska-Shretter, A., Linhart, B., Verdino, P., Keller W., Schulmeister, U., Sperr, W.R., Valent, P., Peltre, G., Quirce, S., Douladiris, N., Papadopoulos, N.G., Valenta, R., Spitzauer, S: Recombinant carp parvalbumin for fish allergy diagnosis. *The Journal of Immunology of The American Association of Immunologists*, 2007, vol. 178, pp. 6290-6296.

[13] Penn, Y.Y., Glattauer, V., Ramshaw, J.A.M., Werkmeister, J.A.; Evaluation of the immunogenicity and cell compatibility of avian collagen for biomedical applications. *Journal of Biomedical Research*, 2010, vol. 93, pp. 1235-1244.

[14] Scanes, C. G.: The Global Importance of Poultry. *Poultry Science*, 2007, vol. 86, pp. 1057-1058.

[15] Matovic, D.: Preface. In *Biomass – Detection, Production and Usage*. Ed. D. Matovic. Intech, Rijeka, Croatia, 2011, p. 9-10. ISBN 978-953-307-492-4.

[16] Pastorek, Z., Kára, J., Jevič, P.: *Biomass - Renewable Energy Source ("Biomasa – obnovitelný zdroj energie").* FCC Public, 2004, ISBN 80-86534-06-5.

[17] Mielenz, J.R.: Ethanol production from biomass: technology and commercialization

status. *Current Opinion in Microbiology*, 2001, vol. 4, pp. 324–329.Allen, J., DePaula, W., Puthiyaveethil, S., Nield, J.: A structural phylogenetic map for chloroplast photosynthesis. *Trends in Plant Science*, 2011, vol. 16, no. 12, pp. 645-655.
[18] Kamm, B., Kamm, M.: Biorefineries – Multi Product Processes. In *White Biotechnology. Advances in Biochemical Engineering & Biotechnology. Ed. R.* Ulber, S. Dieter. Springer-Verlag, Berlin-Heidelberg, 2007, p. 176-184. ISBN 978-3-540-45695-7.
[19] Pulz, O., Gross, W.: Valuable products from biotechnology of microalgae. *Applied Microbiology and Biotechnology*, 2004, vol. 65, pp. 635–648.
[20] Hollar, S.: *A closer look at Bacteria, Algae and Protozoa*. Britannica Educational Publishing, 2012. ISBN 978-1-61530-584-1.
[21] Djukic, D., Jemcev, V.: *General and Industrial Microbiology ("Opšta i industrijska mikrobiologija")*. Stylos, Belgrade, 2004. ISBN 86-7473-144-9.
[22] Spolaore, P., Joannis-Cassan, C., Duran, E., Isambert, A.: Commercial applications of microalgae. *Journal of Bioscience* & *Bioengineering*, 2006, vol. 101, pp. 87–96.
[23] Becker, E.W.: Micro-algae as a source of protein. *Biotechnology Advances*, 2007, vol. 25, pp. 207-210.
[24] Wijffels, R.H., Barbosa, M.J.: An outlook on microalgal biofuels. *Science*, 2010, vol. 329, pp. 796–799.
[25] Blanken, W., Cuaresma, M., Wijffels, R., Janssen, M.: Cultivation of microalgae on artificial light comes at a cost. Review article. *Algal Research*, 2013, vol. 2, pp. 333–340.
[26] Stengel, D.B., Connan, S., Popper, Z.A.: Algal chemodiversity and bioactivity: Sources of natural variability and implications for commercial application. *Biotechnology Advances*, 2011, vol. 29, pp. 483-501.
[27] Becker, E.W.: Microalgae in Human and Animal Nutrition. In *Handbook of Microalgal Culture: Biotechnology and Applied Phycology*. Ed. A. Richmond. United Kingdom: Blackwell Science, 2005, p. 312-347. ISBN 0-632-05953-2.
[28] Whitman, W. B., Coleman, D. C., Wiebe, W. J.: Prokaryotes: the unseen majority. *Proceedings of the National Academy of Sciences of the USA*, 1998, vol. 95, pp. 6578–6583.
[29] Ahmad, I., Ahmad, F., Pichtel, J.: *Microbes and Microbial Technology*. Springer, 2011. ISBN 978-1-4419-7930-8.
[30] Okafor, N.: *Modern Industrial Microbiology and Biotechnology.* Science Publishers, 2007. ISBN 978-1-57808-434-0.
[31] Olaizola, M.: Commercial development of microalgal biotechnology: from the test tube to the marketplace. *Biomolecular Engineering*, 2003, vol. 20, pp. 459-466.
[32] Tomaselli, L.: The Microalgal Cell. In: *Handbook of Microalgal Culture: Biotechnology and Applied Phycology*. Ed. A. Richmond, Blackwell Science, London, 2005, p. 3-19. ISBN 0-632-05953-2.
[33] Blankenship, R.E.: *Molecular Mechanisms of Photosynthesis*. Blackwell Science Ltd. 2002. 330 p. ISBN 0-632-04321-0.
[34] Lodish, H.: *Molecular Cell Biology*. Fifth Edition, 2003, 960 p. ISBN 978-0-716-74366-8.
[35] Rodríguez-Salinas, E., Riveros-Rosas, H., Li, Z., Fučíková, K., Brand, J.J., Lewis, L.A., González-Halphen, D.: Lineage-specific fragmentation and nuclear relocation of the mitochondrial cox2 gene in chlorophycean green algae (Chlorophyta). *Molecular Phylogenetic and Evolution*, 2012, vol. 64, pp. 166–176.
[36] Pröschold, T., Leliaert, F.: Systematics of The Green Algae: Conflict of Classic and

Modern Approaches. In *Unravelling the Algae: The Past, Present, and Future of Algal Systematics*. Eds. J. Brodie, J. Lewis. CRC Press, London, UK, 2007, p. 123–135. ISBN 978-0-849-37989-5.
[37] Lewis, L.A., McCourt, R.M.: Green algae and the origin of land plants. *American Journal of Botany*, 2004, vol. 91, pp. 1535–1556.
[38] Bock, C., Krienitz, L., Pröschold, T.: Taxonomic reassessment of the genus *Chlorella* (Trebouxiophyceae) using molecular signatures (barcodes), including description of seven new species. *Fottea*, 2011, vol. 11, pp. 293–312.
[39] Pröschold, T., Marin, B., Schlösser, U.G., Melkonian, M.: Molecular Phylogeny and Taxonomic Revision of *Chlamydomonas* (Chlorophyta). I. Emendation of *Chlamydomonas* Ehrenberg and Chloromonas Gobi, and Description of Oogamochlamys gen. nov. and Lobochlamys gen. nov.1. *Protista*, 2001, vol. 152, pp. 265–300.
[40] Beherepatil, K.H., Deore, L.T.: Genus *Scenedesmus* from different habitats of Nashik and it's environs (M.S.) India. *International Journal of Bioassays*, 2013, vol. 2, no. 4, pp. 727-734.
[41] Morlon, H., Fortin, C., Floriani, M., Adam, C., Granier-Laplace, J., Boudou, A.: Toxicity of selenite in the unicellular green alga *Chlamydomonas reinhardtii*: comparison between effects at the population and sub-cellular level. *Aquatic Toxicology*, 2005, vol. 73, pp. 65–78.
[42] Morlon, H., Fortin, C., Adam, C., Garnier-Laplace, J.: Cellular quotas and induced toxicity of selenite in the unicellular green alga *Chlamydomonas reinhardtii. Radioprotection*, 2005, vol. 40, pp. 101-106.
[43] Morlon, H., Fortin, C., Adam, C., Garnier-Laplace, J.: Selenite transport and its inhibition in the unicellular green alga *Chlamydomonas reinhardtii. Environmental Toxicology & Chemistry*, 2006, vol. 25, no. 5, pp.1408–1417.
[44] Geoffroy, L., Gilbin, R., Simon, O., Floriani, M., Adam, C., Pradines, C., Cournac, L., Garnier-Laplace, J.: Effect of selenate on growth and photosynthesis of *Chlamydomonas reinhardtii. Aquatic Toxicology*, 2007, vol. 83, pp. 149–158.
[45] Umysová, D., Vítová, M., Doušková, I., Bišová, K., Hlavová, M., Žížková, M., Machát, J., Doucha, J., Zachleder, V.: Bioaccumulation and toxicity of selenium compounds in the green alga *Scenedesmus quadricauda. BMC Plant Biology*, 2009, vol. 9, pp. 58-74.
[46] Fournier, E., Adam-Guillermin, C., Potin-Gautier, M., Pannier, F.: Selenate Bioaccumulation and toxicity in *Chlamydomonas reinhardtii*. Influence of ambient sulphate ion concentration. *Aquatic Toxicology*, 2010, vol. 97, pp. 51-57.
[47] Vítová, M., Bišová, K., Hlavová, M., Zachleder, V., Rucki, M., Čížková, M.: Glutathione peroxidase activity in the selenium-treated alga *Scenedesmus quadricauda. Aquatic Toxicology*, 2011, vol. 102, pp. 87-94.
[48] Gojkovic, Z., Garbayo-Nores, I., Gomez-Jacinto, V., García-Barrera, T., Gómez-Ariza, J.L., Márová, I., Vílchez-Lobato, C.: Continuous production of selenomethionine-enriched *Chlorella sorokiniana* biomass in a photobioreactor. *Process Biochemistry*, 2013, vol. 48, pp. 1235–1241.
[49] Gojkovic, Z., Vílchez, C., Torronteras, R., Vigara, J., Gomez-Jacinto, V., Janzer, N., Gómez-Ariza, J.L., Márová, I., Garbayo-Nores, I.: Effect of selenate on viability and selenomethionine accumulation of *Chlorella sorokiniana* grown in batch culture. *The Scientific World Journal*, 2014, http://dx.doi.org/10.1155/2014/401265.
[50] Cuaresma, M.: *Cultivation of Microalgae in a High Irradiance Area*. Ph.D. Thesis.

Netherlands: Wageningen University, 2011. 187 p.
[51] Young, A., Britton, G.: *Carotenoids in Photosynthesis.* Springer, London, 2012, 512 p. ISBN 978-9-401-04942-9.
[52] Guveia, L., Veloso, V., Reis A., Fernandes, B., Novais, J., Empis, J.: Evolution of pigment composition in *Chlorella vulgaris*. *Bioresource Technology,* 1996, *Vol.* 57, pp. 157-163.
[53] Rowan, KS.: *Photosynthetic Pigments of Algae*. Cambridge University Press: Cambridge, 1989. 317 p. ISBN 0-521-30176-9.
[54] Hsiu-Ping, L., Gwo-Ching, G., Tung-Ming, H.: Phytoplankton pigment analysis by HPLC and its application from a eutrophic lake on Aland, Southwest Finland. *Water Research,* 2002, vol. 23, pp. 481-486.
[55] Masojídek, J., Koblížek, M., Torzillo, G.: Photosynthesis in Microalgae. In *Handbook of microalgal culture: Biotechnology and Applied Phycology*, Ed. A. Richmond. Blackwell Science, London, 2005, p. 20-39. ISBN 0-632-05953-2.
[56] Allen, J. DePaula,W., Puthiyaveethil, S., Nield, J.: A structural phylogenetic map for chloroplast photosynthesis. *Trends in Plant Science,* 2011, vol. 16, no. 12, pp. 645-655.
[57] Zhu, X.G., Long, S.P., Ort DR.: What is the maximum efficiency with which photosynthesis can convert solar energy into biomass? *Current Opinion in Biotechnology,* 2008, vol. 19, no. 2, pp. 153-159.
[58] Available from: <http://www.cie.co.at> [2014].
[59] Kliphuis, A., Klok, A., Martens, D., Lamers, P., Janssen, M., Wijffels, R.: Metabolic modeling of *Chlamydomonas reinhardtii*: energy requirements for photoautotrophic growth and maintenance. *Journal of Applied Phycology*, 2011, pp. 1–14.
[60] Eriksen, N.T.: The technology of microalgal culturing. *Biotechnology Letters,* 2008, vol. 30, pp. 1525–1536.
[61] Harun, R., Singh, M., Forde, G.M., Danquah M.K..: Bioprocess engineering of microalgae to produce a variety of consumer products. *Renewable and Sustainable Energy Reviews,* 2010, vol. 14, pp. 1037–1047.
[62] Borowitzka, M.A.: Fats oils and hydrocarbons. In *Microalgal Biotechnology.* Eds. M.A. Borowitzka and L.J. Borowitzka, Cambridge University Press. Cambridge, 1988, p. 257-287, ISBN 978-0-521-32349-9.
[63] Vilchez, C., Garbayo, I., Lobato, M.V., Vega, J.M: Microalgae-mediated chemicals production and wastes removal, *Enzyme & Microbial Technology,* 1997, vol. 20, pp. 562-572.
[64] Pirt, S. J., Lee, Y. K., Walach, M. R., Pirt, M. W., Balyuzi, H.H., Bazin, M.J.: A tubular bioreactor for photosynthetic production of biomass from carbon-dioxide: design and performance. *Journal of Chemical Technology & Biotechnology,* 1983, vol. 33, pp. 35-58.
[65] Richmond, A., Boussiba, S., Vonshak, A., Kopel, R.: A new tubular reactor for mass production of microalgae outdoors. *Journal of Applied Phycology,* 1993, vol. 5, pp. 327-332.
[66] Mandalam, R., Palsson, B.: Elemental balancing of biomass and medium composition enhances growth capacity in high-density *Chlorella vulgaris* cultures. *Biotechnology* & *Bioengineering,* 1998, vol. 59, no. 5, pp. 605–611.
[67] Quiao, H., Wang, G.: Effect of carbon source on growth and lipid accumulation in *C. sorokiniana* GXNN01. *Chineese Journal of Oceanology* & *Limnology,* 2009, vol. 27, no. 4, pp. 762-768.
[68] Huisman, J., Matthijs, H.C.P., Visser, P.M., Balke, H., Sigon, C.A.M., Passarge, J., Weissing, F.J., Mur, LR.: Principles of the light-limited chemostat: Theory and ecological

applications. *Antonie Van Leeuwenhoek*, 2002, vol. 81, pp. 117–133.
[69] Cuaresma, M., Janssen, M., Vilchez, C., Wijffels, R.H.: Productivity of *C. sorokiniana* in a SLP Panel Photobioreactor Under High Irradiance. *Biotechnology & Bioengineering*, 2009, vol. 104, no. 2, pp. 352-359.
[70] Rayman, M.P: Dietary selenium: time to act. *BMJ*, 1997, vol. 8, pp. 314-318.
[71] Brown, K.M., Arthur, J.R.: Selenium, selenoproteins and human health: a review. *Public Health & Nutrition*, 2001, vol. 4, no. 2, pp. 593-599.
[72] Arthur, J.R., McKenzie, R.C., Beckett, G.J.: Selenium in the immune system. *Journal of Nutrition*, 2004, vol. 133, no. 5 , pp. 1457-1459.
[73] Rayman, M.P.: The use of high-selenium yeast to raise selenium status: how does it measure up? *British Journal of Nutrition*, 2004, vol. 92, no. 4, pp. 557-573.
[74] Letavayova, L., Vlčkova, V., Brozmanova, J.: Selenium: From cancer prevention to DNA damage. *Toxicology*, 2006, vol. 227, no. 1–2, pp.1-14.
[75] Martens, D.A.: Selenium. In *Encyclopedia of Water Sciences.* Eds. B.A. Stewart, T.A. Howel. Marcel Dekker, New York, 2003, p. 840-842. ISBN 0-8247-4241-9.
[76] Riedel, G.F., Sanders, J.G., Gilmour, C.: Uptake, transformation, and impact of selenium in freshwater phytoplankton and bacterioplankton communities. *Aquatic Microbiology and Ecology*, 1996, vol. 11, pp. 43-51.
[77] Hu, M., Yang, Y., Martin, J.M., Yin, K., Harrison, P.J.: Preferential uptake of Se(IV) over Se(VI) and the production of dissolved organic Se by marine phytoplankton. *Marine Environmental Research*, 1996, vol. 44, no. 2, pp. 225-231.
[78] Hasanuzzaman, M., Hossain M.A., Fujita M.: Selenium in higher plants: Physiological role, antioxidant metabolism and abiotic stress tolerance. *Journal of Plant Sciences*, 2010, vol. 5, no. 4, pp. 354-375.
[79] Kramárová, Z., Fargašová, A., Molnárová, M., Bujdoš, M.: Arsenic and selenium interactive effect on alga *Desmodesmus quadricauda. Ecotoxicology & Environmental Safety*, 2012, vol. 86, pp. 1-6.
[80] Li, Z.Y., Guo, S.Y., Li, L.: Bioeffects of selenite on the growth of *Spirulina platensis* and its biotransformation. *Bioresource Technology*, 2003, vol. 89, pp. 171–176.
[81] Wrench, J.J.: (1978) Selenium Metabolism in the Marine Phytoplankters *Tetraselmis tetrathele* and *Dunaliella minuta. Marine Biology*, 1978, vol. 49, pp. 231-236.
[82] Wheeler, A.E., Zingaro, R.A., Irgolic, K.: The effect of selenate, selenite and sulfate on growth of six unicellular marine algae. *Journal of Experimental Marine Biology and Ecology*, 1982, vol. 57, pp. 181-194.
[83] Bottino, N.R., Banks, C.H., Irgolic, K.J., Micks, P., Wheeler, A.E., Zingaro, R.A.: Selenium containing amino acids and proteins in marine algae. *Phycochemistry*, 1984, vol. 23, no. 11, pp. 2445-2452.
[84] Bennett, W.: Assessment of selenium toxicity in algae using turbidostat culture. *Water Research*, 1988, vol. 22, no. 7, pp. 939-942.
[85] Besser, J.M., Huckins, J.N., Clark, R.C.: Separation of selenium species released from Se-exposed algae. *Chemosphere*, 1994, vol. 29, no. 4, pp.771-780.
[86] Boisson, F., Gnassia-Barelli, M., Romeo, M.: Toxicity and accumulation of selenite and selenate in the unicellular marine alga *Cricosphaera elongata. Archives of Environmental Contamination Toxicology*, 1995, vol. 28, pp.487–493.
[87] Danbara, A., Shiraiwa, Y.: The Requirement of Selenium for the Growth of Marine Coccolithophorids, *Emiliania huxleyi*, *Gephyrocapsa oceanica* and *Helladosphaera* sp. *Plant*

Cell Physiology, vol. 40, no. 7, pp. 762-766.
[88] Araie, H., Shiraiwa, Y.: Selenium Utilization Strategy by Microalgae. *Molecules*, 2009, vol. 14, pp. 4880-4891.
[89] Reunova, Y.A., Aizdaicher, N.A., Khristoforova, N.K., Reunov, A.A.: Effects of selenium on growth and ultrastructure of the marine unicellular alga *Dunaliella salina* (Chlorophyta). *Russian Journal of Marine Biology*, 2007, vol. 33, pp.125–132.
[90] Schiavon, M., Moro, I., Pilon-Smits, E.A.H., Matozzo, V., Malagoli, M., Della-Vecchia, F.: Accumulation of selenium in *Ulva sp.* and effects on morphology, ultrastructure and antioxidant enzymes and metabolites. *Aquatic Toxicology*, vol. 122-123, pp. 222–231.
[91] Neumann, P.M., DeSouza, M.P, Pickering, I.J., Terry, N.: Rapid microalgal metabolism of selenate to volatile dimethylselenide. *Plant Cell & Environment*, 2003, vol. 26, pp. 897–905.
[92] Pelah, D., Cohen, E.: Cellular response of *Chlorella zofingiensis* to exogenous stress. *Journal of Plant Growth Regulation*, 2005, vol. 45, pp. 225-232.
[93] Simmons, D.B.D., Emery, R.J.N.: Phytochelatin induction by selenate in *Chlorella vulgaris* and regulation of effect by sulfate levels. *Environmental Toxicology & Chemistry*, 2011, vol. 30, no. 2, pp. 469-476.
[94] Bock, K.J., Daum, K.A., Merian, E., Newland, L.W., Pearson, C.R., Stache, H., Zander H.: *The Handbook of Environmental Chemistry / Anthropogenic Co*mpounds. Springer-Verlag, New York, 1982, ISBN 978-3-540-11108-5.
[95] Novoselov, S.,V., Rao, M., Onoshko, N., Zhi, H., Kryukov, G. V.: Selenoproteins and selenocysteine insertion system in the model plant cell system, *Chlamydomonas reinhardtii*. *The EMBO Journal*, 2002, vol. 21, no. 14, pp. 3681-3693.
[96] Turanov, A., Xu, X., Carlson, B., Yoo, M., Gladyshev, V.: Biosynthesis of Selenocysteine, the 21st Amino Acid in the Genetic Code, and a Novel Pathway for Cysteine Biosynthesis. *American Society for Nutrition - Advances in Nutrition*, 2011, vol. 2, pp. 122–128.
[97] Hawrylak-Nowak, B.: Comparative effects of selenite and selenate on growth and selenium accumulation in lettuce plants under hydroponic conditions. *Plant Growth Regulation*, 2013, vol. 70, pp.149–157.
[98] Eisler, R.: *Selenium hazards to fish, wildlife and invertebrates: a synoptic review*. U.S. Fish and Wildlife Service Biological Report, 1985, no. 1.5, pp.1-41. Available from: <http://pubs.er.usgs.gov/publication/5200062> [2014].
[99] Levander, O., Whanger, P.: Deliberations and evaluations of the approaches, endpoints and paradigms for selenium and iodine dietary recommendations. *Journal of Nutrition*, 1996, vol. 126, pp. 2427-2434.
[100] Schrauzer, G.N.: Selenomethionine: a review of its natural significance, metabolism and toxicity. *Journal of Nutrition*, 2000, vol. 130, pp. 1653–1656.
[101] Zeng, H.: Selenium as an essential micronutrient: Roles in cell cycle and apoptosis. *Molecules*, 2009, vol. 14, pp.1263-1278.
[102] Williams, E., Harrison, M.: Selenium: From health to the biological food chain. *Journal of Biotech Research*, 2010, vol. 2, pp.112-120.
[103] Sors, T.G., Ellis, D.R., Salt, D.E.: Selenium uptake, translocation, assimilation and metabolic fate in plants. *Photosynthesis Research*, 2005, vol. 86, pp. 373-389.
[104] Pilon-Smits, E.A.H., Quinn, C.F.: Selenium Metabolism in Plants. In *Cell Biology of Metals and Nutrients*. Eds. R. Hell, R.R. Mendel. Plant Cell Monographs, Springer-Verlag,

Berlin Heidelberg, 2010, p. 225-240. ISBN 978-3-642-10613-2.
[105] Ellis, D.R., Salt, D.E.: Plants, selenium and human health. *Current Opinion in Plant Biology*, 2003, vol. 6, pp. 273–279.
[106] Zhu, Y.G., Pilon-Smits, E.A.H., Zhao, F.J., Williams, P.N., Meharg, A.A: Selenium in higher plants: understanding mechanisms for biofortification and phytoremediation. *Trends in Plant Science*, 2009, vol. 14, pp. 436–442.
[107] Lowry, O.H., Rosebrough, N.J., Farr, A.L., Randall, R.J.: Protein measurement with the Folin phenol reagent. *The Journal of Biological Chemistry*, 1951, vol. 193, pp. 265-275.
[108] Samuel, C.S.: Determination of collagen content, concentration, and sub-types in kidney tissue. *Methods in Molecular Biology*, 2009, vol. 466, pp. 223-235.
[109] Biego, G.H., Joyeux, M., Hartemann, P., Debry, G.: Daily intake of essential minerals and metallic micropollutants from foods in France. *The Science of Total Environment*, 1998, vol. 217, pp. 27-36.
[110] Gitelson, A., Qiuang, H., Richmond, A.: Photic volume in photobioreactors supporting ultrahigh population densities of the photoautotroph *Spirulina platensis. Applied Environmental Microbiology*, 1996, vol. 62, no. 5, pp. 1570–1573.
[111] Norris, J.R., Tempest, D.W, Richmond M.H.: *Dynamics of Microbial Growth*. John Wiley & Sons Ltd, 1978, 35 p. ISBN 978-0-471-99564-7.
[112] Sánchez, J.F., Fernández-Sevilla, J.M., Acién, F.G., Cerón, M.C., Pérez-Parra, J., Molina-Grima, J.: Biomass and lutein productivity of *Scenedesmus almeriensis*: influence of irradiance, dilution rate and temperature. *Applied Microbiology* & *Biotechnology,* 2008, *vol.* 79, pp. 719–729.
[113] Tsoularis, A.: Analysis of logistic growth model. *Research Letters in Informatics & Mathematical Science*, 2001, vol. 2, pp. 23–46.
[114] Rioboo, C., Gonzalez, O., Herrero, C., Cid, A.: Physiological response of freshwater microalga *Chlorella vulgaris* to triazine and phenylurea herbicides. *Aquatic Toxicology,* 2002, vol. 59, pp. 225-235.
[115] Bagus, M.: *Identification of Algae Growth Kinetics*. Ph.D. Thesis. Netherlands: Agrotechnology and Food Sciences Group, Wageningen University, 2009. 4-7 p.
[116] Yang, J., Rasa, E., Tantayotai, P., Scow, K.M., Yuan, H., Hristova, K.R., Mathematical model of *Chlorella minutissima* UTEX2341 growth and lipid production under photoheterotrophic fermentation conditions. *Bioresource Technology*. 2011, vol. 102, pp. 3077–3082.
[117] R Development Core Team: *R - A Language and Environment for Statistical Computing.* R Foundation for Statistical Computing, 2013, Vienna, Austria.
[118] Ritz, C., Streibig, J.C.: Bioassay Analysis using R. *Journal of Statistical Software,* 2005, vol. 12, no. 5, pp. 1-22.
[119] Liechtenthaler, H.: Chlorophylls and carotenoids: pigments of photosynthetic biomembranes. *Methods in Enzymology*, 1987, vol. 148, pp. 350–382.
[120] Cuaresma, M., Buffing, M.F., Janssen, M., Vilchez, C., Wijffels, R.H.: Performance of *C. sorokiniana* under simulated extreme winter conditions. *Journal of Applied Phycology,* 2012, vol. 24, no. 4, pp. 693–699.
[121] Maxwell, K., Johnson, G.N.: Chlorophyll fluorescence, a practical guide. *Journal of Experimental Botany*, 2000, vol. 51, no. 345, pp. 659–668.
[122] Masojídek, J., Kopecky, J., Giannelli, L., Torzillo, G.: Productivity correlated to photobiochemical performance of *Chlorella* mass cultures grown outdoors in thin-layer

cascades. *Journal of Industrial Microbiology & Biotechnology,* 2011, vol. 38, pp. 307-317.
[123] Harris, E.L.V.: Concentration of The Extract. In *Protein Purification Techniques.* Ed. S. Roe. Oxford University Press, 2001, p. 138-139, ISBN 0-19-963674-5.
[124] Hafiz, A.: *Principles and Reactions of Protein Extraction, Purification, and Characterization.* CRC Press. 2004. 410 p. ISBN: 978-0-203-50743-8.
[125] Baines, D.: Analysis of Protein Purity. In *Protein Purification Techniques.* Ed. S. Roe. Oxford University Press, 2001, p. 38-39, ISBN 0-19-963674-5.
[126] Moreno-Roldán, F., García-Barrera, T., Gómez-Ariza, J.L.: Simultaneous Analysis of Mercury and Selenium Species Including Chiral Forms of Selenomethionine in Human Urine and Serum By HPLC Column-Switching coupled to ICP-MS. *Analyst,* 2010, vol. 135. pp. 2700-2705.
[127] Gómez-Jacinto, V., García-Barrera, T., Garbayo-Nores, I., Vilchez-Lobato, C., Gómez-Ariza, J.L.: Metal-metabolomics of microalga *C. sorokiniana* growing in selenium- and iodine-enriched media. *Chemical Papers*, 2012, vol. 66, no. 9, pp. 821-828.
[128] Rodziewicz-Motowidło, S., Śladewska, A., Mulkiewicz, E., Kołodziejczyk, A., Aleksandrowicz, A., Miszkiewicz J., Stepanowski P.: Isolation and characterization of a thermally stable collagen preparation from the outer skin of the silver carp *Hypophthalmichthys molitrix*. *Aquaculture,* 2008, vol. 285, pp. 130–134.
[129] Buckin., V., O'Driscoll, B., Smyth, C.: Ultrasonic spectroscopy for material analysis. Recent advances. *Spectroscopy Europe*, 2003, vol. 15, no. 1, pp. 120-158.
[130] Zhongkai, Z., Guoying L., Shi, B.: Physicochemical properties of collagen, gelatin and collagen hydrolysate derived from bovine limed split wastes. *Journal of the Society of Leather Technologists & Chemists*, 2005, vol. 90, pp. 23-29.
[131] Gojkovic, Z., Márová, I., Matoušková, P., Obruča, S., Pekař, M.: Use of ultrasonic spectroscopy and viscosimetry for the characterization of chicken skin collagen in comparison with collagens from other animal tissues. *Preparative Biochemistry and Biotechnology,* 2013a, doi:10.1080/10826068.2013.867869.
[132] Doucha, J., Lívanský, K., Kotrbáček, V., Zachleder, V.: Production of *Chlorella* biomass enriched by selenium and its use in animal nutrition: a review. *Applied Microbiology & Biotechnology,* 2009, vol. 83, pp. 1001–1008.
[133] Svoboda, M., Kotrbáček, V., Ficek, R., Drábek, J.: Effect of organic selenium from Se-enriched alga (*Chlorella spp.*) on selenium transfer from sows to their progeny. *Acta Veterinaria*, 2009, vol. 78, pp. 373-377.
[134] Sallas, L., Luomala, E.M., Utriainen, J., Kainulainen, P., Holopainen, J.K.: Contrasting effects of elevated carbon dioxide concentration and temperature on Rubisco activity, chlorophyll fluorescence, needle ultrastructure and secondary metabolites in conifer seedlings. *Tree Physiology,* 2003, vol. 23, pp. 97-108.
[135] Giacomelli, L., Rudella, A., Van-Wijk, K.J.: High light response of the thylakoid proteome in *Arabidopsis* wild type and the ascorbate-deficient mutant vtc2-2. A comparative proteomics study. *Plant Physiology,* 2006, vol. 141, pp. 685-701.
[136] Steinmüller, D., Tevini M.: Composition and function of plastoglobuli. Isolation and purification from chloroplasts and chromoplasts. *Planta,* 1985, vol. 163, pp. 201-207.
[137] Laizet, Y., Pointer, D., Mache, R., Kuntz, M.: Subfamily organization and phylogenetic origin of genes encoding plastid lipid-associated proteins of the fibrillin type. *Journal of Genome Science & Technology,* 2004, vol. 3, pp. 19-28.
[138] Rinnan, R., Holopainen, T.: Ozone effects on the ultrastructure of peatland plants:

Sphagnum mosses, *Vaccinium oxycoccus*, *Andromeda polifolia* and *Eriophorum vaginatum*. *Annals of Botany*, 2004, vol. 94, pp. 623-634.
[139] Katz, A., Jimenez, C., Pick, U.: Isolation and characterization of a protein associated with carotene globules in the alga *Dunaliella bardawii*. *Plant Physiology*, 1995, vol. 108, pp. 1657-1664.
[140] Li, F.: Autophagy: a multifaceted intracellular system for bulk and selective recycling. *Trends in Plant Science*, 2012, vol. 17, no. 9, pp.526–537.
[141] Tang, H., Chen, M., Simon-Ng, K.Y., O'Salley, S.: Continuous Microalga Cultivation in a Photobioreactor. *Biotechnology and Bioengineering*, 2012, vol. 109, no. 10, pp. 2468-2474.
[142] Kim, A., Oh, J.H., Park, J.M., Chung, A.S.: Methylselenol generated from selenomethionine by methioninase downregulates integrin expression and induces caspase-mediated apoptosis of $B_{16}F_{10}$ melanoma cells. *Journal of Cell Physiology*, 2007, vol. 212, pp. 386–400.
[143] Vonshak, A., Torzillo, G.: Environmental Stress Physiology. In: *Handbook of Microalgal Culture: Biotechnology and Applied Phycology*, Ed. A. Richmond. Blackwell Science, London, 2005, p. 57-82. ISBN 0-632-05953-2.
[144] Ogawa, T., Aiba, S.: Bioenergetic analysis of mixotrophic growth in *Chlorella vulgaris* and *Scenedesmus acutus*. *Biotechnology & Bioengineering*, 1981, vol. 23, pp. 1121–1132.

10. LIST OF AUTHOR PUBLICATIONS

Papers published in international journals with impact factor:

Gojkovic, Ž., Vílchez, C., Torronteras, R., Vigara, J., Gomez-Jacinto, V., Janzer, N., Gómez-Ariza, J.L., Márová, I., Garbayo-Nores, I.: Effect of selenate on viability and selenomethionine accumulation of *Chlorella sorokiniana* grown in batch culture. *The Scientific World Journal*, 2014, http://dx.doi.org/10.1155/2014/401265.

Gojkovic, Ž., Garbayo-Nores, I., Gomez-Jacinto, V., García-Barrera, T., Gómez-Ariza, J.L., Márová, I., Vílchez-Lobato, C.: Continuous production of selenomethionine-enriched *Chlorella sorokiniana* biomass in a photobioreactor. *Process Biochemistry*, 2013, vol. 48, pp. 1235–1241.

Gojkovic, Ž., Márová, I., Matoušková, P., Obruča, S., Pekař, M.: Use of ultrasonic spectroscopy and viscosimetry for the characterization of chicken skin collagen in comparison with collagens from other animal tissues. *Preparative Biochemistry and Biotechnology*, 2013, doi:10.1080/10826068.2013.867869.

Manuscript submitted to journal with impact factor:

Gojkovic, Ž., Vílchez, C., Márová, I., Garbayo-Nores, I.: Selenium effect on green algae (Chlorophyta). Review paper. Submitted to: *Aquatic Sciences* (March, 2014).

Full text conference proceedings:

Gojkovic, Ž.; Obruča, S., Pekař, M., Kučerík, J., Márová, I.: Analysis of physico chemical properties of collagen isolated from different animal tissues. *Chemické listy*. Brno: 2011. s. 1012-1012. ISSN: 0009- 2770.

Gojkovic, Ž., Mikulíková, Z., Zouharová, L., Obruča, S., Márová, I.: Possible use of chicken skin tissue as alternative source of Type I collagen. *Chemické listy*, 2010, roč. 104, č. 6, s. 581-582. ISSN: 0009- 2770.

Gojkovic, Ž., Mikuliková Z., Zouharová L., Obruča, S., Kučerik J., Márová, I.: Molecular properties of collagen type I derived from different animal skin tissues. XIV. Setkání biochemiků a molekulárních biologů. Brno, Czech Republic, 2010, 53-54 p. ISBN 978-80-210-5164- 5.

Illkova, K., Omelková, J., Pavlačková, J., **Gojkovic, Ž.**: Characterization of preparation for fat separators. *Nova Biotechnologica*, 2009, Vol. 9, No. 3, pp. 225-230. ISSN 1337-8783.

Abstracts from international congresses:

Gojkovic, Ž., Garbayo-Nores, I.,Gómez-Jacinto,V., García-Barrera, T., Gómez-Ariza, J., Márová, I.,Vílchez, C.: Continuous production of microalgae *Chlorella sorokiniana* biomass enriched in selenomethionine. V International Conference on Environmental, Industrial and Applied Microbiology BioMicroWorld2013: Book of Abstracts. Spain 2013. p. 89.

Gojkovic, Ž., Gómez-Jacinto,V., Janzer, N.,Vigara-Fernández, J., Torronteras-Santiago, R., García-Barrera, T., Gómez-Ariza, J., Márová, I., Vílchez, C., Garbayo-Nores, I.: Selenate effect on growth, cell morphology, protein expression and SeMet accumulation of *Chlorella sorokiniana* cultivated in batch culture. V International Conference on Environmental, Industrial and Applied Microbiology BioMicroWorld2013: Book of Abstracts. Spain 2013. p.

139.
Gojkovic, Ž., Márová, I.: *Controlled production of Se-enriched biomass by microalgae C. sorokiniana.* 7th CRF International Conference on Chemical reaction in Foods: Book of Abstracts. 2012. s. 252-252. ISBN: 978-80-7080-836- 8
Gojkovic, Ž., Márová, I., Obruča, S., Pekař, M.: Physical chemical properties of chicken skin collagen in comparison with collagens from other animal tissues. 7th CRF International Conference on Chemical reaction in Foods: Book of Abstracts. Praha: 2012. s. 221-221. ISBN: 978-80-7080-836- 8.
Márová, I., Petrik, S., Starečková, T., Hároniková, A., **Gojkovic, Ž**., Čačková, K. Production of carotenoid- rich yeast biomass using selected waste substrates. Vitamins 2011 - 10th International Nutrition ansd Diagnostics Conference, Praha 2010, 4.-7.9. Pardubice: University Pardubice, 2010. s. 85-86. ISBN: 978-80-7395-257- 0.

11. CURRICULUM VITAE

PERSONAL INFORMATION

Name: **Živan Gojkovic**
Address: Vladimira Rolovica 31/32, 34000 Kragujevac, Serbia
Date of birth: 11.07.1978.
Place of birth: Kraljevo, Serbia.
Telephone: (+34) 645743595
e_mail: xcgojkovic@fch.vutbr.cz

EDUCATION

- **PhD student** at Faculty of Chemistry, Brno University of Technology, Brno, Czech Republic. October 2009 – March 2014. Doctoral thesis under joint supervision of Brno University of Technology and University of Huelva.
- **Engineer of Food Technology and Biotechnology,** Faculty of Chemistry. Brno University of Technology. Brno, Czech Republic. June 2009**.**
- **Engineer of Biotechnology and Biochemical Engineering**. Faculty of Technology and Metallurgy, University of Belgrade, Karnegijeva 4, 11000 Belgrade, Serbia (5 yrs.)

WORK EXPERIENCE

- **Algal Biotechnology Group.** University of Huelva, October 2013-March 2014. Junior researcher. Under the grant from Agrifood Campus of International Excellence (ceiA3) for foreign PhD-students. Research related to the doctoral thesis.
- **Algal Biotechnology Group.** University of Huelva, Spain, September 2011-June 2013. Junior researcher. Laboratory investigation for the production of microalgal biomass in batch and continuous cultures, aimed at production of selemethionine-enriched algal biomass.
- **Department of Food Chemistry and Biotechnology, Faculty of Chemistry, Brno University of Technology (BUT)**. September 2009-February 2011. Investigation of physico-chemical characteristics and biological properties of collagen isolated from animal skin tissues as a part of doctoral thesis research.
- **Teacher of Biochemistry**, Food analysis and Thermodynamics subjects in “Prva tehnicka skola” High school, Kragujevac, Serbia. September 2004-July 2007.

INTERNATIONAL EXCHANGE AND GRANTS

- **Agrifood Campus of International Excellence Grant (ceiA3) - Cordoba, Spain, for foreign PhD students.** October 2013-March 2014. University of Huelva, Spain.
- **Erasmus placement program.** February 2012-August 2012. Algal Biotechnology Group of The Faculty of Experimental Sciences. University of Huelva, Spain.
- **Erasmus students exchange program.** February 2011-July 2011. Algal Biotechnology Group and International Centre for Environmental Research (CIECEM). University of

Huelva, Spain.

LANGUAGES

	Understanding		Speaking		Writing
	Listening	Reading	Interaction	Production	
English	C1*	C1	B2	B2	B2
Spanish	C1	C1	B2	B2	B2
Czech	B2	B2	B2	B2	B2
Bulgarian	B2	B2	B1	B1	A2
Serbian	Native speaker				

*C1 - Proficient user; B2 - Independent user; B1- Independent user; A2 - Basic User;